Determining the impact of a flood event: flood hazard mapping and modelling of Ba River, Fiji

School of Science, Faculty of Health, and Environment Science

A thesis submitted to the Auckland University of Technology

in partial fulfilment of the requirements for the degree of Master of Science (Research)

By: Zoyha Zabin Nisha

Primary Supervisor: Dr Bradley Case

Secondary Supervisor: Professor Michael Petterson

Dedication

This dedication honours the story of Alam and Karmaita, who embarked on a journey from India to Fiji as indentured labourers in 1901 aboard the steamship Fulthala. Their perseverance and resilience have been passed down through generations of the Pathaan family, and I am grateful to be their granddaughter.

Abba, I wish you were here today to see how far your ‘joy’ has come in life. I’m sure you will be celebrating in heaven.

Ammi, for providing unwavering support and the freedom of choice, I dedicate this work in recognition of your immense strength.

Acknowledgements

I express my sincere gratitude to Dr Bradley Case, my primary supervisor, for his unwavering support and guidance throughout the research process. Despite encountering some challenges along the way, Dr Case remained dedicated to my success and provided invaluable assistance to help me overcome obstacles.

I also extend my thanks to Professor Michael Petterson, my secondary supervisor, for his encouragement and for pushing me to achieve my academic best. His unwavering faith in my abilities gave me the motivation to persevere when I faced moments of self-doubt.

The success of this research is indebted to the generous support of the Ministry of Foreign Affairs and Trade (MFAT) for awarding me the Manaaki New Zealand Scholarship, which enabled me to pursue my education in New Zealand. I extend my deepest appreciation to the people and government of New Zealand for providing this scholarship to Fiji.

I would like to express my sincere appreciation to the scholarships team, with special thanks to Sandelyn and George for their exceptional support. Sandelyn, your dedication, compassion, and kindness are beyond measure, and I am confident that every student under your care receives the same level of attention and support that you provided me. Your attentiveness and empathy made me feel heard and valued.

I extend my heartfelt appreciation to all the agencies and government authorities in Fiji for their invaluable assistance in providing the necessary datasets. Vinaka Vakalevu for your generous support and cooperation throughout my research.

I would like to express my deepest gratitude to my mother and siblings for their love and support throughout my research journey. Their prayers, well wishes, encouragement, and motivation kept me going during challenging times. I am truly grateful for their presence in my life.

Finally, I would like to dedicate this work to the love of my life, Ashreet, for his unwavering support and encouragement. He has been an incredible source of strength and motivation, cheering me on even when I felt like giving up. Our journey together has been filled with challenges and triumphs, and I look forward to sharing many more adventures with my love in the future.

Attestation of Authorship

"I hereby declare that this submission is my work and that, to the best of my knowledge and belief, it contains no material previously published or written by another person (except where explicitly defined in the acknowledgements), nor material which to a substantial extent has been submitted for the award of any other degree or diploma of a university or other institution of higher learning".

Signed: Date: 05/04/2023

Zoyha Zabin Nisha

Contents

List of Figures

List of Tables

List of Equations

Abstract

Fiji faces recurrent flood events, making it crucial to prioritize efforts in reducing flood risk and its impact. With limited resources available to prepare, respond, and recover from flooding, creating a flood hazard map becomes a vital tool in identifying high-risk areas. By mapping potential flood locations, communities can be better protected, and emergency resource allocation and decisions can be improved. Additionally, such maps can aid in town planning efforts, reducing the risks posed to people and infrastructure. The Ba Town vicinity, located on the western part of Viti Levu, Fiji's main island, is a highly flood-vulnerable area. With a rise in the urban population due to increased commercial and industrial activity and the expansion of the town boundary, Ba Town presents a greater flood risk to people and the economy. This thesis aims to create a flood hazard map and examine flood risk areas using three methodologies. The three methods are: i) Multicriteria Decision Analysis (MCDA) using the Height Above Nearest Drainage (HAND) method; ii) flood mapping using Synthetic Aperture Radar (SAR) imageries on the Sentinel Application Platform (SNAP) software; and iii) simulating a one-dimensional flood in Hydrologic Engineering Centre's River Analysis System (HEC-RAS) for flood extent. The most suitable flood inundation result is generated from the HAND method and is categorized into five risk levels: very high, high, medium, low, and very low. The results are analysed in three zones and against flood heights and land use land cover present in each zone. The results from the HAND method were satisfactory and showed areas at flood risk and supported the field validation data from the National Disaster Management Office. The results from SAR and HEC-RAS methods can be calibrated, and output can be further improved with more accurate input data parameters of the study site. The highlight of this study's findings is the successful development of a flood hazard map using the HAND method, categorizing flood risk levels, and validating results against field data. This comprehensive approach empowers decision-makers in Ba

Town to prioritize mitigation efforts, allocate resources effectively, and implement targeted measures to protect vulnerable communities and critical infrastructure from the increasing threat of recurrent flooding. By providing valuable insights into flood-prone areas and enhancing disaster preparedness, this research contributes significantly to Fiji's resilience against climate-induced hazards and supports sustainable urban development in flood-prone regions.

List of Abbreviations

DEM- Digital Elevation Model

FMS- Fiji Metrological Services

GEE- Google Earth engine

GIS- Geographic Information Systems

HAND- Height Above Nearest Drainage

HEC-RAS- Hydrologic Engineering Centre's River Analysis System

MCDA- Multi-Criteria Decision Analysis

MLMR- Ministry of Land and Mineral Resources

NDMO- National Disaster Management Office

PIC – Pacific Island Countries

SAR- Synthetic Aperture Radar

SIDS- Small Island Developing States

SNAP- Sentinel Application Platform

Chapter 1: Introduction

Flooding is a significant challenge for developing countries like Fiji. Fiji, situated in the South Pacific Ocean, is at heightened risk from the effects of climate change, such as an increased occurrence of extreme weather events like tropical cyclones or heavy rainfall, and rising sea levels (Kapoor et al., 2021). Fiji has faced several notable instances of flooding in the past few years, particularly during the period between November and April known as the cyclone season (Fiji, 2017). Flood occurrences arise from a complex interplay of both natural and anthropogenic factors. Among the natural influences, tropical cyclones play a significant role in inducing flooding events by bringing forth intense rainfall and storm surges. On the other hand, human activities, particularly land use changes and deforestation, contribute to exacerbating flood events during periods of heightened precipitation, as they foster amplified runoff and erosion rates (Duaibe, 2008). These intensified floods not only result in considerable infrastructural and property damage but also pose substantial health risks to affected populations, facilitating the transmission of waterborne diseases like typhoid and leptospirosis(Daniela Rincón, Usman T. Khan, & Costas Armenakis, 2018).

Fiji experiences various types of flooding including riverine flooding, flash flooding, and coastal flooding. Riverine flooding happens when a river inundates its banks because of continuous heavy rainfall for days or weeks. It causes significant damage to infrastructure, homes, crops, and livestock, as well as loss of life (Yeo et al., 2017). Flash flooding is another type of flooding that occurs when there is a high amount of precipitation over a short duration, usually within a few hours (Yeo et al., 2010). This overwhelms the drainage systems and causes sudden and swift flooding (WMO, 2018). Flash floods can cause the biggest floods in Fiji as there is little warning timeframe which makes it difficult for people, emergency services, and disaster management authorities to respond effectively.

Furthermore, coastal flooding occurs when sea levels rise during cyclones due to high tide or storm surges and inundate the low-lying areas along the coast (McMichael, 2019). Fiji's population is primarily concentrated along the coast, with approximately 76% residing within 5 kilometres of the shoreline (Andrew et al., 2019). Numerous villages and settlements are located in the coastal areas, predominantly inhabited by the indigenous population (Fiji, 2017). Inundation of coastal areas results in the loss of crops and communities experience displacement and disruption of social and cultural activities (Fiji, 2017).

Evaluating the historical records of flooding, 286 flood events occurred all around Fiji between 1840 to 2009 (Yeo, Mcgree, & Devi, 2010). Analysis of flood records by the Fiji Meteorological Service (FMS) between 2009 to 2022 recorded a further 42 events bringing the total to 328 events in a 180-year timeline (Figure 1).

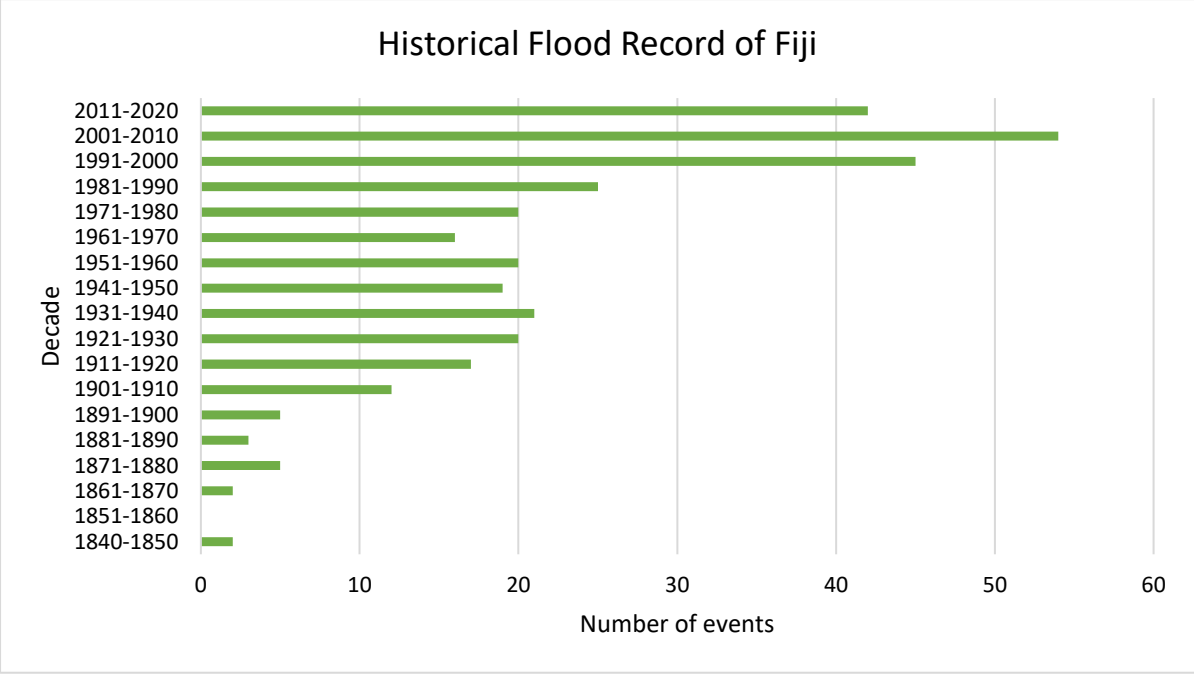

Figure 1 Breakdown of flood history by the decade in Fiji. Updated Yeo et al., (2010) with annual climate summaries from Fiji Meteorological Services.

Catastrophic floods have impacted Fiji far more recently. In 2016, category 5 tropical cyclone (TC) Winston brought devastating winds and rain into Fiji, resulting in an estimated damage of US$1.4 billion, affecting 350,000 people and damaging 31,000 houses (OCHA, 2016). In 2018, TC's Josie and Keni caused widespread flooding across Fiji, displaced 12,000 people, took six lives, and impacted 78,000 people (OCHA, 2018). These two cyclone events and flooding that occurred between 26th March 2018 to 8th April 2018 caused extensive damage to infrastructure and property. The cost of damages is estimated at FJD$91 million (Naikaso, 2018). In 2020, TC Harold in April (category 4) and TC Yasa in December (category 5) impacted Fiji and the combined estimated damage cost was FJD $643 million (RNZ, 2020, 2021). Not long after, in January 2021, category 2 TC Ana impacted 63,000 families in Fiji and devastated the North Island of Vanua Levu, resulting in an estimated damage of FJD$500 million (FMS, 2020, p. 27).

Having less than 10 billion FJD in GDP; it is a significant loss for Fiji to experience multiple hazards in a year (World Bank Group, 2022). There is a general increase in flooding events in Fiji, as illustrated in Figure 1, which highlights the need to identify flood-risk areas across Fiji. Both the Fijian government and global organizations are collaborating to enhance flood management and disaster preparedness in Fiji. This includes the development of flood protection infrastructure, early warning systems, and programs to educate and train communities (Tilly & Fakhruddin, 2020, p. 5). However, most research and flood risk models have been focused on Nadi which is the tourism hub of Fiji (Fiji, 2017, pp. 101,103). This highlights a gap in identifying flood risk areas in other catchments in Fiji.

There is a challenge for flood mapping as there is a lack of up-to-date data which makes it difficult to accurately model flood risks and identify areas that are most vulnerable to flooding (Tilly & Fakhruddin, 2020). The Fiji Meteorological Service (FMS) uses a hydrological model to predict river levels and potential flooding, which helps to inform flood

warnings and emergency response efforts. The FMS also works with other agencies, such as the Fiji National Disaster Management Office (NDMO), to develop flood risk maps and hazard assessments, which can be used to guide land-use planning and disaster preparedness activities. The tools and techniques used to generate flood forecasting are sophisticated and there is a lack of trained and dedicated hydrologists and IT infrastructure for forecasting models to run operationally in Fiji (Tilly & Fakhruddin, 2020). The need for this research is to identify a flood mapping method for Ba Catchment that can be adopted locally and further improved by integrating local knowledge and expertise so that results have improved accuracy and relevance to the local context. This research, therefore, identifies flood risk zones in Ba Catchment (Figure 2) by undertaking three different methodologies to isolate the most suitable method for Fiji with the available datasets.

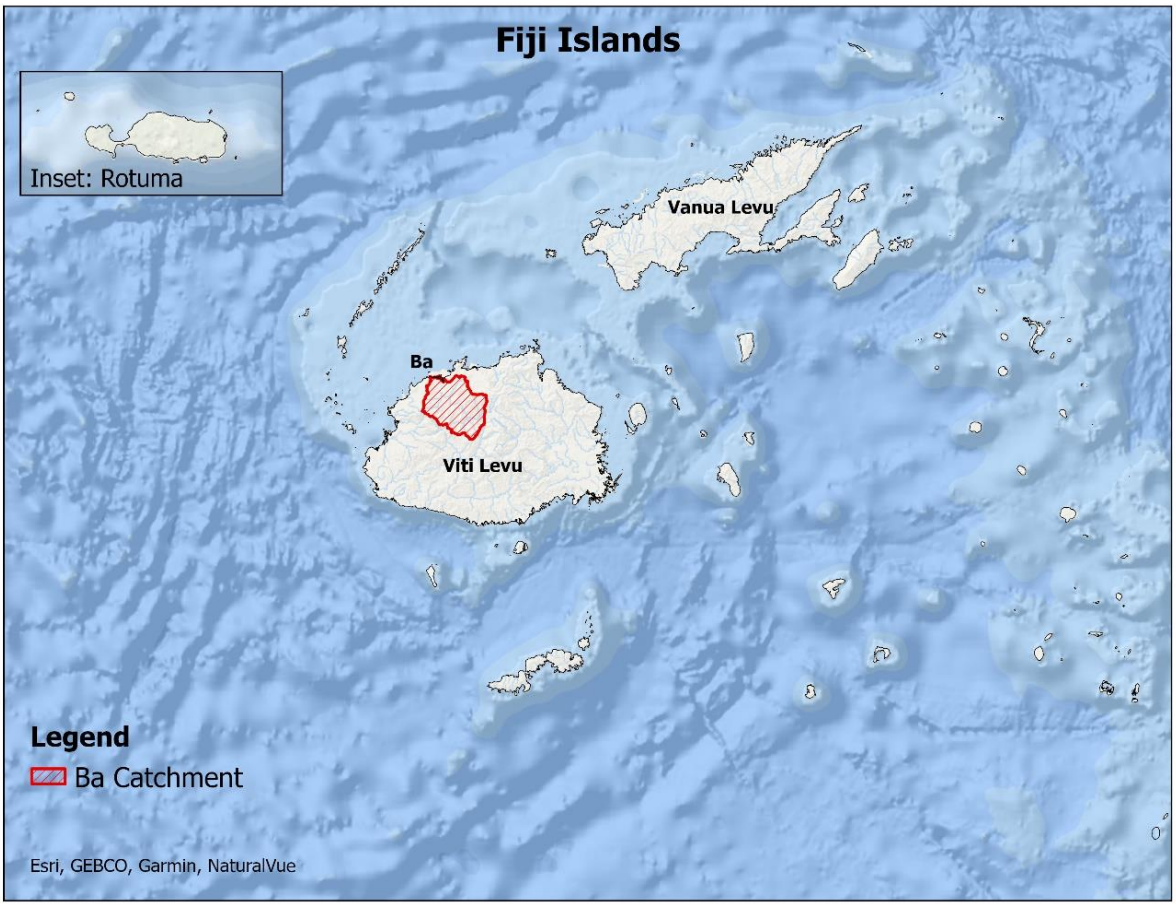

Figure 2 Map of Fiji showing the location of Ba Catchment on Viti Levu Island.

Ba Catchment is selected for this study due to multiple flood events and a need to identify flood-prone areas in smaller urban centres in Fiji. The rise in urban population has resulted in increased housing with more infrastructure developments. A flood hazard mapping of Ba Catchment would assist in identifying potential risk zones and assist people in decision-making.

All the methods here evaluated include the use of Geographic Information Systems (GIS) tools, analysis of synthetic aperture radar (SAR) imageries using remote sensing, and simulation of a one-dimensional flood model for Ba Catchment. Research indicates that participatory flood hazard mapping is a suitable approach in developing countries to effectively respond to and gain a deeper comprehension of the information presented in flood hazard maps (Irvine et al., 2020). The likelihood of flooding is more predictable with GIS and remote sensing, and it is possible to develop effective flood management strategies to reduce economic losses and prevent human fatalities (Paquette & Lowry, 2012). Flood modelling studies can be integrated into disaster management and preparedness plans and flood mitigation strategies. For example, to develop mitigation plans there is a range of flood inundation models available, from simple models using spatial layers in software such as QGIS for general analysis and decision-making to complex flood simulation modelling with more complicated engineering software such as HEC-RAS.

1.1 Aim and research question

The main aim of this research is to map out the possible extent of flooding in the Ba urban area, Fiji.

The overall research question is: What are the flood risk areas in Ba, and the potential consequences for local communities?

In addressing the research question above, the research will focus on preparing a flood hazard map to identify areas prone to flood and explore flood impacts on different land use zones at the lower Ba Catchment.

1.2 Structure of the Thesis

This thesis research consists of seven chapters. Chapter 1 is an introduction to flooding in Fiji and sets out the aims and research question. Chapter 2 is a literature review. Chapter 3 introduces the specifics of the research area. Chapter 4 describes the research methods and design undertaken to carry out flood mapping of the Ba River. Chapter 5 presents the results of the research methods. Chapter 6 presents the discussion and findings of the research. Chapter 7 concludes the research with study limitations and recommendations.

Chapter 2: Literature Review

This chapter will discuss available literature for flood hazard mapping and elaborate on different methods available to undertake flood modelling and mapping. The literature review analyses global case studies and methods to ascertain whether they can be replicated in the Pacific Island countries. The goal of the literature study is to determine methods that can be used in the Ba Catchment with the available datasets to answer the research question. The chapter outlines the flood risk assessment studies, assessment of socio-economic impacts of flooding, development of flood hazard mapping using GIS, flood impacts in the Pacific Island catchments, hydrological collection in the Pacific SIDS, using open-source data, and hydrological modelling for flood mapping

The vulnerability of low-lying areas in the Pacific Islands to the effects of global climate change is a major concern. This vulnerability may result in changes in weather patterns, more frequent and severe El Nino-Southern Oscillation events, extreme weather, and sea-level rise (McAneney, Honert, & Yeo, 2017). However, evaluating flood risk in small island developing states (SIDS) is challenging due to the scarcity of data appropriate for long-term trend analysis. This lack of data is a worldwide issue (Kundzewicz et al., 2014), and the Pacific Islands region is particularly affected because of the lack of specialized technical expertise in hydrology, meteorology, and data analysis which hinders the development and maintenance of effective flood monitoring and modelling systems (Tilly & Fakhruddin, 2020).

Flooding is one of the severe natural hazards that Pacific islanders encounter, and it poses many challenges. It has resulted in the loss of lives and property, emphasizing the significance of having effective mitigation strategies and response mechanisms in place. Apart from the devastating losses caused by flooding, most of the funding is typically

allocated toward restoring the affected communities' livelihoods. However, having accessible flood hazard maps can help mitigate the impact of floods and reduce the financial burden of flood events. This is because people will be aware of the areas most likely to be flooded beforehand, enabling prioritization of mitigation efforts. As a result, the amount of money spent on flood events should be expected to decrease (Forkuo, 2011).

2.1 Flood risk assessment studies

According to the European Flood Directive, flood risk refers to the likelihood of a flood occurring and the negative consequences it could have on human health, the environment, cultural heritage, and economic activity (Löschner et al., 2017). Kundzewicz, et al. (2014, p. 19) discuss the risk of floods and climate change in Oceania, specifically referring to instances of floods in Australia and New Zealand but not mentioning any such instances in the Pacific Islands. With scarce verified historical records of previous events, a reasonable approach is to look at the currently available datasets to gauge the impact of flooding on the environment and communities for Pacific SIDS, such as Fiji, for better flood risk planning. However, it is crucial to conduct risk assessments that consider both the probability and impact of flooding. This is necessary to quantify flood risk accurately and to compare the economic benefits of different options for managing flood risk. Risk assessments in Fiji have traditionally relied on analyzing individual flood events, such as assessing the benefit-cost of the "Navua Flood Warning Scheme based on the assessed damage from the April 2004 flood" (Holland, 2008). The benefit-cost of different flood management schemes in Fiji has been evaluated by estimating the damage caused by the January 1993 flood and projecting it to other design events. (JICA, 1998).

Flood extent mapping in Fiji has been limited to occasional historical flood extents; for example, the Secretariat of Pacific Community (SPC) has mapped the extent of the

January 2009 flood (Yeo, 2013). The latest available Light Detection and Ranging (LiDAR) imagery of the Ba Town area is from 2012 and is used to generate a high-resolution digital elevation model to understand the elevation of Ba Town. A study using GIS-based Multi-Criteria Decision Analysis (GIS-MCDA) methodology, with the highest weight on elevation, has provided another approach to modelling flood hazards in Nadi, however, a limitation identified was the inability to identify micro-topography features using the existing elevation dataset as the entire catchment was not surveyed with differential GPS (Paquette & Lowry, 2012). The suggested solution to this limitation was the use of LiDAR data to correct the missing and/or inaccurate data in the elevation layer. At present, Fiji's most sophisticated flood study and mapping tools have been developed for the Nadi floodplain. These tools utilize LiDAR technology to establish topography, a two-dimensional flood model, and data from the March 2012 flood to create flood depth, velocity, and hydraulic hazard maps (Bind et al., 2014; Yeo et al., 2017). This advancement provides a means to fill the gaps identified earlier by Pacquette & Lowry (2012) in capturing accurate topographic data for the Nadi region and paves the way for research in Ba Catchment using a similar methodology.

Studies of natural hazards in Fiji are mainly focused on flood risk and damage, particularly in Nadi and the Ba River basin (Ambroz, 2009; Yeo, Mcgree, & Devi, 2010). By constructing a flood series in the Ba River using recorded flood levels, Yeo, et al. (2007) emphasised the need to develop strategies to address flood-related problems in the Ba River basin. Their study suggested revising the flood planning level due to the inadequacy of the 5.0m above mean sea level flood frequency level at Rarawai Mill. Yeo et al. (2010) evaluated the effectiveness of existing infrastructure development and ecosystem-based adaptation on future flood damages through an assessment of 2012 flood damages. Most of these studies are based on flood risk assessment and provide recommendations to address flood problems, such as early warning systems and community preparedness for flooding. However, there is a

lack of investigation of adequate infrastructure that the government can adopt for flood risk reduction.

2.2 Assessing socioeconomic impacts of Flooding

An essential aspect of effective flood risk management is to examine and map the vulnerability and exposure of communities, taking into account future urban growth projections. By combining flood hazards with community exposure and susceptibility, flood risk can be evaluated, including the financial and life risks associated with floods (Yeo et al., 2017). Once the flood risk is identified, various interventions can be evaluated, such as flood gates, levees, flood mitigation dams, riparian vegetation, catchment afforestation, and urban planning, to develop a strategic plan with prioritized actions for managing the flood risk (Coenen et al., 2019; Yeo et al., 2017).

The term "resilience" refers to a community's ability to endure, withstand, recover from, and adapt to changes in flood risks. According to Mark & Djordjević (2006), resilient communities have enhanced capacities at every stage of the flood management cycle, including mitigation, preparedness, response, and recovery. The authors suggest that flood-resilient cities and individuals possess an understanding of the flood risk they face, are adequately prepared, and can respond more effectively in the event of a flood.

Assessing the impact of floods is a crucial aspect of managing the risks associated with them. Different stakeholders can use the estimates of the impacts for different purposes, such as spatial and land-use planning, emergency preparedness and response, disaster recovery, decision-making, risk management, and policy-making (Mark & Djordjević, 2006). One of the first steps of the impact assessment is a review of past events. Such retrospective assessments usually comprise considerations of the possible flooding scenarios to be expected in the future and factors affecting the degree of danger to local populations. These

types of studies provide one useful method for developing effective response strategies and determining how responsibility for action should be delegated to responsible authorities. Therefore, developing strategies and models for flood protection and response can help with flood mitigation (Mark & Djordjević, 2006). Geographic Information Systems (GIS) provide a means to characterise existing drainage infrastructure and to model the effects of surface flows in a high rainfall event, to understand the impact on the infrastructure supporting water flows (Mark & Djordjević, 2006).

Since flood impact assessment is a crucial aspect of flood risk management, it is essential to ensure that any damage estimates meet specific reliability and accuracy standards (Mark & Djordjević, 2006). Regarding the reliability of flood damage estimates, a major issue is the challenge of obtaining accurate historical data, which is necessary for conducting research into flood damage estimation. According to Downton & Pielke (2005), discrepancies often exist between damage estimates produced by various organizations or agencies, especially for floods that occur in small, localized areas. However, in larger and more widespread floods, inconsistencies in damage estimates tend to balance out. The study of damage estimates is usually derived from various sources, including collaborations with local authorities, insurance agents, and news reports, as well as detailed surveys that could take up to five years to finish after a flood event. From the Fijian perspective, the lack of reliable and complete hydrological records would mean that such data would have to be assessed for accuracy and validated before it could be used within a flood hazard mapping to minimize errors in different modelled scenarios (Yeo, 2013).

2.3 Flood hazard mapping using GIS

Flood hazard mapping is vital for recommending appropriate land uses in flooded areas. There have been several global case studies to measure the effectiveness of using GIS as a

tool in flood mapping. GIS-based flood hazard mapping, carried out for many decades in developed countries, is now being adopted in developing countries to assist in hazard mitigation. In Lagos, Nigeria, GIS was used to create a hydrological model of flood-prone zones in the Surulere region (Okoye & Ojeh, 2015). Researchers used ENVI 4.7 and ArcGIS 10.0 software to map flood-prone zones in Surulere. Surulere experienced flooding due to several factors, including a high concentration of precipitation, patterns of land use, human activities, and urban expansion. To obtain accurate results, researchers (Okoye & Ojeh, 2015) studied 20 years of rainfall data to analyze the flooding patterns in the region. The authors also used Ikonos satellite imagery to generate a land use map and digital elevation models (DEM) in ArcGIS, which helped to identify the areas of Surulere that were at high risk of flooding. The result concluded that most terrestrial areas were in the flood zone such as in areas like Ebute-metta, Cele, and Aguda, resulting in damaged infrastructure and loss of lives. Thus, it was crucial to adopt the appropriate techniques, knowledge, and investigations to minimize flood occurrences in the Surulere area. The case study highlights that the primary advantage of employing GIS in flood management is its capability to not only provide a flood visualization but also generate a potential for in-depth analysis of the estimated damage caused by floods. GIS allows for the integration of three-dimensional and non-spatial topographic data, including rainfall and tributary movements, river cross-sections, and river basin characteristics. This technology facilitates the identification of high-risk areas and prioritizes their mitigation efforts.

Forkuo (2011) discusses the use of GIS and remote sensing data to formulate flood vulnerability maps in the Northern Region of Ghana, where floods pose a recurrent danger. A composite flood hazard index was created using datasets such as topographical, land cover, and demographic data. Land use classes were defined through supervised classification by using Aster satellite imagery. Land use data complemented the workflow of the flood model

and DEM was created from topographic maps. The research created a map at the district level, illustrating regions that are susceptible to flood hazards. The composite flood hazard index employed variables such as rivers, population density, the number of towns in each district, cultivated crop areas, and the availability of high ground. GIS tools and applications, along with rainfall data and satellite imagery, were utilized to map the maximum flood hazard zones in the study area

The studies conducted by Forkuo (2011) and Okoye & Ojeh (2015) highlight the potential of these tools and methods in producing flood hazard maps for flood-prone areas. Developing countries such as Fiji face many challenges during and after a flood hazard, and GIS and remote sensing can be similarly utilised to compile relevant datasets, including those related to flood impacts for further analyses. A flood hazard model can help plan and mitigate disaster risk reduction after results have been verified on the ground by communities who have traditional knowledge of approximate flood extent zones.

Rincón et al., (2018) focused on the development of a flood risk mapping approach using GIS and multi-criteria analysis in the Greater Toronto Area in Canada. The study aimed to identify areas that are vulnerable to flooding and to prioritize it for flood management planning. The methodology involved the identification of various flood-related criteria, such as proximity to rivers, slope, elevation, and soil type, which were analyzed using GIS tools. The criteria were then combined using the Analytic Hierarchy Process (AHP) to develop a flood risk index that identified areas at high risk of flooding. The results of the study indicated that areas close to the rivers were at high risk of flooding, with the highest risk located in the Don River Watershed. The study also revealed that areas with low elevation, high slopes, and high soil erodibility were also vulnerable to flooding. Overall, the study provides valuable insights into the use of GIS and multi-criteria analysis for flood risk mapping and management planning in urban areas. The findings can help policymakers and

city planners to develop effective flood management strategies and to reduce the risks of flooding in the future.

Lyu et al.,(2016) conducted a study in China that evaluated the relationship between levels of urbanization and flood hazard using GIS mapping and analysis. The authors found that even moderate rainfall with an intensity of 50 mm was enough to cause flooding in the area. The study highlighted the negative effects of subway lines and drainage systems on exacerbating the flood hazard in Guangzhou. The researchers concluded that alongside improvements in the drainage system, mechanisms were required to store rainwater during such events, such as a "sponge city" approach. They also recommended the use of a combined model of GIS and Building Information Modeling to evaluate and monitor flood risk in urban areas.

Zheng et al.,(2018) utilized high-resolution terrain analysis to develop a flood inundation mapping workflow for the Colorado River using the GeoFlood software. They employed the HAND method to compute channel hydraulic parameters and synthetic stage-discharge rating curves and evaluated their results by comparing them to the 100-year floodplains obtained from the Federal Emergency Management Agency (FEMA). The study found that GeoFlood is a computationally efficient and straightforward approach for generating inundation extents and water depth grids at multiple stage levels and can support future flood mapping efforts.

In Brazil, the approach to flood hazard mapping involved a flow frequency analysis using the HAND model researched by Speckhann et al., (2018). The authors evaluated the model's accuracy as 90% compared with a flood extent map of 2011 derived from observation. The authors suggested the advantage of this approach was the possibility of

applying the tool in city management and identifying hotspots for more detailed inundation studies.

The framework developed by Abedin & Stephen, (2019) provides a comprehensive approach to mapping urban flooding, considering both spatiotemporal variability and the impact of clogging factors. The inclusion of various inputs such as watershed delineation, generation of run-off hydrographs, and mapping of inundation depths and flood extent in the framework is noteworthy. Additionally, the calibration and validation of the framework using different DEM and rainfall temporal resolutions and historical news reports and photographs, respectively, provide confidence in the accuracy and reliability of the results. The flexibility and compatibility of the framework with various software such as ArcGIS and Quantum GIS are also advantageous, enabling its wide applicability in different contexts.

2.4 Flood Impacts on Pacific Island Catchments

The small catchment size of rivers in Pacific SIDS is one reason why flooding events impact these island nations significantly. The larger island nations are from the Melanesian region and have rugged mountain peaks at higher elevations. When comparing the three largest river basins in Pacific SIDS by region and island, Papua New Guinea has the two largest river basins, followed by the Rewa River basin in Fiji (Table 1).

Table 1 Selected Pacific Island countries showing the largest river basins by basin area, with estimated river lengths (in kilometres) within each catchment (source: SPC Statistics for Development Programme). Table modified and reproduced from Gehrke et al.,(2011).

Pacific Island Countries & Territories	**Island**	**Largest river**	**Basin area (km^2)**	**River length (km)**
Papua New Guinea	New Guinea	Sepik	96000	1126
Papua New Guinea	New Guinea	Fly	76000	1050
Fiji	Viti Levu	Rewa	2918	145
Solomon Islands	Malaita	Wairaha	486	33
Solomon Islands	Guadalcanal	Lungga	394	50
Vanuatu	Espiritu Santo	Jourdain	369	53
Fiji	Vanua Levu	Dreketi	317	65
New Caledonia	Grande Terre	Le Diahot	317	65
Vanuatu	Efate	Teouma	91	28
French Polynesia	Tahiti	Papenoo	91	23
Guam	Guam	Talofofo	60	12.6
Samoa	Savai'i	Sili	51	11
Palau	Babeldaob	Ngerdorch	39	15
Samoa	Upolu	Vaisigano	33	12
American Samoa	Ta'u	Laufuti	8	3
Federated States of Micronesia	Pohnpei	Nanpil Kiewp	7.8	10
Cook Islands	Rarotonga	Avatiu	5.5	5
Tonga	Eua	Eua Creek	2.3	2

Low-lying islands are also impacted by tidal surges, which inundate coastal areas and affect the livelihood of small island nations' coastal populations. An example is Tonga, where a projected rise of 0.3m in sea level would affect 20,000 people living along the coast (Mimura & Pelesikoti, 1997). Similarly, even if coastal protection measures are implemented

in the Pacific Islands of Kiribati and Tuvalu, these are currently at the highest risk from sea level rise, threatening their livelihoods and sovereignty (Donner & Webber, 2014).

Tropical storms that bring heavy rainfall can cause severe weather conditions on Pacific islands, particularly those with high topographic elevations. This can lead to intense rainfalls, as demonstrated by a recording of 928mm of rain within 24 hours at a Fiji station in 2009, which caused flooding. Additionally, excessive soil moisture due to heavy or prolonged rainfall reduces the soil's capacity to absorb water, leading to increased surface runoff that overwhelms drainage systems and natural watercourses, resulting in flooding. Saturated soil can trigger landslides, destabilize slopes, and exacerbate flash floods, further elevating the risk and severity of flooding events, as seen in the severe floods of January and March 2012 in western Viti Levu, according to (Kuleshov et al., 2014).

Flood inundation of properties has caused hundreds of fatalities in Pacific Island countries (Yeo et al., 2017, p. 7). Although the number of fatalities from floods in Pacific Island countries may not seem high globally, it has a significant impact when considered in proportion to the total population of the country. Based on a risk-to-life model by Bind et al. (2014), a flood in the Nadi catchment area with a 1-in-100-year likelihood of happening would result in the loss of 12 to 15 lives, even if there was some prior warning time available for partial evacuation.

There is a possibility of even greater loss of life, as illustrated by the potential scenario of the Mataniko River flash flood hitting Honiara at night. In such a case, houses would be fully occupied, and the darkness would make it harder to detect and escape, resulting in several hundred lives being at risk (World Bank., 2014). This level of disaster fatalities is not uncommon in Pacific Island countries. For instance, Yeo & Blong (2010) reported that there were at least 225 deaths in Fiji in 1931 and at least 111 deaths in the

Solomon Islands in 1986 due to severe floods and landslides caused by slow-moving tropical cyclones.

2.5 History of Tropical Cyclones in Fiji

Fiji is affected by extreme environmental events, including earthquakes, tsunamis, landslides, and droughts (Buri et al., 2022), but tropical cyclones and flooding cause the most frequent and widespread destruction (Lucas, 2020). Between 1972 to 2022, 50 tropical cyclones have impacted Fiji, and the occurrence of category 3 and above has increased in the last decade (Figure 3). Between 2010 and 2022, 17 tropical cyclones have hit Fiji, and 12 have been above category 3, causing massive destruction to the island group.

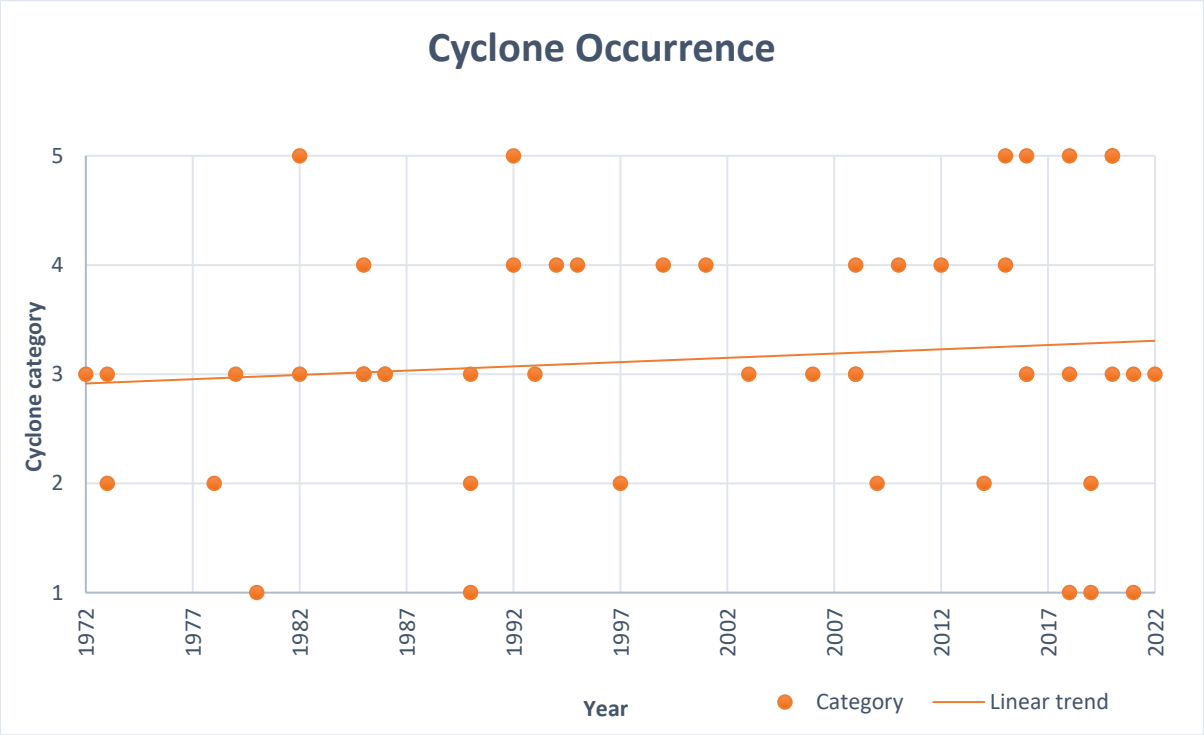

Figure 3 A record of tropical cyclone events in Fiji between 1972- 2022, shows that recent events have been category 3 and 5 cyclones. Data until 2012 is sourced from the National Disaster Management Office and updated by Zoyha Nisha from 2013-2022.

Tropical cyclone Winston in February 2016 was the strongest tropical cyclone on record for Fiji, with winds up to 280 km/hr (OCHA, 2016). It affected up to 350,000 people, injured 126, killed 44, and caused over FJD$1 billion in losses (RNZ, 2016). Between 1972

and 2022, six Category 5 cyclones struck Fiji, the latest being in 2020. After a decade gap between the occurrence of Category 5 tropical cyclones from 1982 to 1992, four events occurred in 2015, 2016, 2018, and 2020 respectively (Figure 3). This shows the increased frequency of extremely dangerous cyclones experienced in Fiji over the last decade in particular. The most common cyclone category is Category 3, a severe event with mean wind speeds ranging between 119-157 km/h (MetService, 2022).2.5 Hydrological data collection in the Pacific SIDS

After the 2009 flood in Fiji, inadequacies were discovered in the hydrological monitoring process. However, in recent years, Fiji has taken steps to improve its rainfall measurement system by increasing the number of equipment maintained by the Fiji Meteorological Services. For instance, the National Institute of Water and Atmospheric Research (NIWA) installed multiple rain gauges that were used to collect data for calibrating flood models as a component of the Integrated Water Resources Management pilot in the Nadi basin (Bind et al., 2014). Historically, flood modelling in Samoa has been challenging because of the limited hydrological data available, as noted by Lumbroso et al. (2008). However, the rainfall occurring at sub-hourly intervals, a partial hydrograph of the flow, and the flood levels observed during the Vaisigano River flood that occurred due to Tropical Cyclone Evan in December 2012, were found to be beneficial in the development of recent flood models, as per Yeo et al. (2017). During the 2014 Honiara floods in the Solomon Islands, none of the rain or water level recording devices that were set up near Honiara between 2007 and 2010 as part of the Pacific Hydrological Cycle Observing System mission was in working order due to limited resources for gauge maintenance and acts of vandalism (World Bank., 2017). The flood data available for the Honiara Flood Risk Management Plan consists of rainfall data recorded at one site every three hours, flood extents observed in two floodplains, and surveyed flood peak levels. The limited availability of data poses a challenge

in Honiara in calibrating the flood models. Similarly, developing flood models for Port Vila and Luganville was complicated due to inadequate hydrological data, often stemming from institutional problems like the absence of personnel to download data from the recorder located at the Sarakata River flood during tropical cyclone Pam (Yeo et al., 2017).

2.6 Using open source Digital Elevation Models (DEM)

When detailed country-specific data is unavailable, SIDS resort to using open-source Digital Elevation Models (DEM) that are obtained from satellite data, to develop flood models. Some examples of DEM datasets include the Shuttle Radar Topography Mission (SRTM), TanDEM- X, and the Multi-Error-Removed Improved- Terrain (MERIT). These open-source DEMs fill a gap in data requirements for hydrological analysis; however, the drawback of such datasets is low spatial resolution, which impedes the ability to model fine scale variation in topography and hydrological processes, especially in smaller catchments of Pacific SIDS (Archer et al., 2018). In comparing the above three open-source DEM datasets within the LISFLOOD hydrodynamic model, Archer, et al., (2018) concluded that TanDEM-X data is most suitable for flood modelling in the Ba River catchment, Fiji. Since fine-detailed LiDAR-based DEM data for Ba Catchment is available for only a small portion of the area, flood modelling is still highly dependent on spaceborne elevation datasets. An important consideration, however, is that the TanDEM-X dataset involves additional processing, including the removal of vegetation cover, to make it usable.

Similarly, Hawker et al.,(2018) conducted a study on simulating a digital elevation model derived from SRTM and MERIT to understand how vertical errors varied spatially. MERIT DEM is derived from SRTM; however, it is error-reduced, and the data remains at ~ 90m resolution. The study used the simulated DEMs to generate statistically plausible

topographies which allowed different topographies to be input into the simulations. It resulted in the flood model utilizing uncertain topographies to predict flood extent. This research showed that using an ensemble of simulated MERIT DEMs, the results were close to benchmark flood models as the spatial error had been disaggregated by different land cover classes generated from the topography. Hawker et al.,(2018) conducted a test for Ba Catchment and were the first to utilize simulated DEMs in flood models at a small-scale catchment. As demonstrated by these studies, open-source DEM data can be used to generate flood models for smaller catchments such as those of Pacific SIDS. However, it must be utilized after errors have been corrected to create results close to benchmark flood models which use data such as LiDAR (Hawker et al., 2018).

2.7. Hydrological modelling for flood mapping

A hydrological model is commonly used for flood mapping. It can simulate the flow of water through a watershed to predict the extent and depth of flooding in different areas. By combining a high-resolution digital terrain model and other data, such as buildings, infrastructure, and population, flood maps can be created that show areas at risk of flooding and to what extent. Many different types of hydrological models can be used for flood mapping, ranging from simple empirical models to more complex models that simulate detailed processes of the water cycle.

Sene (2008) discusses that hydrodynamic models of an advanced nature incorporate extra factors into their calculations. These variables may include backwater effects caused by tidal and upstream influences, the overflow of water from a channel, natural floodplains, water lodging in embanked river channels, the impact of artificial structures such as bridges, dams, and levees, and the inflow of water from tributaries. Creating hydrodynamic models necessitates specific prerequisites for data collection. These requirements generally comprise

setting up a network of river gauges to keep track of water inflow and outflow at various points in the basin, creating comprehensive river cross-sections to compute diverse parameters for channel flow, obtaining a highly accurate digital terrain model of the entire vicinity to model the geometry of channels and floodplains, and possessing adequate knowledge of the area to determine variables such as roughness coefficients that impact flow. The more advanced hydrodynamic models are significantly more precise and prove to be particularly beneficial for the operational management of flood defence structures and real-time monitoring of flood situations, as noted by Bates and De Roo (2000). To estimate flows and river levels, hydrodynamic models rely on the use of dimensional approximations of the mass and momentum equations, as explained by Sene (2008). Wright et al. (2008) describe the existence of hydrodynamic models in different dimensions, such as one-dimensional, two-dimensional, and three-dimensional models. Additionally, some hybrid models merge one-dimensional and two-dimensional approaches.

Hydrological data has been included in the assessment of flood risks in some catchments for Fiji, Samoa, Solomon Islands, and Vanuatu. However, results are compromised due to the poor quality of hydrological data available for hydrodynamic modelling (Yeo et al., 2017, p. 4). Despite the challenges, notable progress has been made in flood mapping and modelling for certain urban floodplains in the region in recent times. To improve hydrological data collection, storage, and reliability, several gauges were installed in the Nadi basin to record data for calibrating flood models (Bind et al., 2014). A study by the Japan International Cooperation Agency in 1998 has provided data on design, discharge volumes, hydraulics, and options for interventions which is a starting point and reference material to conduct new flood modelling in Ba and Rakiraki Catchments in Fiji (Coenen et al., 2019)

Chapter 3: Description of the study area, Ba River Catchment

3.1 Summary of study Site

Ba is a common name in Fiji. It is a name of a province, district, town, and river. The Ba Province is the most populated in Fiji and contains eight districts, one of which is the Ba District. Within Ba District is Ba Township, less than 15 km from the sea. The town is divided into 5 wards: Varoka (Ba Town Central), Varadoli, Rarawai, Yalalevu, and Namosau; areas outside these ward boundaries are mainly rural. The Ba River is the primary river within the Ba Catchment, flowing towards the northwest and originating from the mountainous central regions of Viti Levu. It discharges into the South Pacific 15 km downstream of Ba Town (Figure 4).

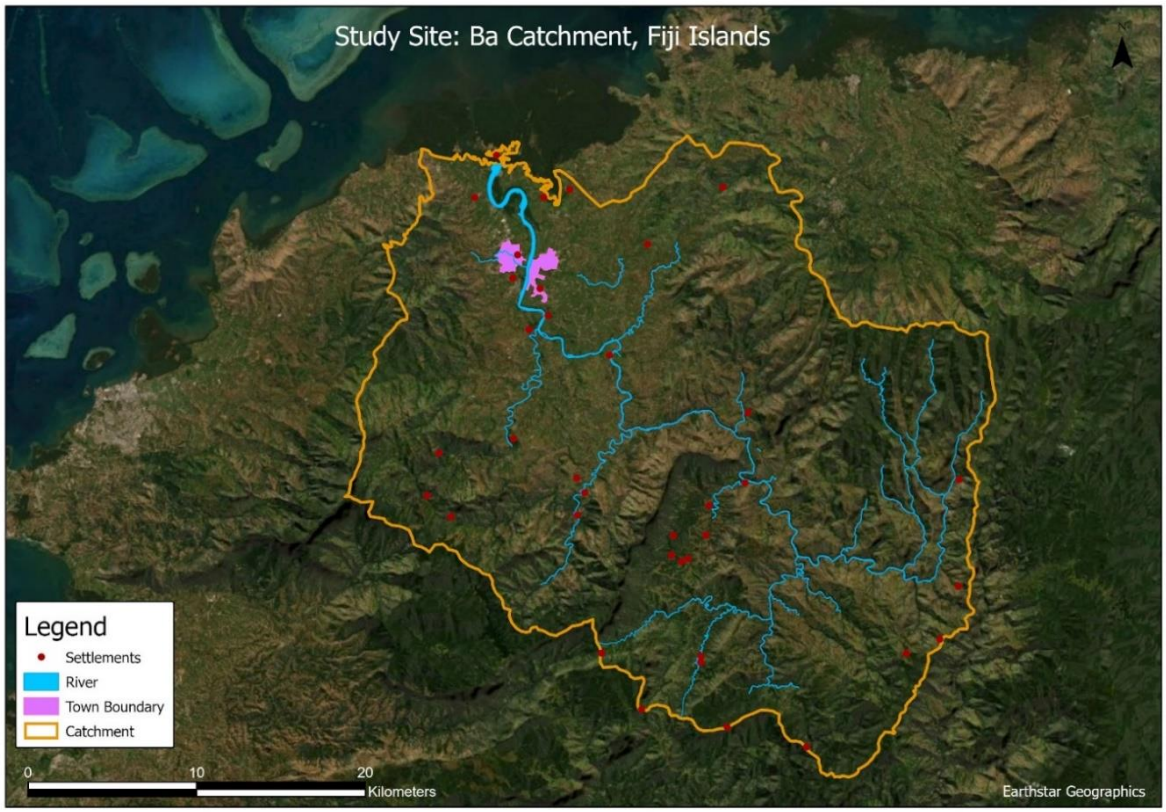

Figure 4 The Ba River watershed boundary and the major river channels that contribute to the Ba River (data source: Ministry of Lands and Mineral Resources).

Various tributaries contribute to the Ba River, and during heavy rainfall periods, it results in flash flooding in the lower reaches of the river due to the high water flow rates caused by the steep topography in the upper Ba Catchment area. The length of the Ba River is approximately 84 km, beginning at an elevation of 1,060m, and drains an area of approximately 948 km^2 (Figure 5). The Ba Township is situated on the banks of the lower Ba River zone and is severely impacted during every flood event as one of the tributaries, Elevuka Creek, runs through the Town Centre (Coenen et al., 2019).

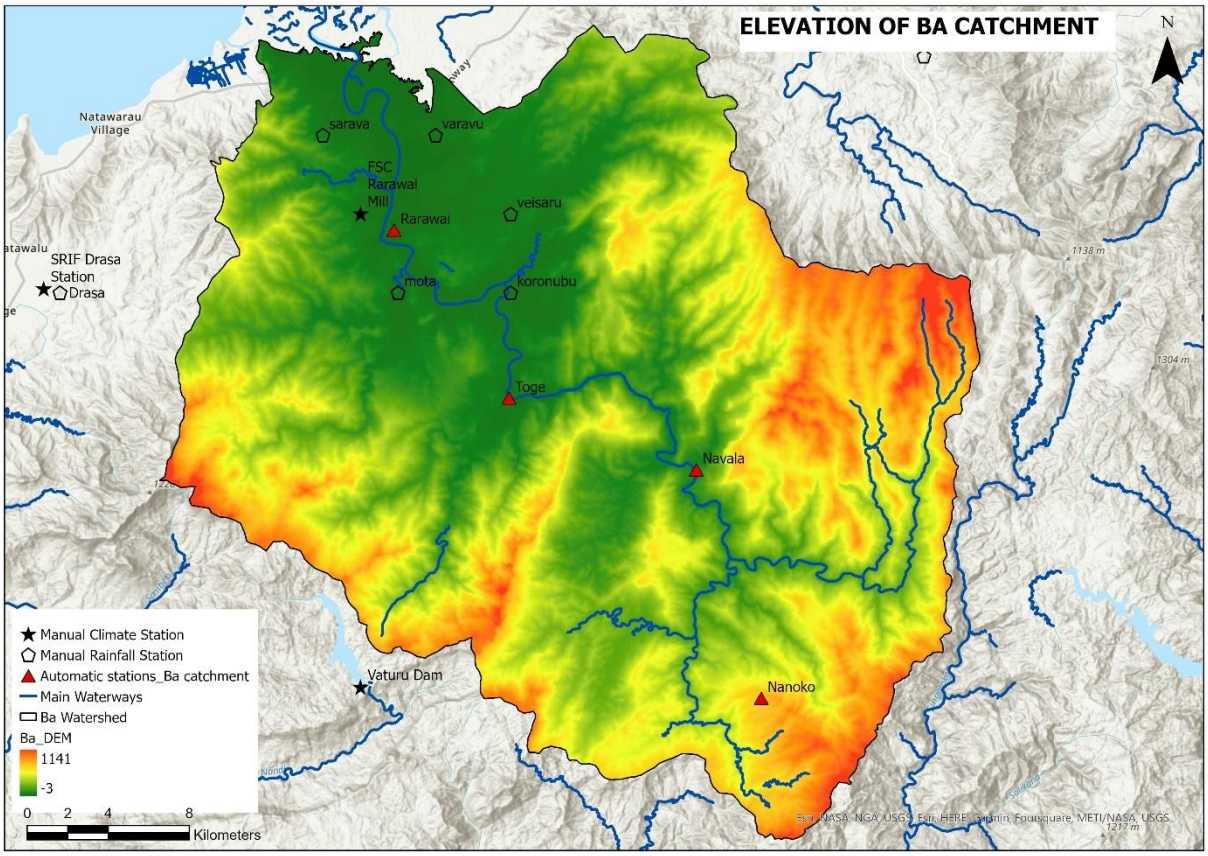

Figure 5 Ba Catchment elevation shows the highest spot at 1141 meters. The hydro-meteorological observation stations are spread across the catchment, with more manual stations based at the lower catchment along the main Ba River.

An elevation profile is obtained by digitizing the Ba River path on Google Earth Pro. The elevation begins at the river head and ends at the river mouth. The highest point is approximately 851 meters above mean sea level, and the total length of the river is 83.4

kilometres in this profile (Figure 6). The longitudinal profile gives a picture of the steepness of the Ba River.

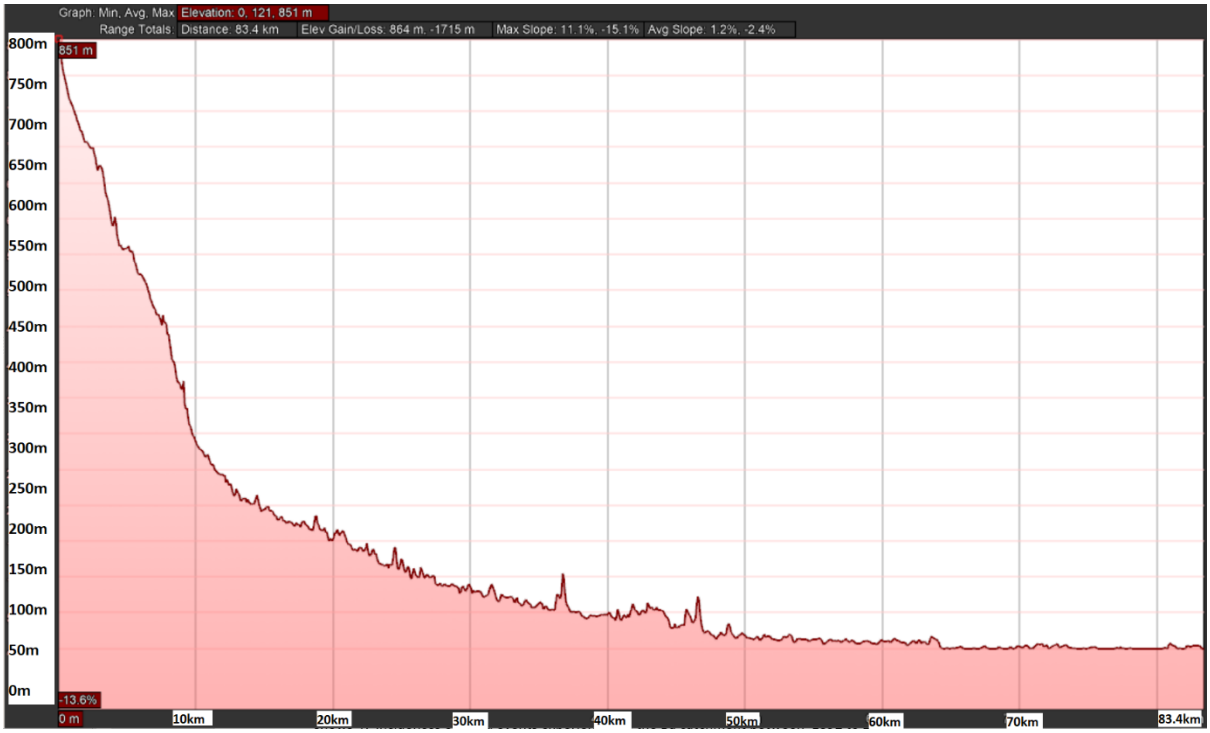

Figure 6 Ba River elevation profile created using Google Earth Pro software using the Google Earth Basemap.

The riverbeds within the Ba Catchment exhibit a distinct feature, with a gentle gradient (slope 2 to 8 degrees) from the mouth to the middle reach, and a sudden steepness in the upper reach (greater than 9 degrees). A flood report by JICA (1998) undertook a longitudinal profile of the Ba River. The Ba River has a lower reach of between 0- 40 kilometres from the river mouth, a middle reach between 40- 70 kilometres, and an upper reach of 70-83 kilometres. Metherall, Beavis, Holland, & Vinaka (2021) found that the elevation at the foothills of Ba decreases to 15 meters from a mean of 40 meters. Further downstream, near Ba Town, the elevation decreases from 10 meters to sea level. The Ba River gradient identified by the JICA report is 1/1,300 at the lower, 1/200 at the middle, and

1/20 at the upper reach (JICA, 1998). The gradient information reveals the steepness of elevation at the upper reach of the Ba River (Figure 7).

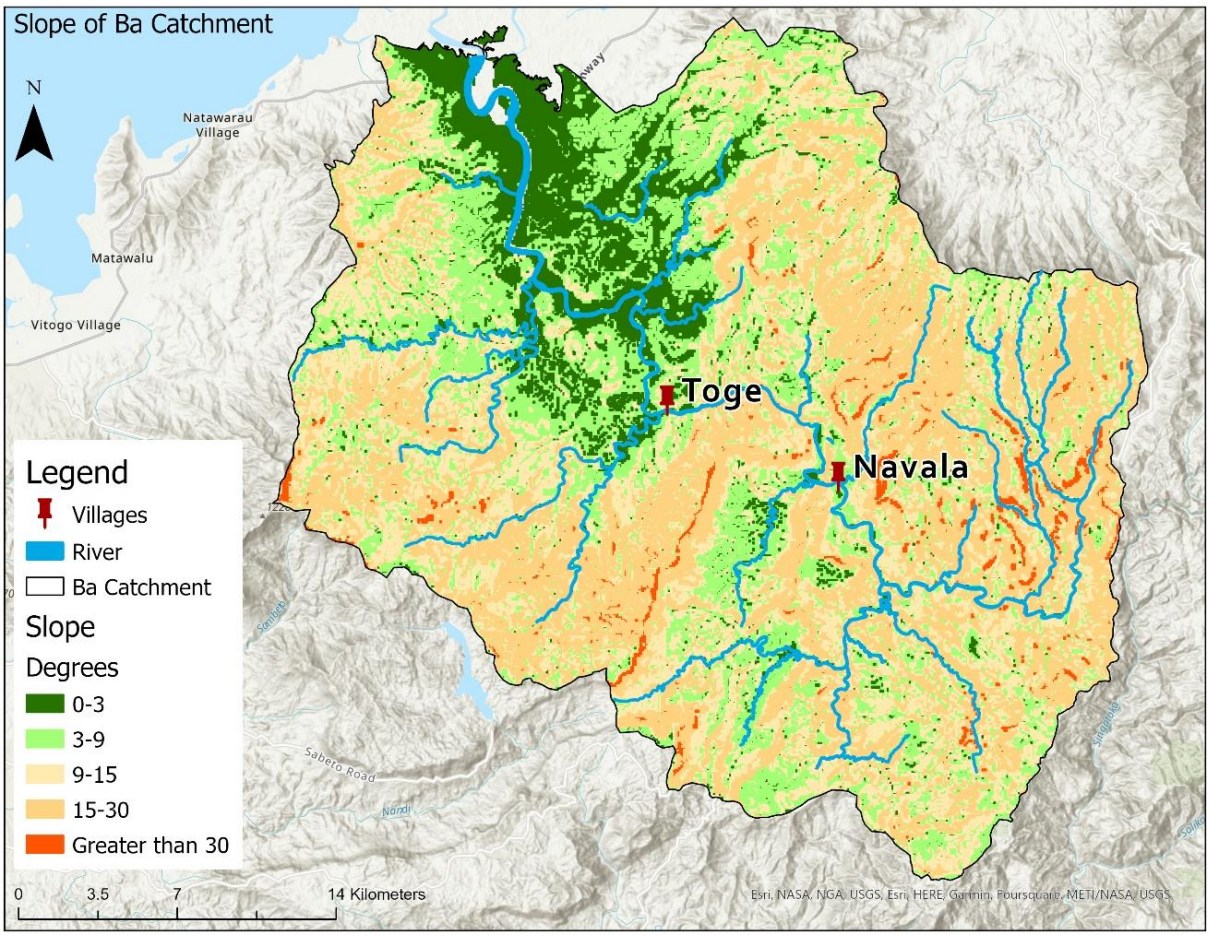

Figure 7 Slope gradient showing the change in steepness from the middle reach towards the upper reach of catchment area. Map by Zoyha Nisha.

3.2 Summary of Land use Conditions

Forest

Yeo, (2000) summarized natural native forest cover as approximately 30.69%, ranging from scattered to medium-dense forest (Figure 8). There are pine plantations situated on the northwest side of the catchment which would be harvested when ready. According to a study by Stephens, Lowry, & Ram (2018), pine plantations in Eastern Ba Catchment are on their second planting cycle and have a shallow rooting system. This resulted in weak soil stability thus leading to soil loss and debris flow during the 2012 flood. A grassland with small,

scattered wood expands in the middle reach of the catchment while a large mangrove forest is found in the coastal area of the delta.

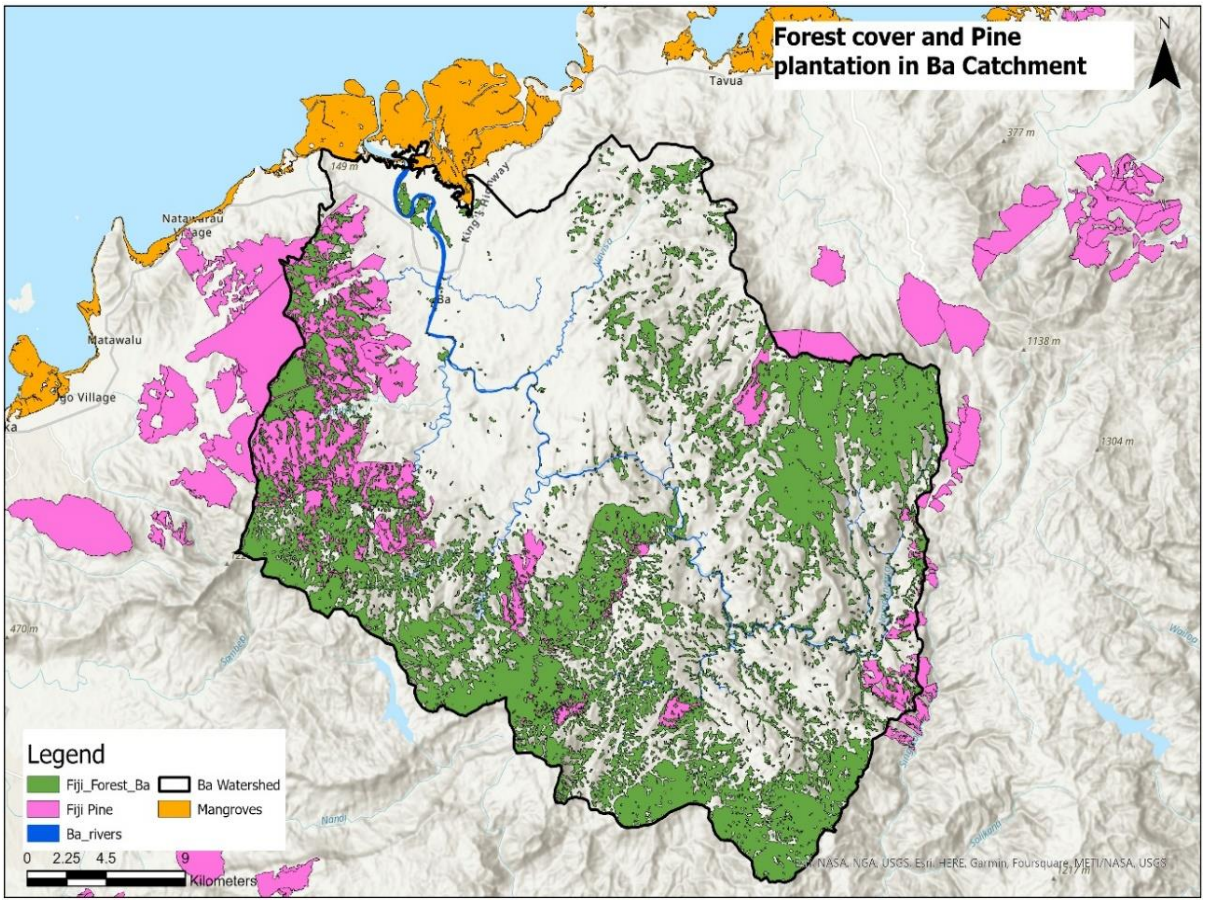

Figure 8 Forest cover of Ba catchment showing locations of mangrove forest and pine plantations. Map by Zoyha Nisha.

Soil erosion and agriculture

Soil erosion in most watersheds is severe except in plains and parts of forested areas (Stephens, Lowry, & Ram, 2018). Deforestation for farming, urban development, road building, and logging in surface water catchments has resulted in erosion, and degrading water quality (Kumar, 2010). Additionally, the steep topography of the islands has led to floods, landslides, loss of vegetation, and significant soil erosion. (Stephens, Lowry, & Ram, 2018). It is anticipated that soil erosion is high in the grassland, grazing, and sugarcane areas and leads to high sedimentation at the river mouth (Metherall et al., 2021). An estimated 4.6mm/year of soil is lost in the Ba watershed (Coenen et al., 2019).

The river mouth is also the site for black sand extraction, posing severe threats to the mangrove and other habitats at the site (Richards et al., 2021). The Fiji Sugar Corporation's (FSC) Rarawai Mill sugar mill is situated along the Ba Riverbank and is 1 km away from central Ba Town (McAneney, Honert, & Yeo, 2017). According to Naidu et al. (2017), sugarcane is among the most significant crops cultivated in Fiji. It has served as a crucial primary agricultural industry and a significant source of exports for Fiji's economy throughout the majority of the 19th and 20th centuries. Cropland is one of the dominant land cover classes in the Ba River basin (Figure 9).

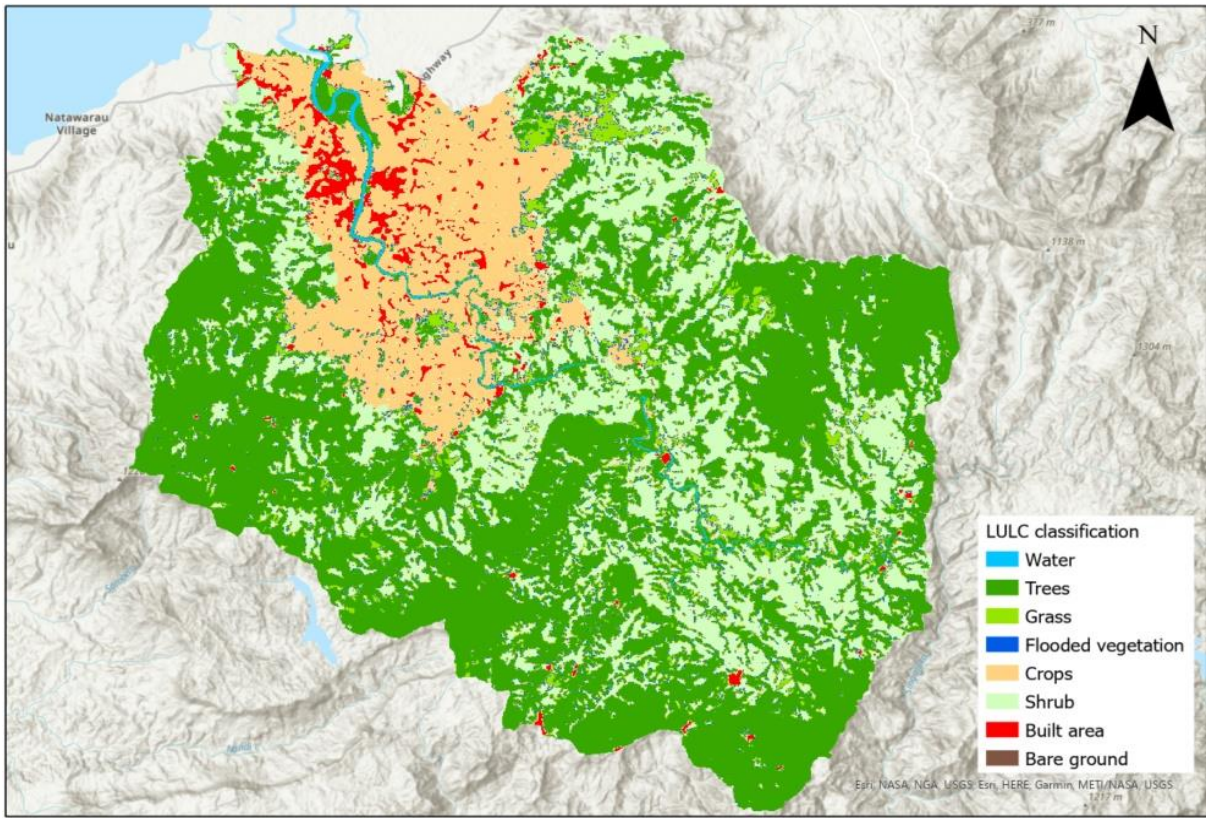

Figure 9 Land cover map of the Ba catchement derived from the Global Land Cover Dataset produced by ESRI and Impact Observatory institute using the existing sentinel 2 satellite repository (ESRI, 2021). It is modified in ArcGIS Pro software to suit the Ba Catchment zone. Flooded vegetation refers to the mangroves in inter-tidal zone.

Urban use

The commercial area of Ba Town has developed further, including new residential developments extending South and West of town in Koronubu, Yalalevu, and Namousau.

Rarawai mill and its related facilities of FSC are in the town area. There are town and rural planning schemes in and around the major cities and towns, designating land use based on the town and country planning guidelines, as per the Town Planning Act. The guideline sets the minimum flood level of habitable rooms in a flood-prone area ("Town Planning Act- Chapter 139- General Provisions," 1999). In Ba, the minimum floor level is set at 5 meters above mean sea level, nearly the existing ground level. As outlined in Yeo & Blong, (2010), flood levels show inundated depths above 5 meters. Therefore, new maps of flood-prone areas should be prepared, and floor level or usage regulations should be determined based on the information on flood maps.

Population

The population of Ba district in the 2017 census was 39,372, with an urban resident population of 15,846 (FBoS, 2018). Table 2 combines Ba's population information from published statistical records showing an increase in the last decade. The population has increased greatly in both urban and rural areas indicating a change in land use and an increase in demands for developments to cater to the needs of a growing population.

Table 2 Population and housing census data, modified from census 2017 ("2017 Population and Housing Census," 2018).

Ba Census	**1976**	**1986**	**1996**	**2007**	**2017**
Town	3849	6515	6314	6826	15846
Peri-urban	4460	3745	8402	11710	23526
Total Population	**8309**	**10260**	**14716**	**18526**	**39372**

Ba flood history

Yeo et al.,(2007) gave a comprehensive 122-year historical record of flooding in Ba up to 2012. This research supplements that publication by updating flood event information in Ba from 2012 until February 2022. Flood event records for Ba from 1892 to 2022 highlight that, of the total 47 events that have occurred during this period, most have occurred during the months from December through April, coinciding with the Fijian cyclone season; one event occurred in October, caused by the Category 3 tropical cyclone Bebe in 1972 (Figure 10).

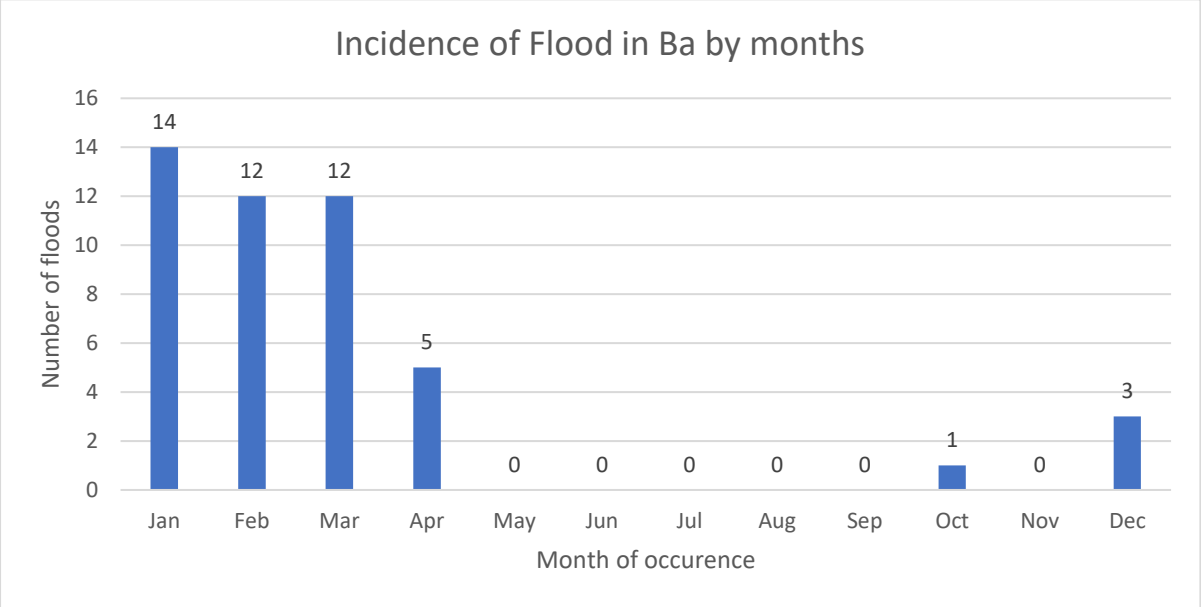

Figure 10 incidence of floods occurring by month between the years 1892 to 2022. The events occurred mostly between January and March, with some events also occurring in December, April, and October. Updated McAneney et al.,(2017) based on flood records on the EM-DAT database (2022).

Rain data of Ba Catchment

There are seven automatic and telemetered rainfall stations in and near Ba Catchment, with 6 additional manual stations based around the lower catchment (Table 3, Figure 11).

Table 3 Manual station ID and name for which 40 years of rainfall data is available.

Manual stations in the catchment					
V77562	**V77563**	**V77571**	**V77572**	**V77574**	**V77575**
Mota	Sarava	Veisaru	Koronubu	Varavu	Rarawai

There is one operating water level station at Toge Village. The addition of automatic stations has improved data collection and credibility for further analysis. Rainfall datasets were acquired from Fiji Meteorological Services for Ba Catchment from 1980 to 2020. The 10-minute rainfall data was requested for all stations in the catchment; these data were available for different date ranges because the automatic weather station was established in stages across the catchment; hence, different temporal datasets were available from each station (Table 4).

Automatic stations in the catchment

Analysis of rainfall data shows that Navala station did not have records of the April 2018 flood event in Ba whereas Toge station recorded 8mm of rainfall on the day of the major flood event (see appendix).

Table 4 Temporal data range of four automatic stations along Ba River in the catchment

Station	**Month/year**	**To date**
Toge	September 2015	2022
Navala	November 2018	2022
Rarawai	October 2010	2022
Nanoko	July 2017	2022

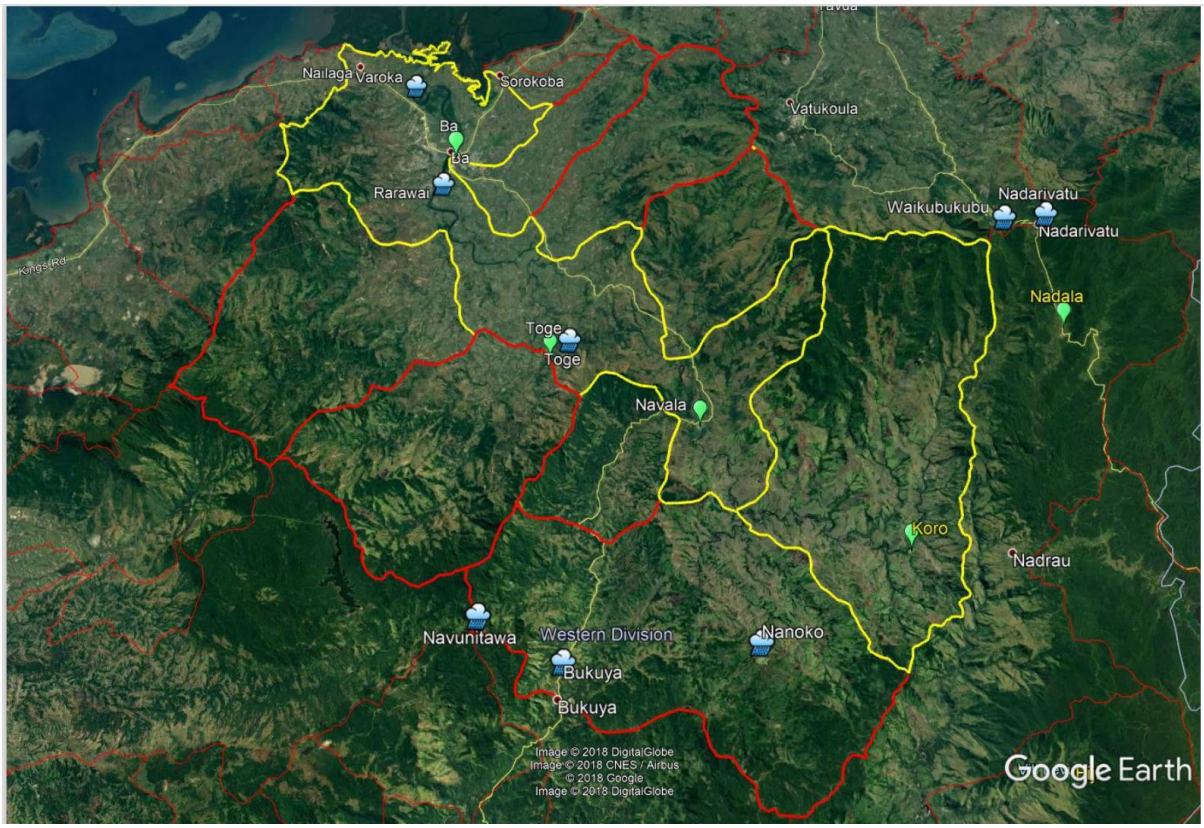

Figure 11 Location of telemetered stations and automatic weather stations in Ba Catchment. The stations are Varoka, Nailaga, Sorokoba, Rarawai, Navunitawa, Bukuya, Nanoko, Koro, Navala, Toge and Waikubukubu.

The rainfall data is analysed to see the water level on the rainfall leading to flooding in April 2018, as all stations had data for 2018 hence a reason to select the year 2018 for rainfall data analysis. There was an antecedent rainfall period due to tropical cyclone Josie impacting Fiji, resulting in significant flooding (Moishin et al., 2021). The most intense rainfall occurred over 2 hours on 1st April 2018, between 7 am and 9 am. The stations had the following readings: Toge- 117mm/hr, Bukuya- 90mm/hr, Navunitawa- 75mm/hr, Nanoko- 54mm/hr, and Waikubukubu- 56mm/hr (Figure 12).

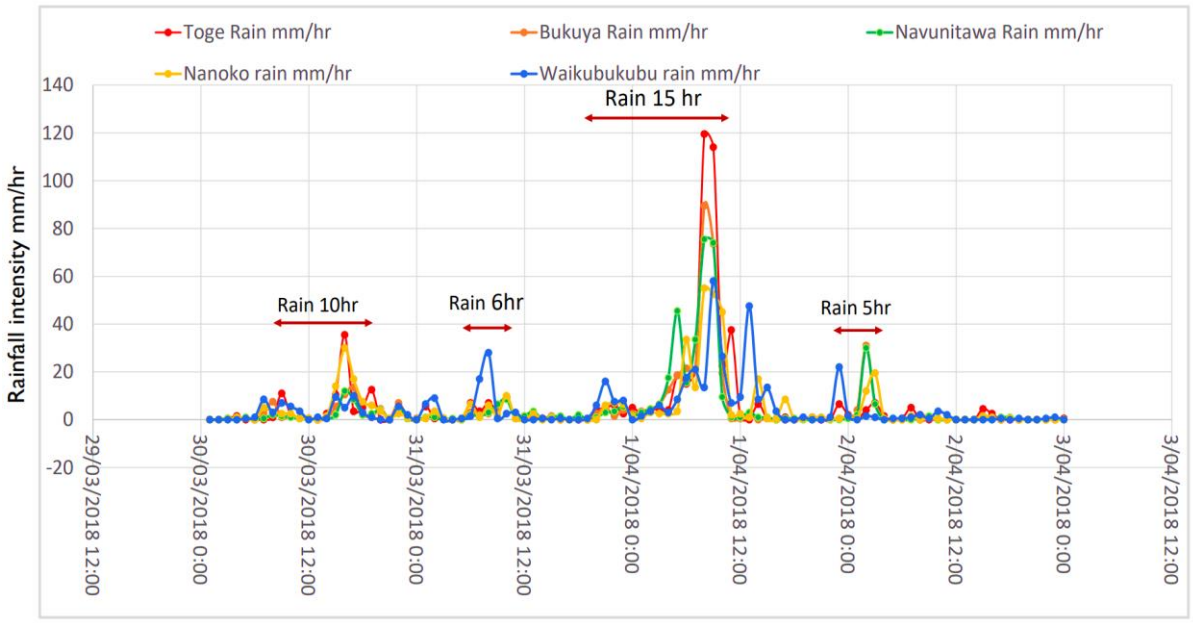

Figure 12 Summarised rainfall distribution in Ba Catchment 30 March – 3 April 2018. The highest rainfall occurred on 1st April.

Chapter 4: Methodology

The research is carried out using three different methods to see which of them is suitable for flood mapping in Ba, Fiji based on the available datasets. The first method is Height at Nearest Drainage (HAND) in QGIS software. This methodology involves the use of DEM generated from LiDAR data. However, this high-resolution DEM is limited to the Ba urban area as the coverage for LiDAR is not of the entire Ba Catchment. LiDAR provides high-resolution imagery to verify outputs from the analysis using ground truth data from the National Disaster Management Office. The second method was using Synthetic Aperture Radar (SAR) imageries in Sentinel Application Platform (SNAP) software and examining output on Google Earth Pro and Google Earth Engine. The last method was creating a simple one-dimensional flood simulation Hydrologic Engineering Centre's River Analysis System (HEC-RAS) software. All the results from each method are compared for its output to determine whether it is suitable for Ba Catchment with the available datasets.

4.1 Multi-Criteria Decision Making (MCDA) using the HAND Method

Flood events can have several immediate effects such as loss of life, displacement of a large number of people, and damaging or destroying properties and infrastructure. Over the long term, floods can cause disease outbreaks and crop destruction, leading to food insecurity. The displaced residents and the local authorities are left to rebuild after every catastrophic flood event. Schools and health centres are utilized as evacuation centres in Fiji. Therefore, the education and health system are disrupted during these emergencies (Yeo et al., 2017, p. 8).

Flood hazard maps assist in emergency response, research, and planning and are a foundation to manage and understand flood risk (Yeo et al., 2017, p. 18). However, most of the methods to derive flood hazard maps require complicated modelling techniques that are time and resource-intensive. A simpler alternative can be the Height Above Nearest Drainage

(HAND) model, which is used to understand flooding susceptibility from the hydrologic analysis.

Diagram of steps undertaken in this method:

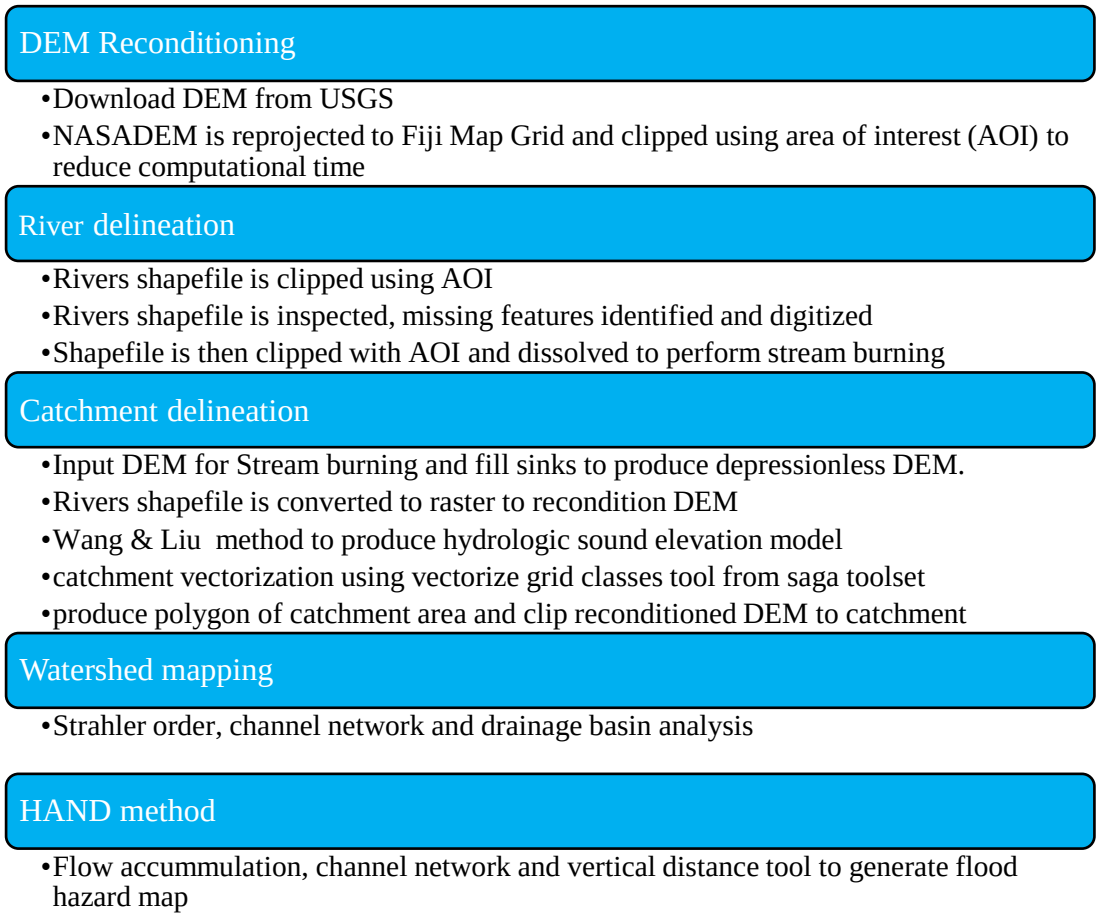

Figure 13 Diagram of key steps for flood mapping using the HAND method

The HAND model has been proven to have a strong correlation with the depth of the water table, offering a precise spatial representation of soil-water environments. By utilizing the relative vertical flow path distances to the nearest drainages, normalized draining potentials can be categorized, resulting in various classes of soil-water environments. Hydrological modelling and flood susceptibility assessment were undertaken using QGIS Desktop 3.16 with GRASS 7.8.4 software, SNAP software, and Hec-RAS software to analyze areas prone to flooding in Ba Catchment. Geospatial tools are utilized to carry out fundamental terrain analysis to delineate different features of the Ba watershed in Fiji. These

pre-processed inputs are used to calculate flood susceptibility using the Height Above Nearest Drainage (HAND) method.

Table 5 data used in the HAND model

Data	**Source**
Digital elevation model (DEM)	NASADEM (JPL, 2013)
River & creeks	Ministry of Lands and Mineral Resources- Fiji
Roads	Open street map
Building outlines	Open street map
Village and settlements	Ministry of Lands and Mineral Resources- Fiji
Flood records- Ground truth data	National Disaster Management Office

NASADEM is an open-source DEM dataset downloaded for Viti Levu, Fiji Islands. The river dataset is used as an input to verify river data generated from the DEM and to carry out other processes. NASADEM builds on the success of the Shuttle Radar Topography Mission (SRTM) by enhancing the accuracy of the digital elevation model (DEM) height and extending data coverage while offering extra SRTM radar-related data products. To accomplish this, the original SRTM radar signal and telemetry data are reprocessed utilizing updated algorithms and auxiliary data that were unavailable during the initial SRTM processing.

DEM Reconditioning, River and Catchment Delineation

In a new QGIS project, the first step taken is to set the default projection to Fiji 1986 Map Grid (FMG) so that all analysis is carried out in the projected coordinate system of Fiji. This step ensures all datasets added to the project will process outputs in FMG.

DEM Reconditioning

NASADEM is downloaded from the United States Geological Survey (USGS) website, and the selected filename is s18e177.hgt. This file extension (.hgt) represents DEM file data (Figure 14).

Name	Type	Size
s18e177.hgt	HGT File	25,327 KB
s18e177.num	NUM File	12,664 KB
s18e177.swb	SWB File	12,664 KB

Figure 14 File downloaded from Earth Data platform for DEM data of Viti Levu

This data has a resolution of 30 meters and is in horizontal datum WGS84. The DEM is reprojected into the Fiji map grid (FMG) and resampled using the bilinear method. The output resolution for the DEM is 30 meters. Lastly, the DEM is clipped with an area of interest (AOI) polygon boundary. The AOI is a polygon shapefile with a digitized rectangle covering the study area (Figure 15).

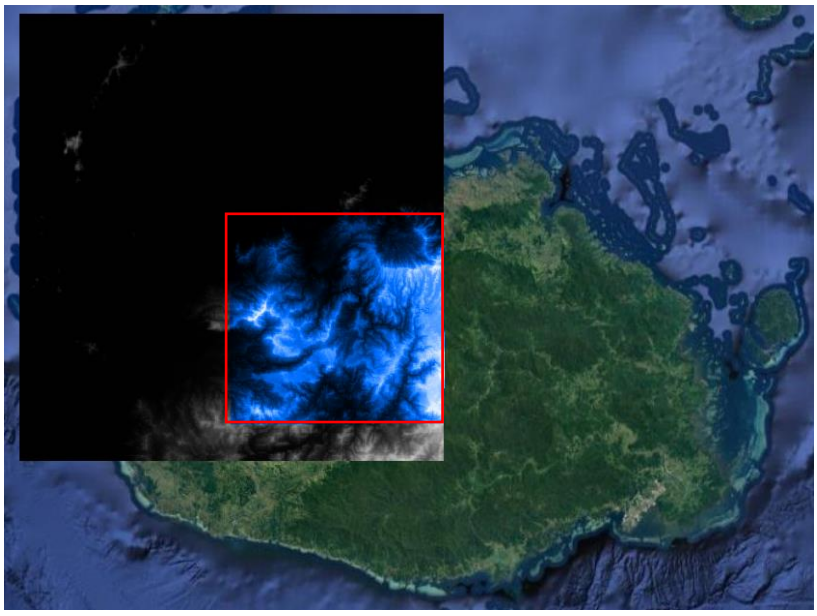

Figure 15 The original DEM raster is clipped to a smaller AOI (red square).

This clipped area also has data that fall outside the Ba Catchment area but significantly narrows the DEM to a localized area, improving the processing timeframe.

Editing rivers

River's shapefile is requested from the Fiji Ministry of Lands and Mineral Resources. The dataset provided was for the whole of Fiji (Figure 16a); therefore, an area of interest was used to clip rivers in the Ba Catchment on Viti Levu. The clipped river shapefile is inspected (Figure 16b), missing rivers and major creeks are digitized against the ESRI satellite base map (Figure 16c), and the shapefile is updated. The river's shapefile is dissolved into one feature to perform stream burning (Figure 16d).

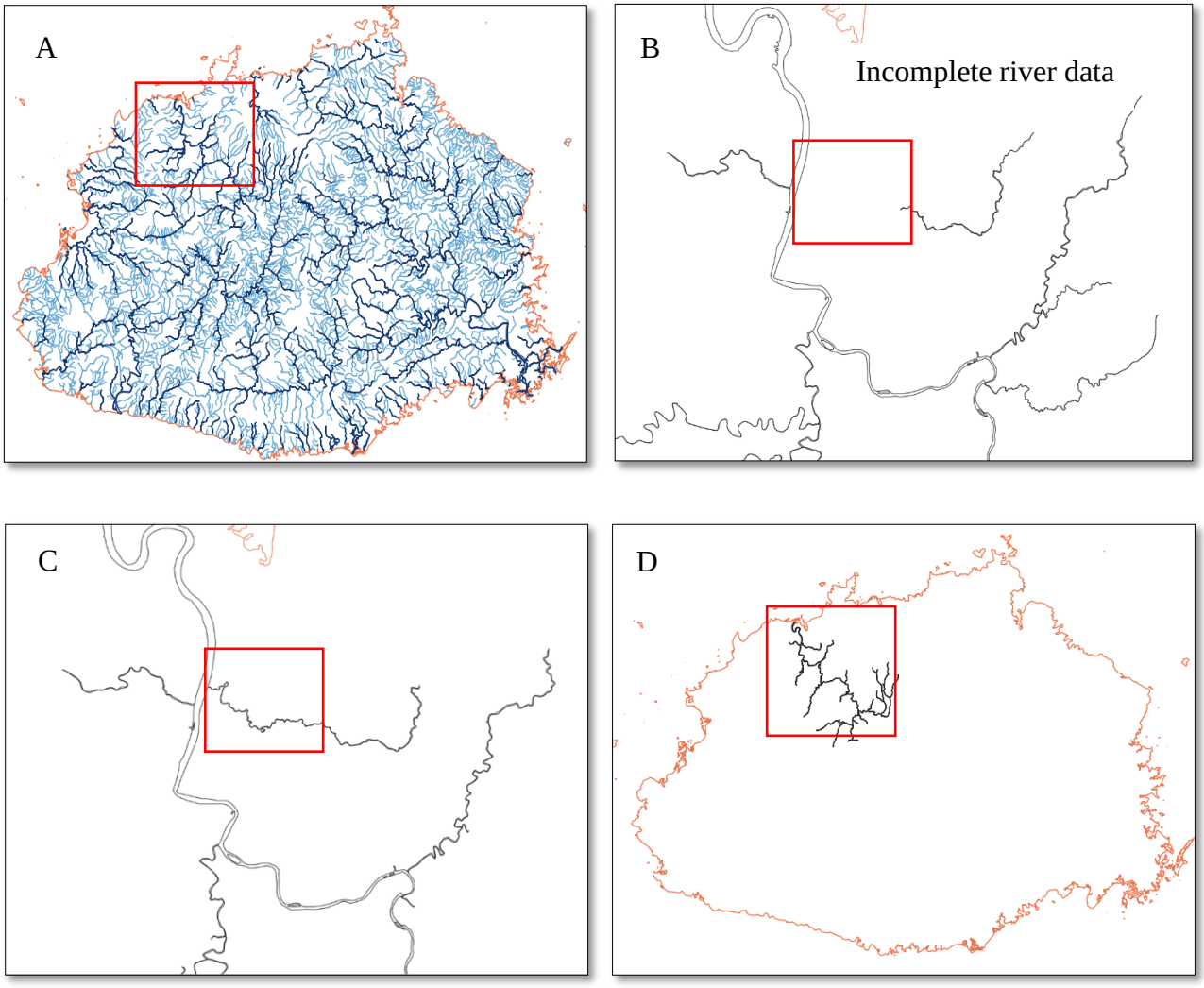

Figure 16 a-d preparing river data for further analysis.

Stream Burning and fill sinks

Stream burning ensures water flow is forced to the cells corresponding to the stream's true location. The 'Burns stream network into DEM (SAGA algorithm)' toolbox is available in QGIS to perform stream burning. The tool requires DEM and river data with raster format as input; therefore, the river's shapefile is converted into a raster format. This step produces a reconditioned DEM with sharper rivers. The "Wang and Liu" algorithm approach allows the production of hydrologic sound elevation models, which include filling depressions and maintaining a downward slope along the flow channel. For this step, a depression-free DEM, a flow path grid, and a grid with watershed basins are created by maintaining a minimum slope gradient between cells.

Delineate Catchment Using Upslope Area Algorithm

The upslope area tool specifies target cells for which the upslope contributing area is identified. SAGA tool upslope area is used to delineate catchment by selecting an area by the Ba River mouth where it meets the sea to identify the area from which water flows out the river mouth. Once the tool finishes processing, the result generates a raster with two values, 0 and 100, where 100 refers to the catchment area for the river mouth defined (Figure 17).

Figure 17 results showing the catchment area leading to flow out through the river mouth.

Vectorize the Catchment

The vectorizing grid classes tool from the SAGA toolset is used to vectorize pixels with values 100. The output gives a catchment area polygon, which can become the updated AOI boundary for further processes. This further reduces the working area of all remaining steps as now there is a refined catchment area from the previous AOI.

Clip the Reconditioned DEM to the Catchment

The DEM generated earlier in the ‘fill sinks’ step is now clipped using the vectorized catchment. The result is a hydrologically reconditioned DEM clipped to the extent of Ba Catchment (Figure 18).

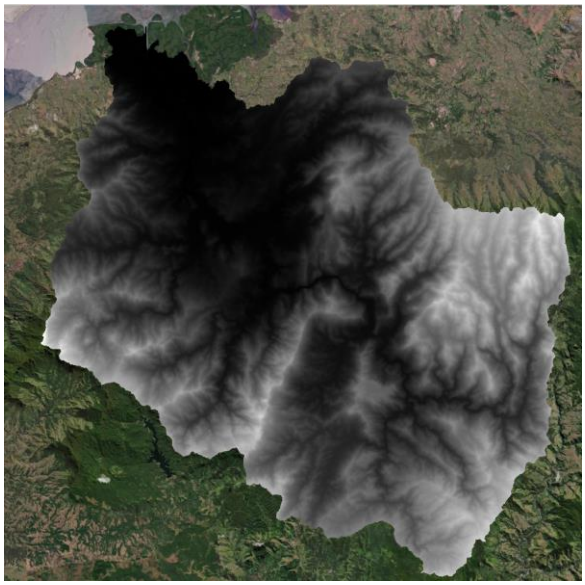

Figure 18 Result of filled watershed DEM of Ba Catchment

Watershed Mapping with Hydrologic Processing

Strahler Order

In the fields of geomorphology and hydrology, the stream order is a numerical value that represents the degree of branching in a river system (Strahler, 1952). Strahler's "top-down"

approach designates the first-order rivers as the furthest tributaries. When two streams of equal order join, the resulting stream receives a value that is one number higher. However, when two rivers of different stream orders converge, the resulting stream is assigned the higher of the two numbers.

The Strahler ordering method starts with the smallest tributaries from the source and gives it order one (Pradhan & Ghose, 2012). When two of order one join, it becomes order two. And when two of order two join, it becomes order three. Simply, when two of the same order joins, there is an increase in order number. However, when a smaller order joins a higher order, there is no increase. For example, when order one joins order three, it remains order three. In this way, the orders increase towards the outlet. The higher the order, the bigger the river. The Strahler order tool is under Saga tools in QGIS. The 'filled DEM' from the earlier step is input in this tool to produce the streams in the DEM (Figure 19).

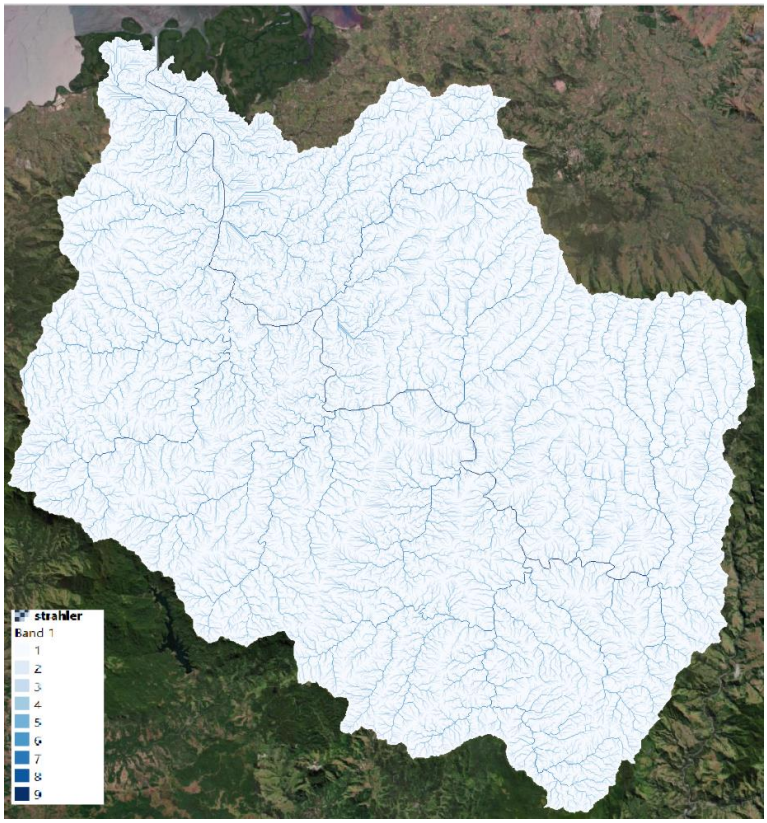

Figure 19 Strahler order output order 1 to 9

The symbology is refined to show the 5 larger orders and below is the output (Figure 20).

Figure 20 Strahler order showing only the largest four orders (5-9) to show the main tributaries

Channel Network and Drainage Basin Analysis

Channels and junctions are generated using flow direction, filled DEM of Ba watershed as elevation input, and the Strahler threshold of 5 main tributaries from Strahler order. The junctions show the intersection of streams and tributaries (Figure 21). This complements the channel's output, indicating each channel's endpoint.

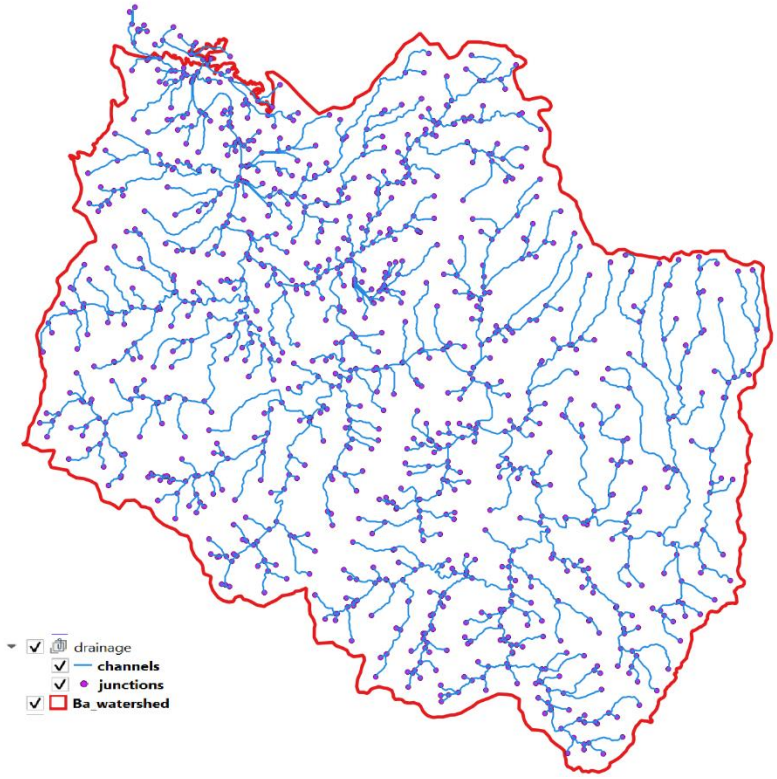

Figure 21 Junctions produced from 'filled watershed DEM' output to show flow direction, channels, and junction

Flood Susceptibility Mapping- Height Above Nearest Drainage (HAND) Method

The HAND method is a method of creating flood maps by using elevation data, streamflow inputs, and discharge-height relationships (Nobre et al., 2011). It works by calculating the vertical distance between a location and its nearest stream, which is shown on a Height Above Nearest Drainage (HAND) map. This map displays the local relative heights found along the drainage network, providing an idea of the topology of the relative local draining potentials. The HAND technique uses this information to create a distributed predictor of flood potential, which is directly related to the river stage height. Overall, the HAND approach is an uncomplicated and effective method for predicting the risk of flooding in an area.

Calculate Flow Accumulation

Flow accumulation analysis is performed using the "Catchment Area" tool in SAGA. This tool's only input is the reconditioned DEM, and the output is the flow accumulation raster. Every pixel in the flow accumulation raster generates a flow accumulation of 30m X 30m = 900 square meters and shows maximum flow accumulation at the river mouth (Figure 22).

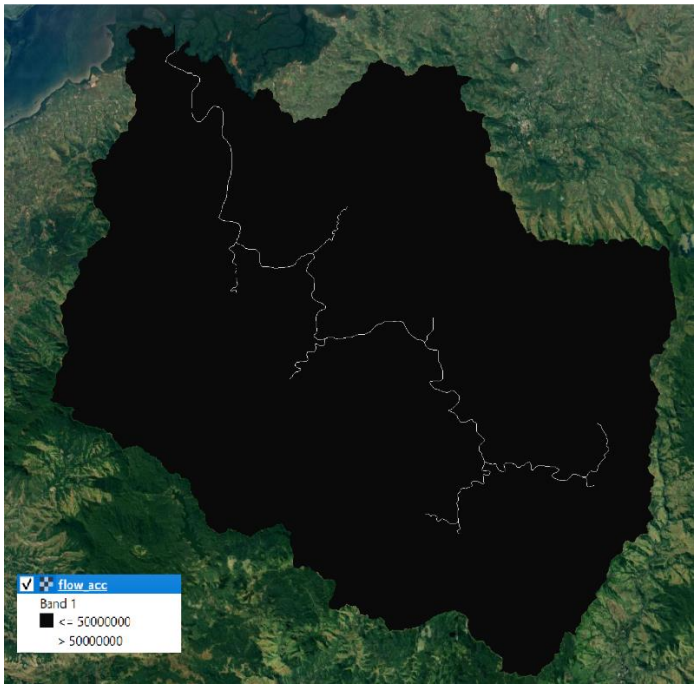

Figure 22 Maximum flow accumulation

Finding Major Channels that May Cause Flooding

In the flow accumulation raster, every cell has an accumulation value, and major channels have more significant accumulation values. Major rivers from generic flow planes can be separated using a threshold accumulation value. In Ba Catchment DEM, the 50,000,000 flow accumulation threshold provides major rivers (Figure 23).

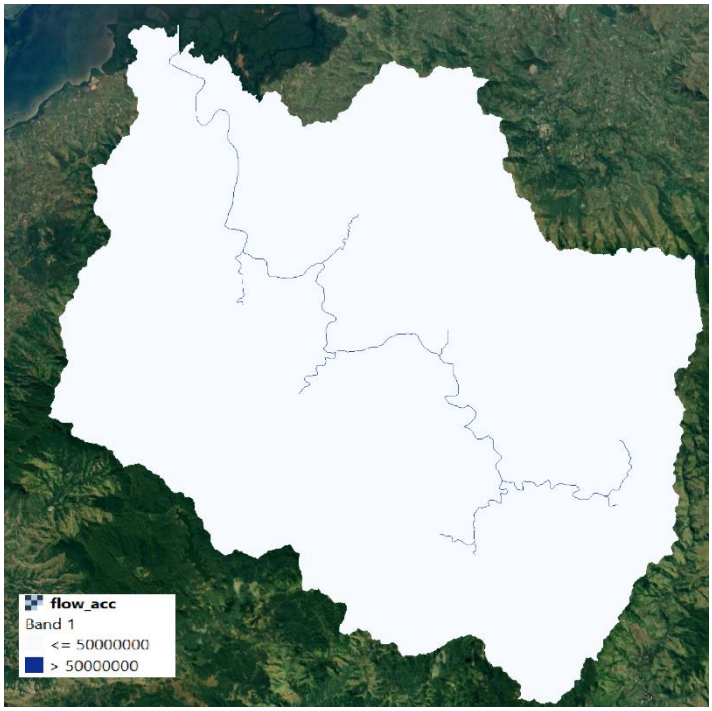

Figure 23 Major flood channels in blue

Generate Channel Network and vertical distance

The channel network is generated using the flow accumulation threshold value of 50,000,000 (Figure 24).

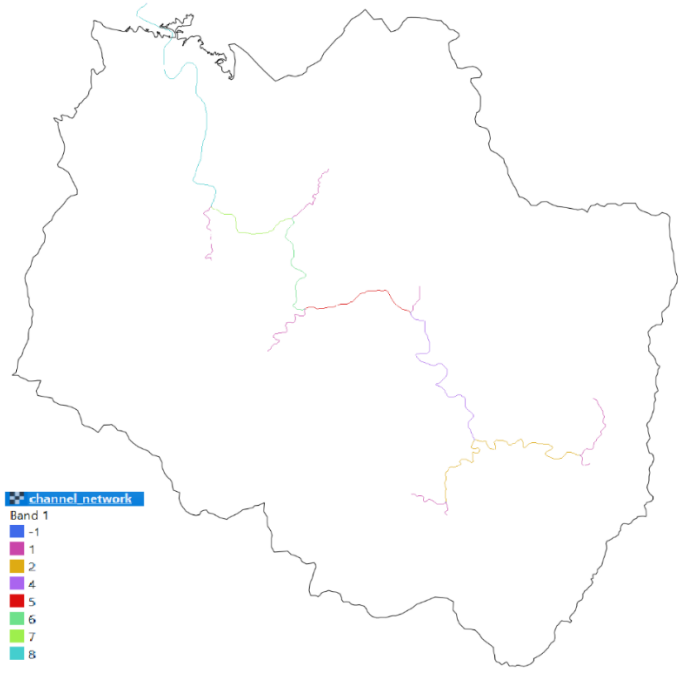

Figure 24 Channel network output.

The vertical distance to the channel network tool is equivalent to the height at the nearest drainage (Figure 25).

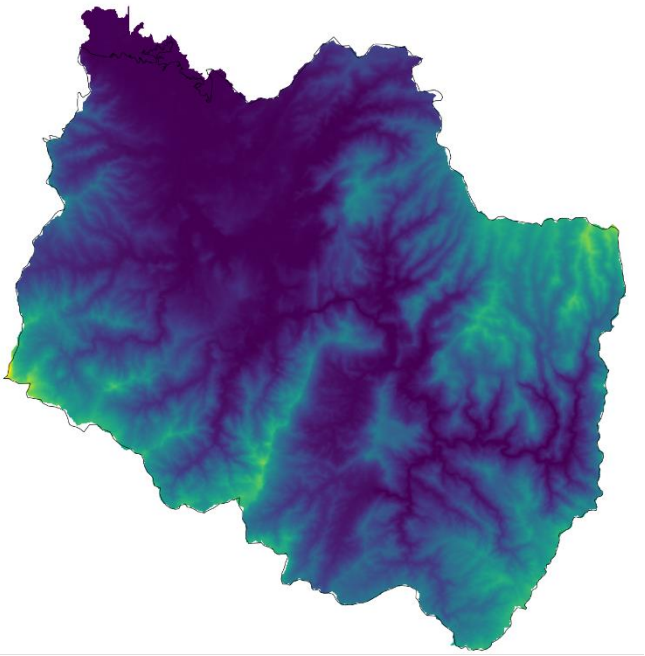

Figure 25 Vertical distance to channel network output.

Classify Vertical Distance to Flood Susceptibility

Areas with high pixel values are highly likely to be inundated by extreme rainfall discharge events. Using this hypothesis, vertical distance raster is classified into flood susceptibility classes (Table 6).

Table 6 Flood susceptibility classes for Ba Catchment.

Vertical distance to stream (m)	**Flood susceptibility class**
0-2	5
2-4	4
4-6	3
6-8	2
8-10	1
10+	0

The flood susceptibility classification table above considers 0-10 m height above the nearest drainage susceptible to flood. It is derived using local knowledge of inundation and research

by Yeo et al., (2010). The table is used to reclassify the results and produce a flood map of Ba Catchment.

4.11 Land use Land cover of Ba Catchment

The land use land cover is digitized to best represent information on the ground. It has been undertaken by the researcher based on various mixed datasets such as building outlines, forestry shapefiles, and river networks obtained from the Fiji Ministry of Lands and Mineral Resources. The final output is different from the open-source ESRI 2021 global land use classification which is purely based on the remote sensing methodology.

4.2 Flood mapping using Synthetic Aperture Radar (SAR) Imageries

The use of Synthetic Aperture Radar (SAR) is beneficial in every stage of the flood disaster process, including prevention, mitigation, and recovery. SAR technology provides valuable information that can assist in the management of floods before they occur, help reduce the impact of flooding during an event, and aid in the recovery efforts after a flood. SAR-derived digital elevation models are input to flood models that predict water runoff and accumulation in the event of flooding. SAR is often the only remote sensing technique that can penetrate habitually dense rain clouds that coincide with most flooding events. On 1st April 2018, following exceptionally heavy rains, the Ba River burst its banks and caused devastating floods, damaging properties, farmland, and infrastructure. It is one of the many flooding events that residents have witnessed over the years. SAR imageries are analyzed to determine flood waters in the Ba Catchment and the method is replicated on the Google Earth Engine platform to change parameters and view flood results.

SAR Data Processing Using Sentinel 1 Toolbox

The software to analyze SAR imagery is Sentinel Application Platform (SNAP) which is an open-source software downloaded from https://step.esa.int/main/download/snap-download/. For SAR data processing, SNAP needs to access relevant DEMs, restituted orbit files, and precise orbit files. The processor automatically downloads relevant auxiliary data however, the auxiliary data from sentinel 1A can also be downloaded from http://step.esa.int/auxdata/orbits/Sentinel-1/POEORB/S1A/ if not updated automatically.

For the study site, the Sentinel 1 Ground Range Detected (GRD) product type is selected as it includes only the amplitude, and the images have been multi-looked; thus, it is smaller in size. The sensor mode is interferometric wide swath (IW), which is most suitable for flood mapping. The data is chosen based on sensing date as it refers to the date on which the image was taken.

To differentiate between flooded regions and permanent water bodies, a technique is used that merges an image captured during a flood event (crisis image) with an image taken before the flood (archive image). The images are freely available to download from the Copernicus hub which can be accessed at https://scihub.copernicus.eu/dhus/. Below is the workflow summary for flood mapping with Sentinel 1 using SNAP software (Figure 26).

Diagram to summarize workflow of flood mapping in SNAP.

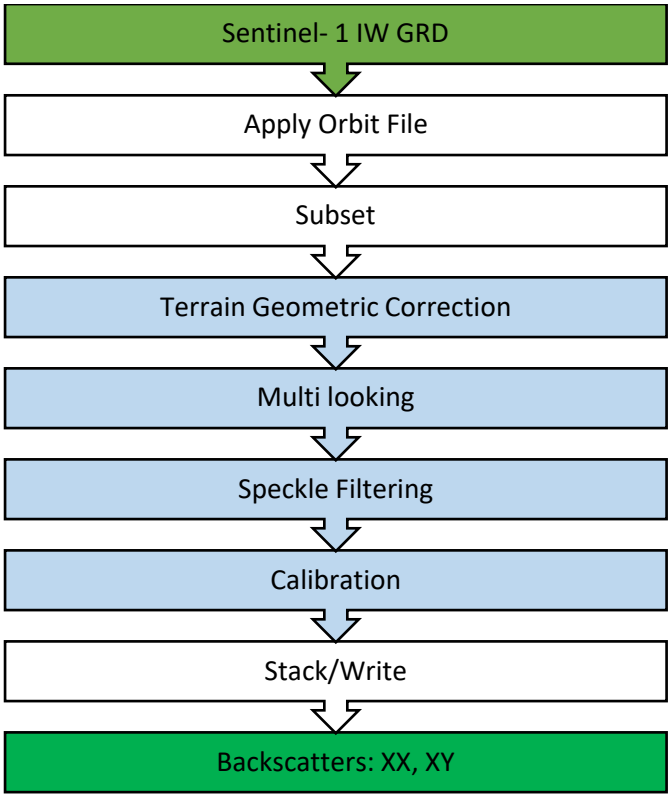

Figure 26 Work flowchart of SAR image analysis for flood mapping using level 1 GRD images.

The date of sensing range for the crisis image was based on the flood event dates which were between the 1st and 4th of April 2018. The archive image date was selected for any available imagery in March 2018.

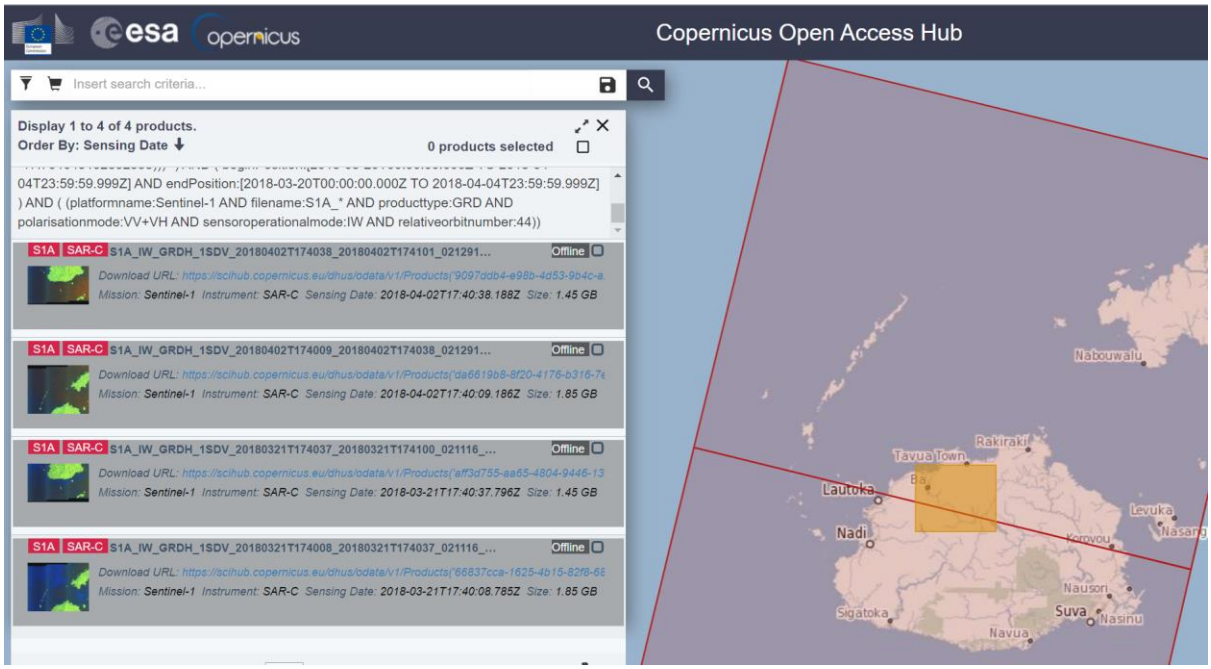

Figure 27 Four SAR images are in the search result of which two are from 21st March 2018 and the other two taken on 4th April 2018. The image on each day is mosaicked before subletting to the area of interest.

Table 7 Files selected for SAR image processing.

Image	**Filename**	**Orbit**	**File Size**	**Pass Direction**	**Polarization**
Crisis	S1A_IW_GRDH_1SDV_20180402T174009_20180402T174038_021291_024A16_EA78	44	1.45gb	Descending	VV VH
Archive	S1A_IW_GRDH_1SDV_20180321T174037_20180321T174100_021116_024491_25A3	44	1.45gb	Descending	VV VH

There are two images available each day however each were mosaicked to cover the Ba Catchment since each image does not fully contain the area of interest as shown in the selection in red (Figure 27, Table 7).

The file name above has several components associated to assist in selecting the right image. S1A refers to Sentinel 1 mission identifier, IW refers to interferometric wide swath mode which is useful for flood mapping and GRDH refers to ground range detected high-

resolution imagery. GRD includes only the amplitude and the images have been georeferenced and multi-looked hence smaller in size. 1SDV refers to level 1 product as the imagery is GRD and it is a standard dual VV + VH polarization. The polarization type is crucial in the detection of open water bodies. For quad-pol (polarimetric) SAR systems, which are transmitted in either horizontal (H) or vertical (V) planes, there are two possible ways that they can be received: horizontally (H) or vertically (V). Therefore, there are two possibilities for co-polarization, which are HH and VV, and two possibilities for cross-polarization, which are HV and VH.

SAR image acquisition

The images selected are band C images with ground range detected projection and with thermal noise removed, radiometric calibration, and terrain correction. It is analysis-ready and hence requires a speckle filter as a minimum input to generate flood extent results. The two selected images are added to SNAP windows explorer to subset and start the processes (Figure 28).

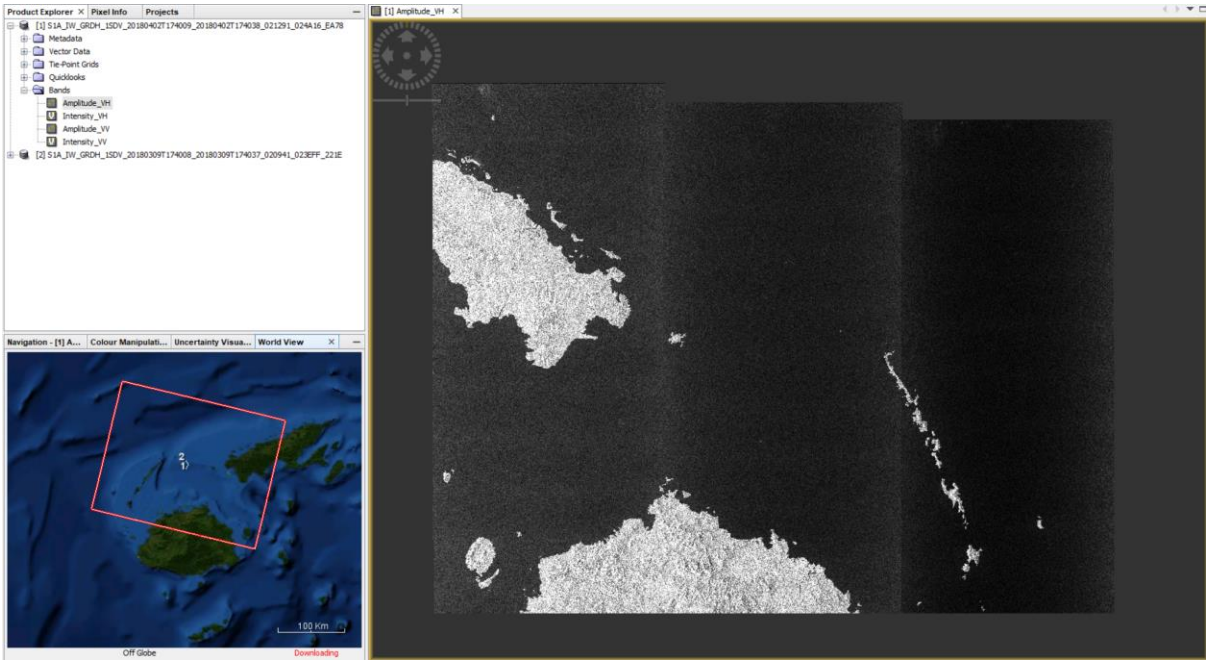

Figure 28 SAR image of the study site is downloaded and opened in SNAP for creating a subset before further analysis

The image is of part of Viti Levu and Vanua Levu as shown on the worldview panel (indicated by the red box). It is currently flipped and covers a large area outside the Ba Catchment.

Terrain Geometric Correction

Range Doppler Terrain correction is carried out for the correction of geometric distortions caused by topography. It is due to foreshortening and shadow effects. This step corrects the location of the pixels based on the SRTM digital elevation model, which is preselected, or a separate DEM can be uploaded onto the tool. The projection selected is WGS84 geographic latitude and longitude projection. The resulting image is no longer flipped, and a subset of the corrected image is saved before further analysis (Figure 29).

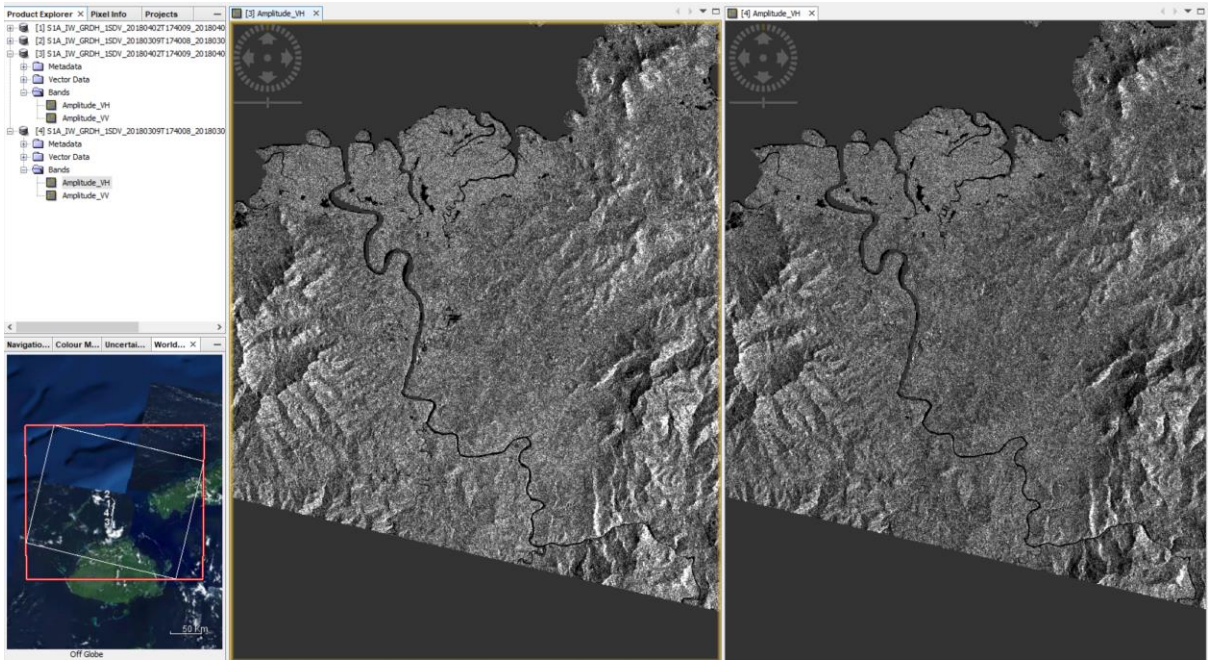

Figure 29 Terrain corrected imagery zoomed into Ba delta. The left image is the crisis image, and the right is the archive image.

Multi looking

This step reduces image size and speckle. Ideally, this step is not applied if the result of flood mapping is needed in high resolution. In areas where flood coverage is large, a low-resolution result is acceptable hence multi looking is applied. The speckle is not changed as the resolution of 10m will enable clarity in flooded areas. This is because the coverage of flood extents in Ba is small and flood waters recede quickly.

Calibration

Calibration enables the comparison of the crisis and archive images. The Sigma nought is a parameter used to describe the backscatter coefficient of a target. The backscatter coefficient is a measure of how much radar energy is scattered back to the radar by a target, relative to the amount of energy initially transmitted by the radar (Copernicus, 2022). It is set as default for both crisis and archive images and an output is generated. The calibrated and multi-looked images have Sigma0 as the name of the band instead of Amplitude and Intensity. Due

to the presence of low backscatter values in numerous pixels and the scarcity of high backscatter values, the images seem dark. To enhance the clarity of the visual representation, the pixel values are transformed from a linear scale to a logarithmic scale (decibel). This enables better differentiation between the pixels representing land and water. The histogram of the transformed image displays two peaks, with the larger peak indicating the land pixels and the smaller peak representing the water pixels (Figure 30).

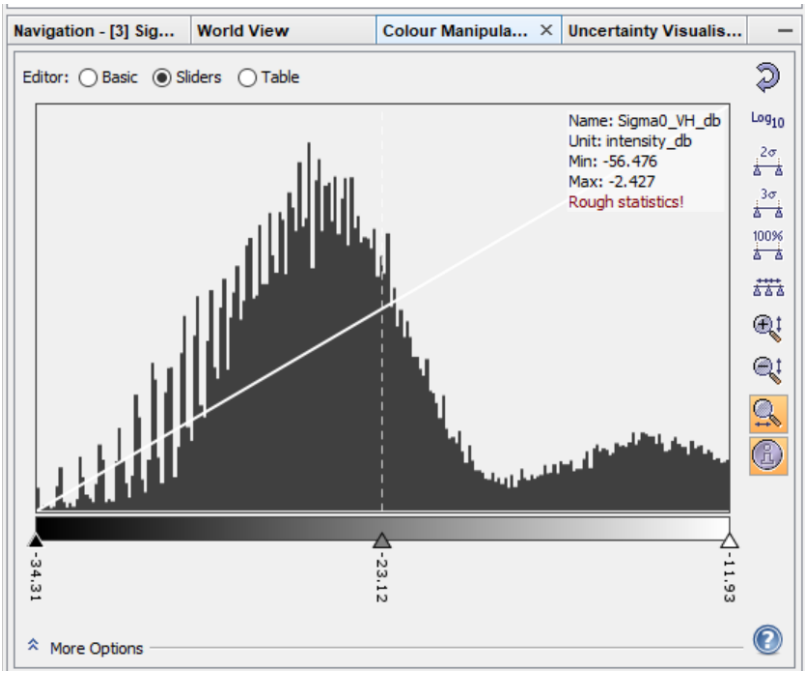

Figure 30 histogram of results shows a high return from land pixels and a low return from water pixels.

Double bounce is the backscatter intensity over a water body appearing as a smooth surface which causes specular scattering, resulting in a radar signal being scattered away from the satellite and appearing very dark (Copernicus, 2022). Applying a speckle filter affects the resolution of the imagery which is currently at 10m. After analysis, thresholding is applied because of the clear distinction between the before and after images (Figure 31). The difference in inundation shows bright areas which are areas inundated and thresholding allows the application of a mask to areas that were inundated.

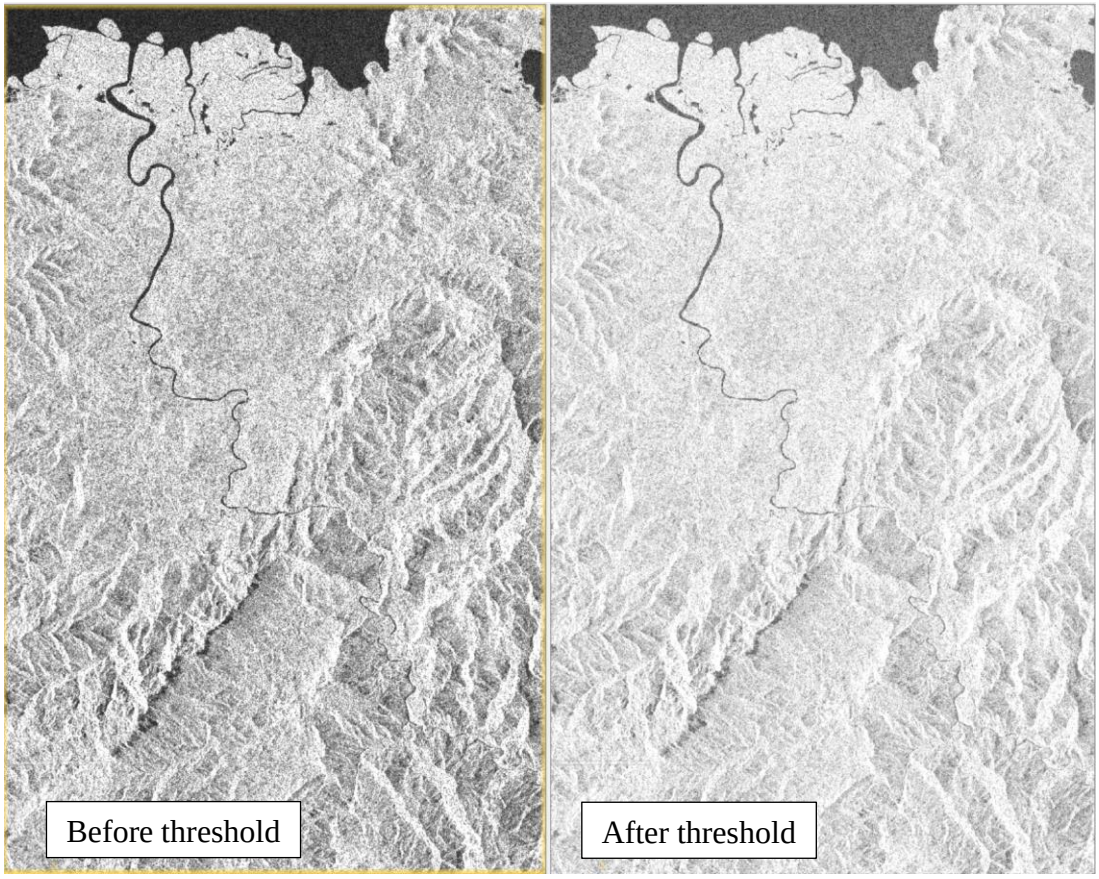

Figure 31 The difference in both images after applying thresholding as a speckle filter has affected the resolution of imagery and affects the results of flash floods.

Stack

The multi-looked, calibrated, and terrain-corrected images of the crisis and archive image are now stacked using its product geolocation as an offset method. The information from the orbit file will register these product overlays accurately. The result is bands of each image put together into one image file. These products can be overlayed and set transparency to visualize the crisis image with the archive and see the flood extent captured by the imagery. Further analysis of this stacked image is done by converting the result into RBG composite image (Figure 32). The red band in the archive image is selected, while the blue and green bands in the crisis image are chosen for the process. This is because flooded regions, which are essentially land areas, will have a strong radar response in the red band. In the archive

image, no flooded areas are expected therefore it will have a high backscatter return. Flooded areas tend to exhibit a low backscatter return in the crisis image, resulting in a high response in the red channel and a low response in the blue and green channels. Therefore, flooded regions are displayed in red, as they will have a strong response in the red channel, but a weak response in the blue and green channels. In areas with no floods, tones of grey should be seen and the backscatter should be similar in red, green, and blue. For permanent water bodies, there is a consistent and weak backscatter return in both the archive and crisis images, resulting in a low response for all the red, green, and blue channels. In the flood map, the flooded areas are highlighted in red, while the river appears dark due to its low response in all channels. The surrounding areas are depicted in various shades of grey.

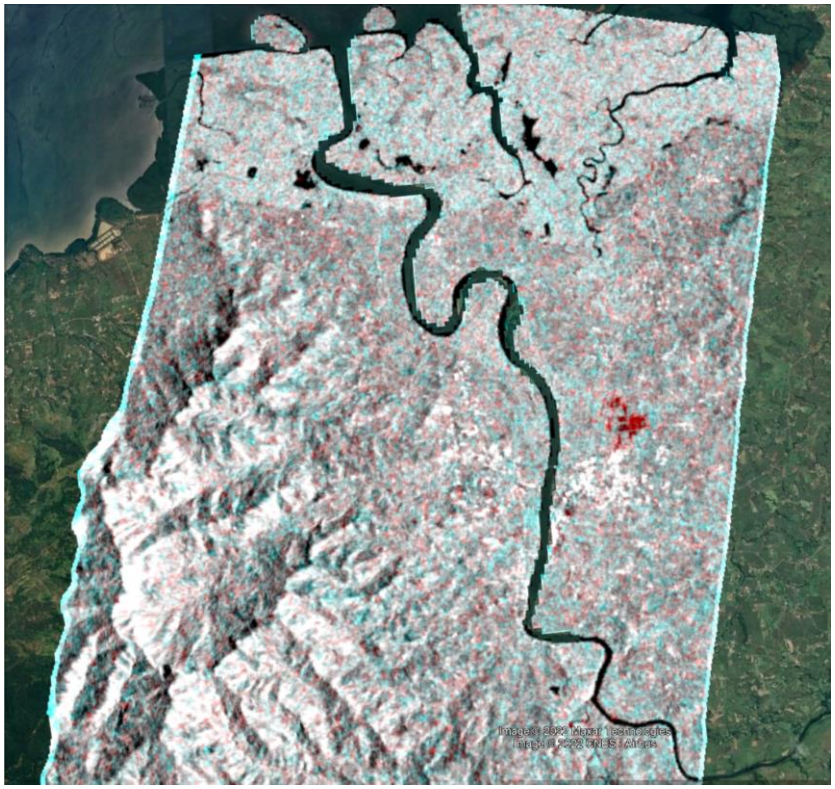

Figure 32 results were exported as .kmz file and viewed on Google Earth Pro. The result is registered properly.

The reason why certain sections may be shaded in blue is because they show a stronger reaction in the crisis picture than in the archive picture. However, this difference could also be attributed to vegetation cover that is not necessarily linked to flooding. The

results can be exported as kmz and viewed on Google Earth Pro. Viewing on Google Earth allows checking the registration of this image to see if it is precise. It can also be colour-manipulated on SNAP to label individual classes and improve visualization of the results (Figure 33).

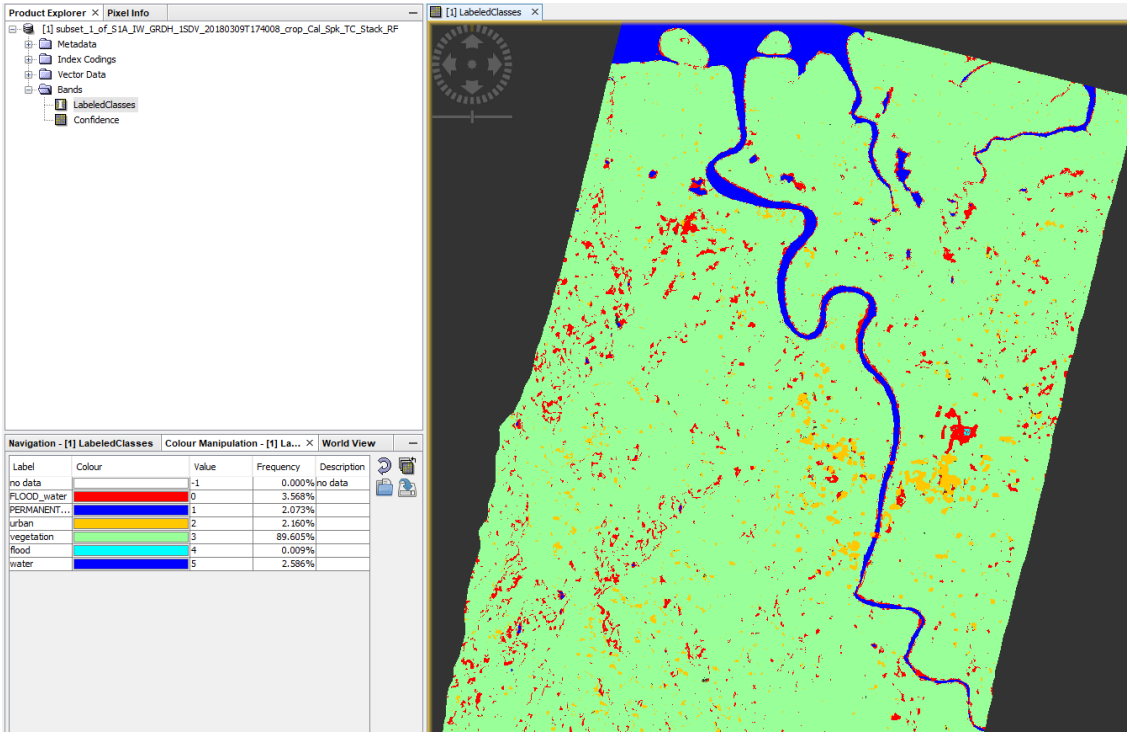

Figure 33 colour manipulation of results in SNAP to show the land use landcover of the site. Red is flood areas, blue is permanent water bodies, yellow is urban, and green is vegetation.

Google Earth Engine

The platform is utilised to execute a script to map flood waters based on analysis of SAR imageries. The before and after flood imageries are filtered by inputting dates of archive and crisis images which is the same as the input for SNAP methodology. The script is adjusted to fit the conditions at the site. The imageries are sentinel 1 ground range detected which has Thermal-Noise Removal, Radiometric calibration, and Terrain-correction hence only a Speckle filter needs to be applied in the pre-processing. The following parameters are set:

- Polarization: VH polarization for flood mapping.
- Pass: Descending imageries are more available in descending pass than ascending. However, both pass is selected to compare the results of the 2018 April flood event.
- Difference threshold: The threshold for the difference image (after flood - before flood) was determined through a process of trial and error. This was necessary because the flood output contained a significant number of negative signals resulting in false-positive output on a threshold above 1.25 hence 1.20 was selected to improve output.
- Instrument mode: Interferometric Wide (IW) swath
- Radar speckle smoothing radius: 50
- Area of interest: polygon geometry created on GEE
- Mask out areas of permanent water bodies and a 5 per cent slope using the Digital Elevation Model from Hydrosheds.

The global gridded datasets on land use land cover and population can also be added to the script to estimate the damage assessment however for Ba Catchment, there was no local gridded population data and national land use data available calibrated for Fiji. Analysis of global datasets was inaccurate as the global datasets, such as population data, did not match local records obtained from census data. Therefore, global population data was not added to the GEE analysis.

4.3 One-Dimensional (1D) Flood mapping using Hec-RAS

Diagram for one dimensional flood mapping in this methodology.

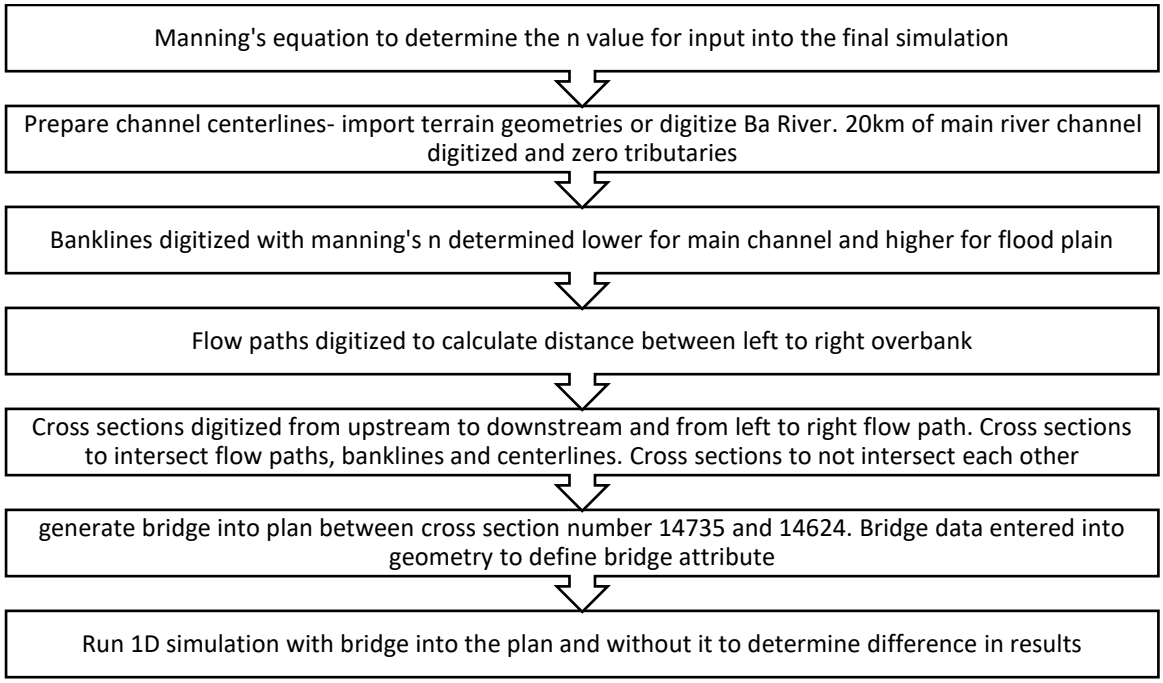

Figure 34 Steps undertaken to run a 1D simulation in HecRAS to determine the flooded area in the lower Ba River.

Discharge estimates using the slope area method

The slope area method is commonly used to estimate peak discharge indirectly by measuring peak discharge from high water marks and debris lines after the flood event (Smith, Cordova, & Wiele, 2010). It is used when instruments to measure flow cannot be deployed, especially during flash floods, making it challenging to install in time to capture data of events.

The formula is (Muste, Thomas, & Bacotiu, 2019):

Discharge = River Slope x Cross Sectional Area (m^3/second) (Equation 1)

Equation 1 formula for calculating discharge of downhill gradient

The debris line is estimated from recordings of interviews with the Toge and Navala Villagers and newspaper articles. It is then marked on Google Earth Pro for elevation data which is corrected based on information provided by the Secretariat of the Pacific

Community (SPC). SPC conducted a Real-Time Kinematic (RTK) based GPS survey at Toge and Navala Village after April 2018 flood (Figure 35).

Figure 35 cross-section of estimated flood height at Toge Village.

The cross-section information enables the estimation of water discharge in the Ba River at Toge and Navala Village to provide insights into the large flood events. In addition, flood heights in Ba were surveyed by the Secretariat of the Pacific Community to allow comparison with previous floods and to use in future investigations. This information, coupled with the water level and rain station data, provided a better understanding of the flood's impact at different locations within the catchment and consider how communities may respond to similar events in the future. Below is the cross-section of the Ba River at Toge (Figure 36).

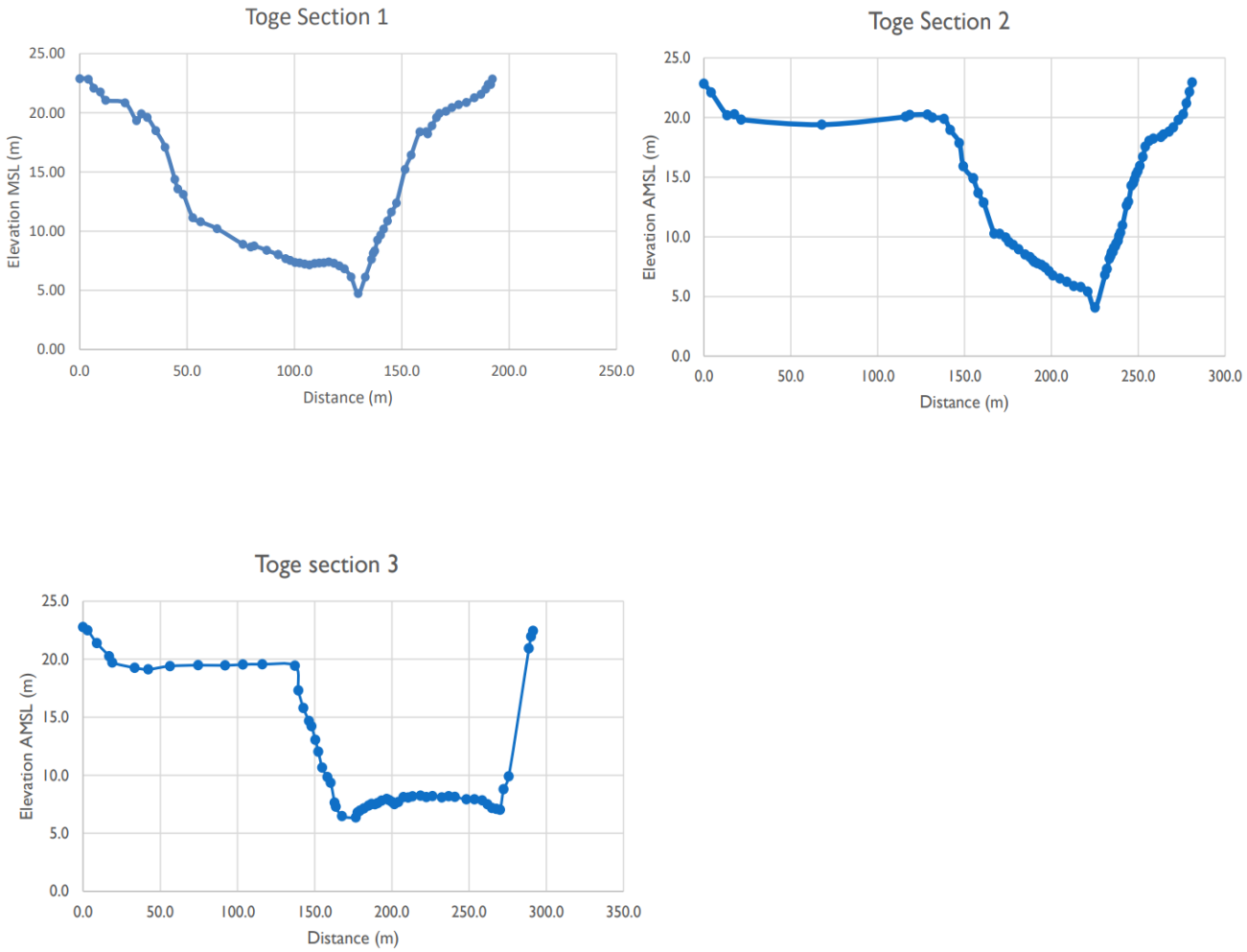

Figure 36 cross sections taken at Toge village from left bank to right bank facing downstream.

Cross sections of Ba River taken at Navala Village (Figure 37, 38).

Figure 37 cross-section of estimated flood height at Navala Village. Cross section 4 is of the road and bridge into the village.

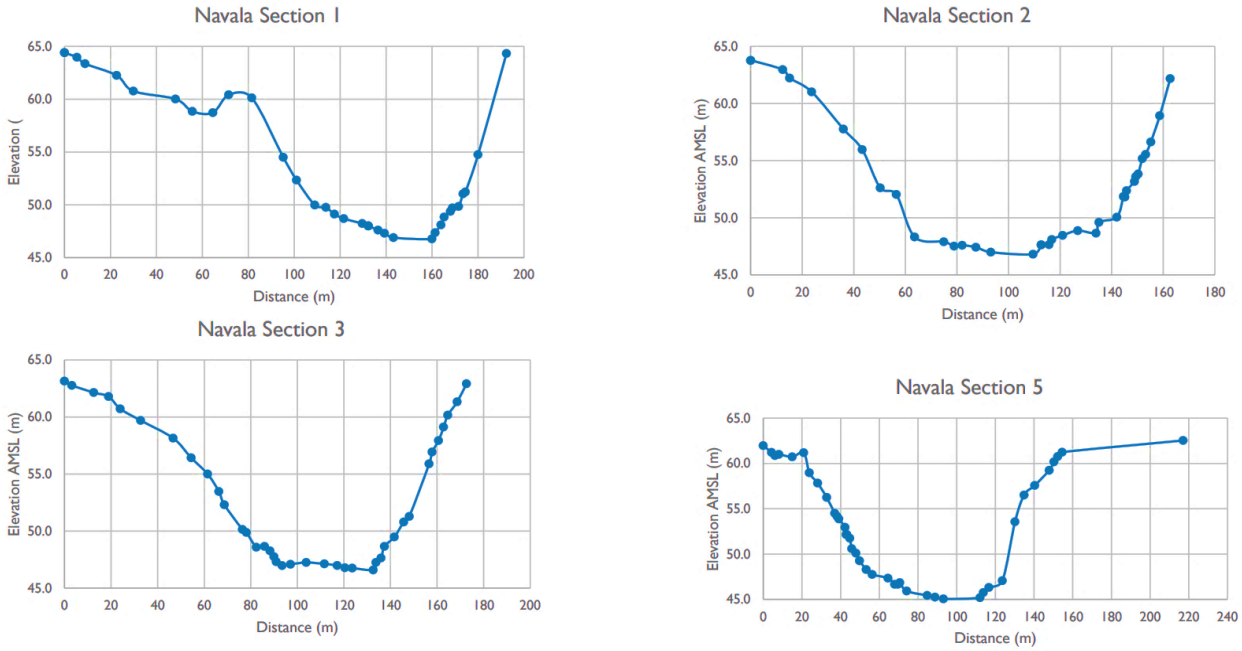

Figure 38 Cross section 1-3 and 5 of Ba River taken at Navala Village.

The cross-section area is determined by calculating the average depth and width between the east and west banks. The cross-section area and velocity are used to calculate the discharge from Equation 1.

Manning's equation

When water flows through a channel, there is a conservation of mass, energy, and momentum. These are some of the many forces that act in Manning's equation. The gravitational force drives flow direction in the channel which is met by resistance from the channel's cross-sectional shape and roughness as it opposes flow. The hydraulic properties such as depth and velocity are dictated by the balance of gravity and flow resistance. The formula for Manning's equation is (Muste, Thomas, & Bacotiu, 2019):

$$Q = (C/n)A(R2/3)(S1/2) \qquad \text{(Equation 2)}$$

Equation 2 formula for calculating Manning's equation

The velocity of flow = C/n. C is the conversion factor which is 1 for S1 units and n is Manning's roughness parameter which tells how rough or smooth the channel is. The n value is smaller for smooth channels and higher for rough channels.

One of the properties used in hydraulic design and Manning's equation is the hydraulic radius. The equation of it is the cross-sectional area of the flow divided by the weighted perimeter of the flow:

$$R = A/P$$

Where A is the cross-sectional area of the flow which takes into account the depth of the water in the channel and P is the wetted perimeter and which deals with how deep the water is when calculating the perimeter.

S= Slope of channel bed

Assuming that there is a uniform flow, the slope expression gives velocity which is the energy driving the flow. Slope information is established for two sites in Ba Catchment: Toge Village and Navala Village.

One part of Manning's equation is for channel properties and the other includes gradient. With Manning's equation, if velocity is known it can be used to find discharge. With discharge and velocity known, this part of the expression is used to calculate the hydraulic radius. The hydraulic radius requires knowledge of channel depth which is established for two sites in Ba Catchment; Toge Village and Navala Village situated at the middle reach of the Ba River.

Preparing Ba lower catchment flood model

Table 8 Datasets required in this simple flood model using HECRAS.

Data	Organization	Use
LiDAR of part of Ba lower catchment	Secretariat of the Pacific Community	Terrain base map for the model

The DEM output of LiDAR is used to simulate as it has a resolution of 1m and covers the highly populated areas of the lower Ba Catchment.

Channel Centrelines

Importing terrain data on the project activates the geometries required for the one-dimensional flow model. It allows editing of all possible geometries in the model. The list is extensive however for a simple flood model, few geometries can be created to run a simple simulation. A river geometry defines the form of the river and the Ba River is approximately 84km long. For this model, the first 20km is digitized (Figure 39a). No tributaries are digitized on the model within the first 20km of the lower river as the tributaries are not visible in the terrain dataset (Figure 39b). The Ba River flows north-westerly, and the river is

digitized from 5km above the Ba Bridge to the river mouth following the rule of starting the digitizing from upstream to downstream. The terrain profile can be viewed to check for possible errors in digitizing and the attribute table outlines the river length and name (Figure 39c).

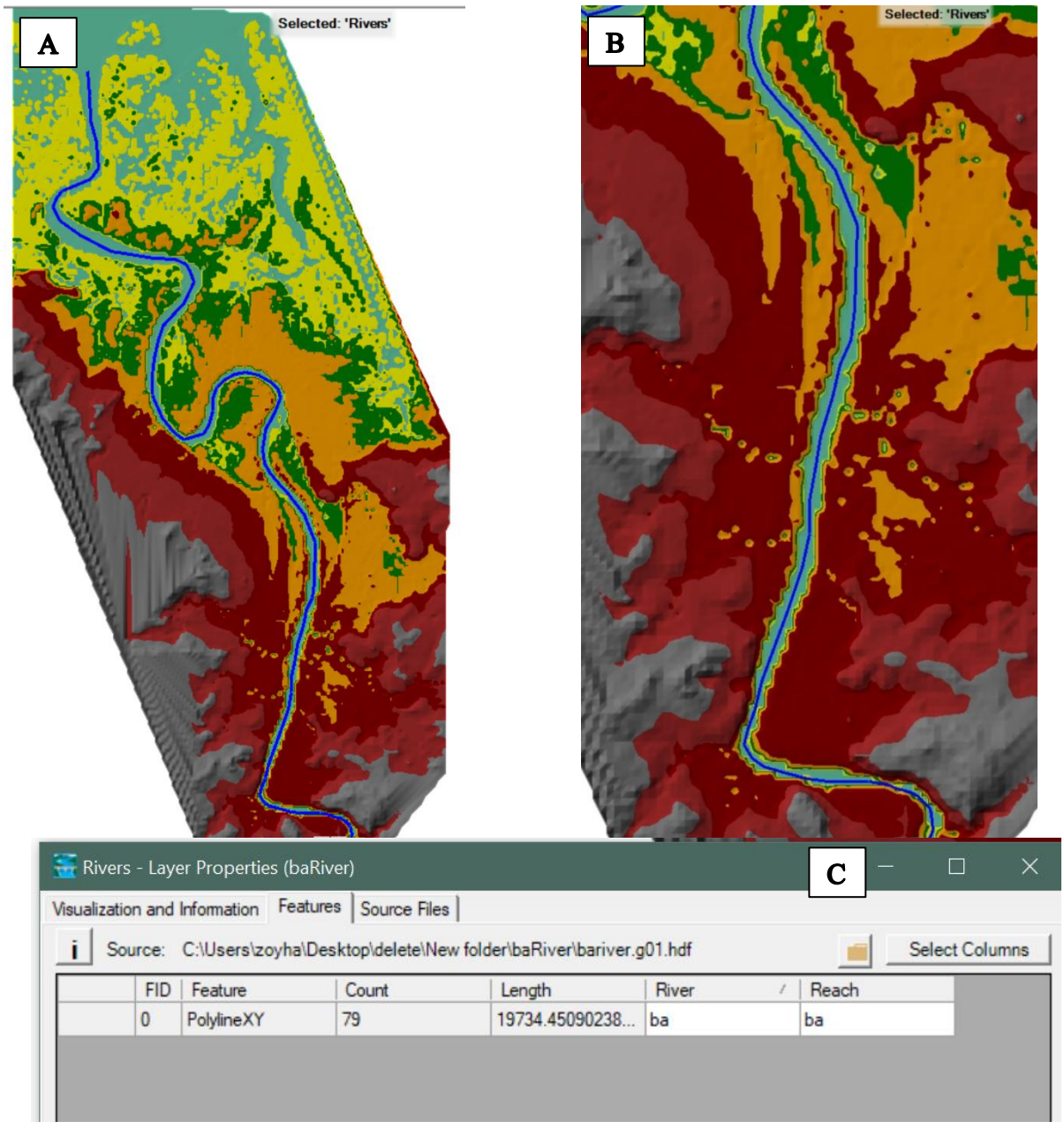

Figure 39 (a) Lower Ba River centreline digitized from terrain data. (b) Hard to estimate smaller tributaries such as Elevuka Creek and Namosau Creek. (c) River length of 20km digitized for the simulation

Banklines

Bank lines are used to distinguish between the main channel and floodplains. It is useful for assigning Manning's n. Manning's n is lower in the main channel than the floodplain due to less resistance as floodplains have vegetation and buildings that obstruct the flow. Therefore, floodplains have higher Manning's n than channels. With clear terrain data, the boundaries of bank lines are visible which assists in the distinction between the main channel and the floodplain (Figure 40a). The digitization of bank lines is from upstream to downstream using terrain data and is both left and right banks (Figure 40b). The bank lines, centrelines, and flow path are needed to generate cross-sections. It is not essential to have one complete bank line, there can be multiple small lines as far as the entire bank line is digitized to later construct cross sections. The digitized polyline properties can be viewed after editing to see the length of each bank line (Figure 40c).

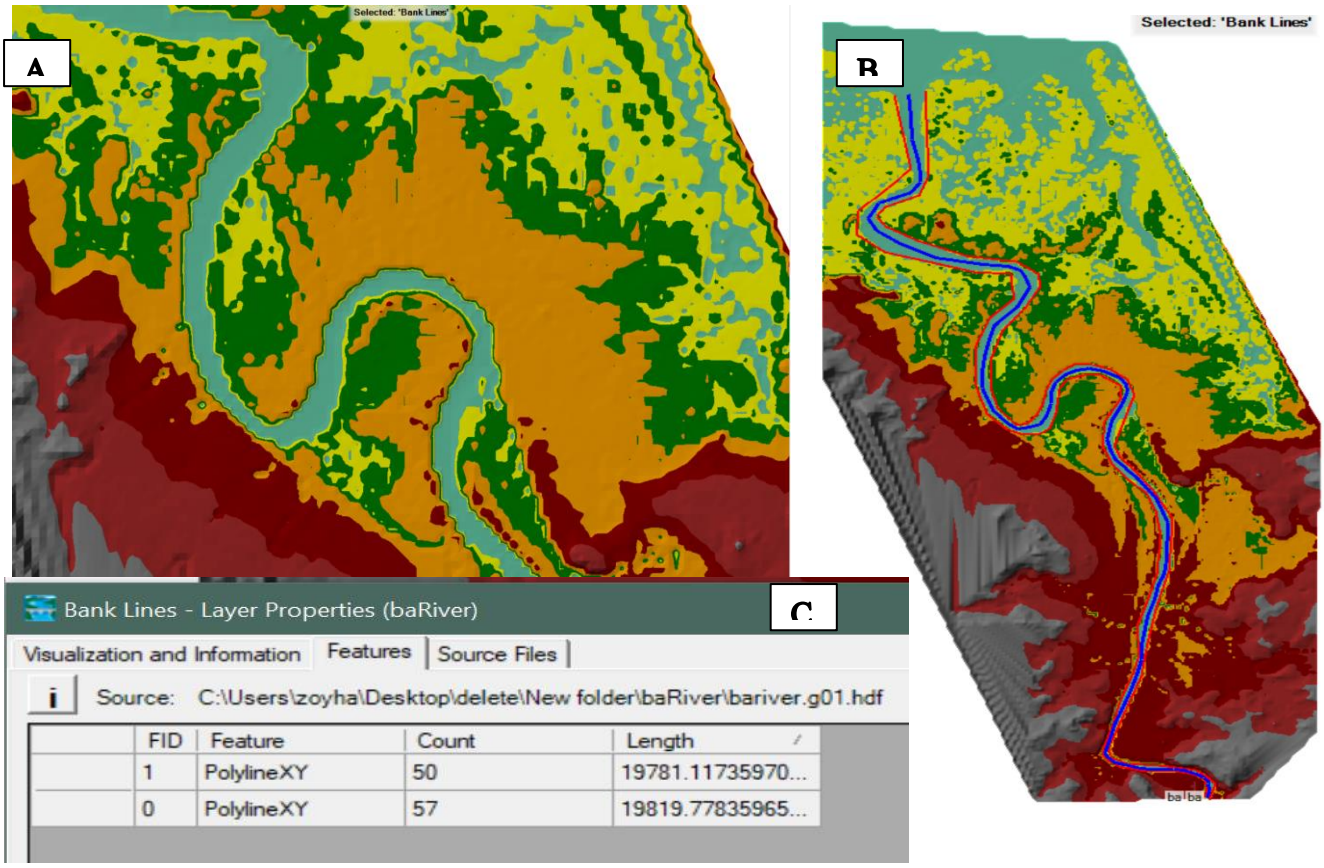

Figure 40 (a) Clear distinction between river channel and banklines help differentiate each boundary. (b) Digitized banklines of lower Ba River (red polyline). (c) 20kms of each bankline digitized for simulation

Flow Paths

Flow paths are also lines running parallel to the centreline and are used to calculate distances along the channel between cross sections (Figure 41a). There are three types of distances used in HEC-RAS. First is the distance along the channel which uses distance along the centreline to find out distances between cross-sections along the channel. Two other distances are used to calculate between adjacent cross sections hence the first is right overbank while the second is left overbank. Flow paths are used to find distances between adjacent cross-sections along the main channel in the right and left overbank. This step involves digitizing flow paths at a distance that will cover enough floodplains to include in the simulation. The base map is a high-resolution topography generated from LiDAR data of Ba Town and the surrounding area only. Zooming into it, the main channel can be easily distinguished similarly to the floodplains in light green symbology. The floodplains are at a higher elevation than the main channel, but lower elevation compared to surrounding features distinguished by symbology. The floodplain can be used as a guide to define flow paths. The digitizing of flow paths has certain criteria. Firstly, to ensure that flow paths do not intersect with any centrelines and bank lines and each reach has an upstream and downstream line representing the left and right flow path accurately. Secondly, if tributaries are added to the simulation, it will have a separate flow path so that the left and right are accurately facing the upstream and downstream flow paths. The left and right banks will be different for river reach and river tributaries. For the Ba flood simulation, there is no tributary added to the simulation because it is unclear in the topography of the correct bankline and channel of Elevuka Creek. The flow paths digitized is for the left and right bank of the lower Ba River measuring approximately 19km (Figure 41b).

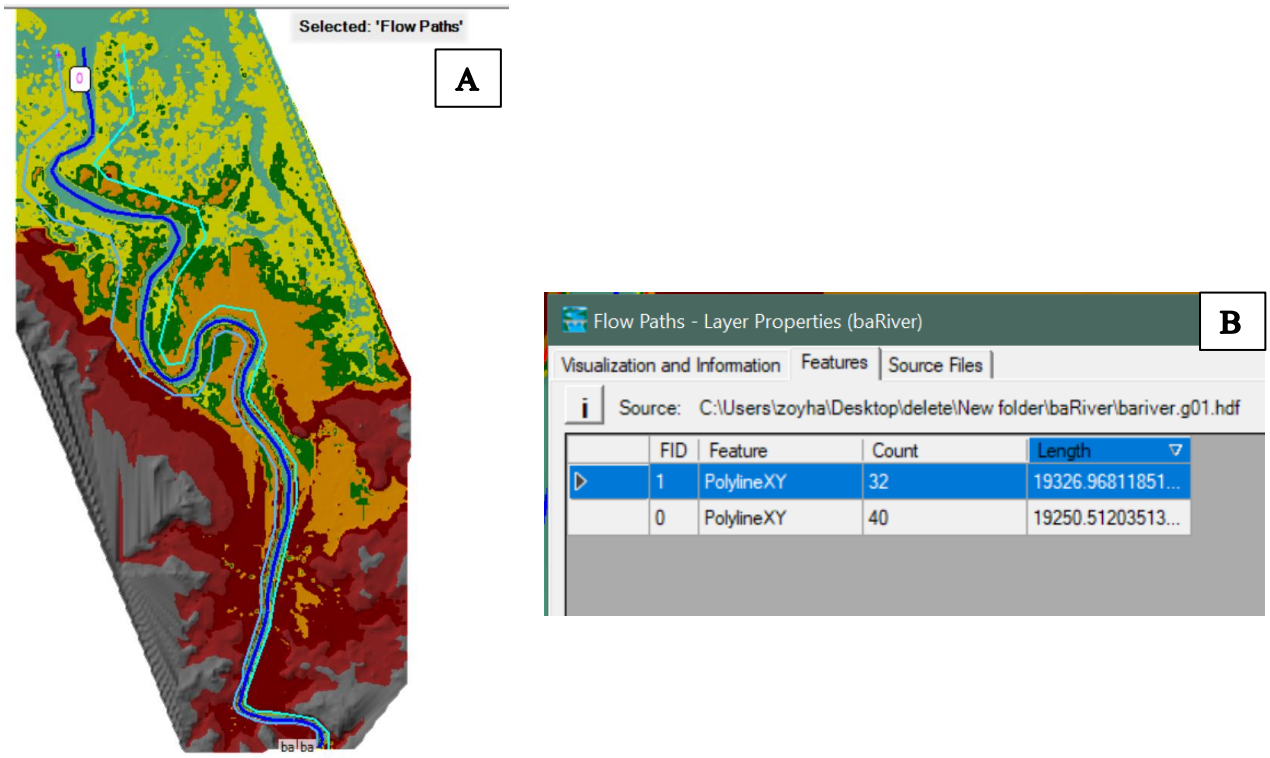

Figure 41 (A) Completed flow path (teal polyline) of lower Ba River and (B) length of flow path of Ba River digitized.

Cross sections

The cross sections are digitized from the left to the right flow path of the river channel followed by digitizing from upstream to downstream. It is important to check that all lines (flow paths, bank lines, and centrelines) are intersected when creating cross sections (Figure 42a). Also, the cross sections do not intersect each other to avoid errors. Moreover, cross-sections perpendicular to centrelines should change directions for cross-sections that cannot be perpendicular so that it avoids intersecting another cross-section.

The digitizing will update the attribute table automatically (Figure 42b). The key information is the length over the left & right overbank region, length of the channel, and left & right bank which defines the points where the cross sections intersect with the bank lines are all defined properly. The left bank is the distance from the left end of the cross-section to

the left bank and then to the right bank. There were 76 cross-sections digitized and for each, the profile can be viewed to see the natural floodplain along the channel.

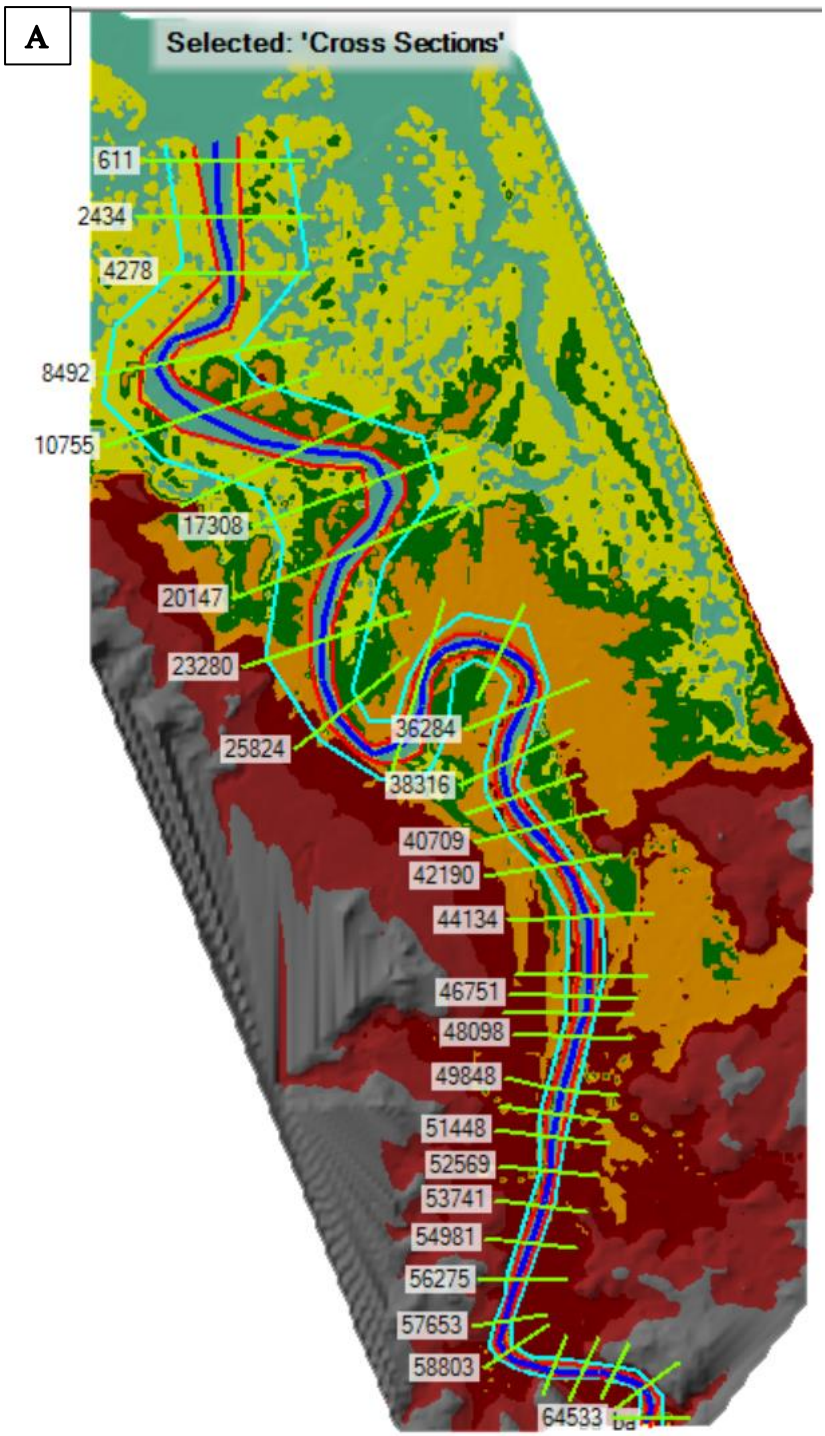

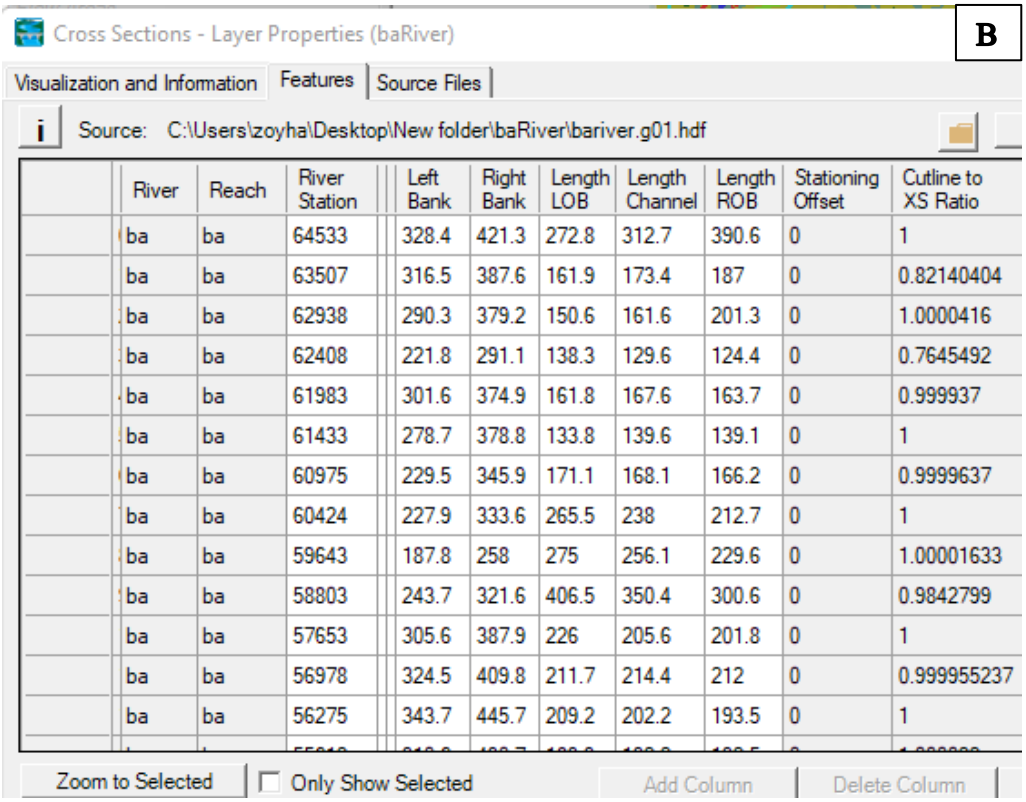

River	Reach	River Station	Left Bank	Right Bank	Length LOB	Length Channel	Length ROB	Stationing Offset	Cutline to XS Ratio
ba	ba	64533	328.4	421.3	272.8	312.7	390.6	0	1
ba	ba	63507	316.5	387.6	161.9	173.4	187	0	0.82140404
ba	ba	62938	290.3	379.2	150.6	161.6	201.3	0	1.0000416
ba	ba	62408	221.8	291.1	138.3	129.6	124.4	0	0.7645492
ba	ba	61983	301.6	374.9	161.8	167.6	163.7	0	0.999937
ba	ba	61433	278.7	378.8	133.8	139.6	139.1	0	1
ba	ba	60975	229.5	345.9	171.1	168.1	166.2	0	0.9999637
ba	ba	60424	227.9	333.6	265.5	238	212.7	0	1
ba	ba	59643	187.8	258	275	256.1	229.6	0	1.00001633
ba	ba	58803	243.7	321.6	406.5	350.4	300.6	0	0.9842799
ba	ba	57653	305.6	387.9	226	205.6	201.8	0	1
ba	ba	56978	324.5	409.8	211.7	214.4	212	0	0.999955237
ba	ba	56275	343.7	445.7	209.2	202.2	193.5	0	1

Figure 42 (a) completed cross-sections of digitized centrelines and (b) attribute table output showing some of the 76 cross-sections digitized.

Bridges

Some more cross sections are added to accommodate a bridge into the simulation. This increases the cross sections list and changes the river station numbers. A bridge is added to the lower Ba River using bridge culvert data. The bridge is created between cross sections 14735 and 14624 and is located approximately 14.6km downstream. The design of the bridge is added based on the estimation of bridge length, width, pier diameters, and the total number of piers. The bridge is estimated to be 200m in length with six piers and it is a two-lane bridge. The cross-section at the site is used to determine the station number upstream and downstream. The distance between the cross-section and the bridge is approximately 100m and the width of road lanes is estimated to be 10m (Figure 43a). The station number is estimated to be 160m for upstream and 350m for downstream with an elevation between 4m to 6.5m (Figure 43b). Since there is no field information, all these figures are estimated to

create the bridge. The opening station for the upper portion of the road is estimated to begin at 0 with openings at 160m, 350m, and closing to be at 500m. The bridge detail can be examined in 3D view to identify the possible error and rectify geometry data before calculating steady 1D simulation (Figure 43c).

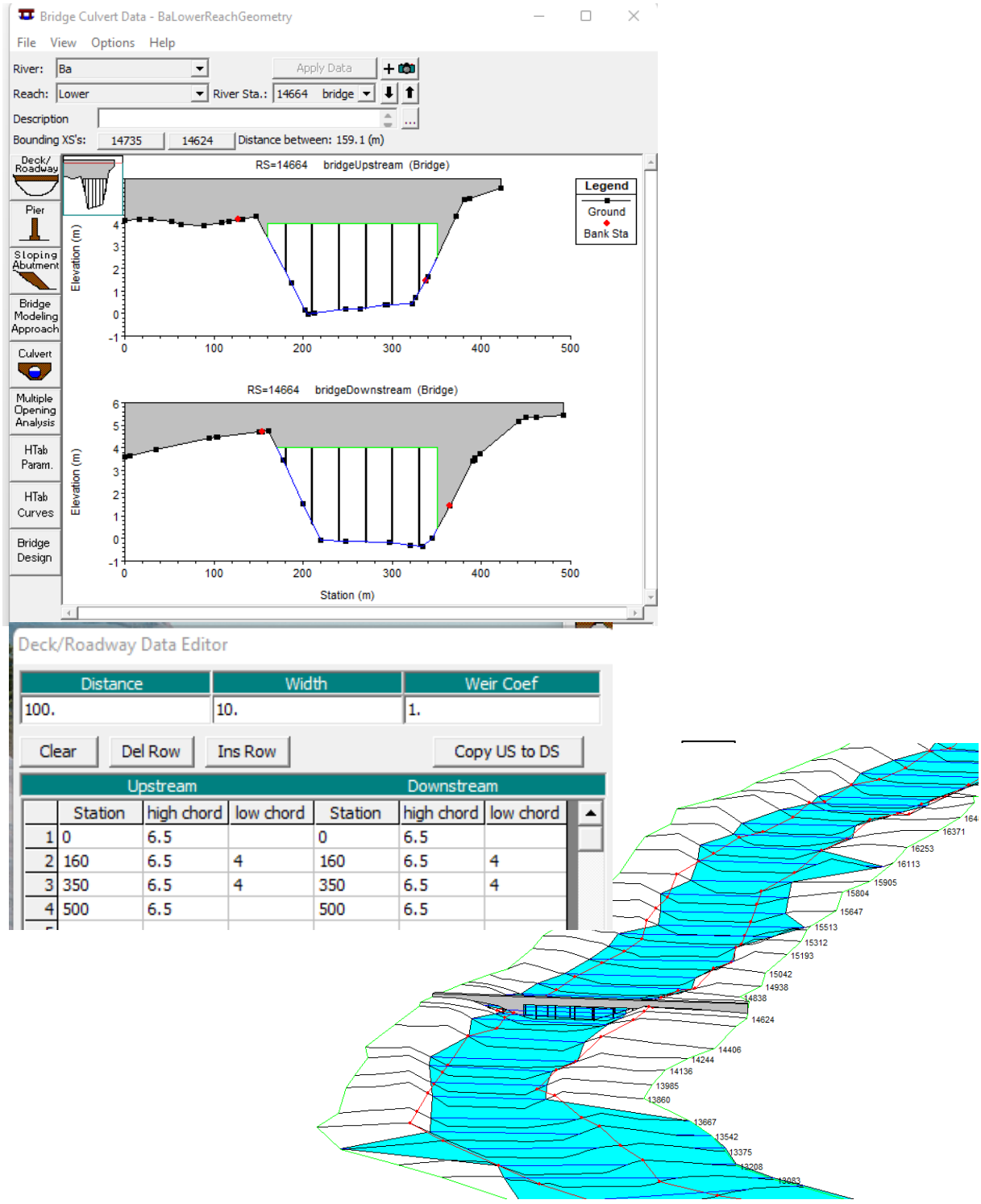

Figure 43 (a) parameters to design bridge geometry, (b) Bridge data entered into the geometry to define bridge attributes and (c) 3D view of completed bridge geometry.

Running 1D Simulation

After finalizing the geometry, manning's n is assigned to run the simulation. Manning's roughness coefficient is determined by Rathnayake & Arachchi, (2015) where the authors have created a HEC-RAS simulation of the Waidina Tributary in Rewa, Fiji. Although the authors have used a slightly higher manning's n, it is not the same as Ba River is smaller than Rewa and the catchment size is also smaller compared to Rewa catchment. Manning's n for river channels that have boulders and cobbles can be between 0.03-0.07 (Arcement & Schneider, 1989). For floodplains with vegetation, as in the case of Ba floodplains, the manning's n can be between 0.025-0.050 for medium to large vegetation. Medium vegetation would have an average flood height one or two times over the vegetation whereas large vegetation includes trees intergrown with weeds and refers to the height of vegetation above average flood depths. For this simulation, Manning's n for river channel is selected as 0.04 and 0.03 for floodplains. Finally, a flow file is generated by assigning boundary conditions to run the simulation. The boundary condition is selected as critical depth to see the impact on the lower Ba River. The first result is generated with the bridge as part of the input (Figure 44a) whereas the second result is generated without the bridge to see the difference (Figure 44b).

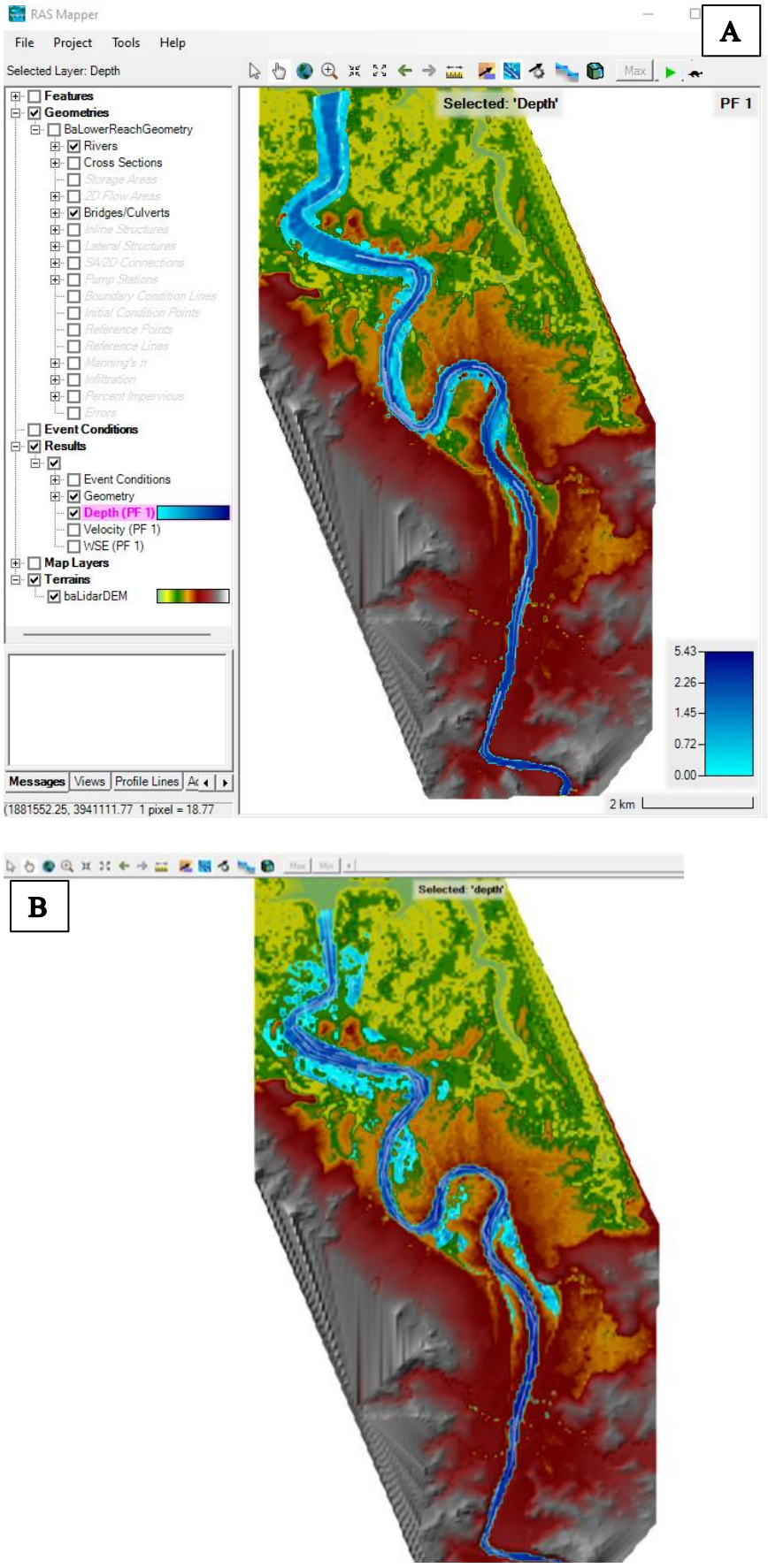

Figure 44 (a) Result of simulation with bridge geometry as part of input and (b) without bridge geometry in input.

4.4 Limitations of the methodologies

The lack of national datasets in gridded or shapefile format is a limitation to accurately creating models that can help in planning adaptation and mitigation strategies for communities residing on the floodplains. There is also a need for improvement in how agencies that have datasets streamline the availability of this information as a lot of time is lost trying to facilitate the data release process. One of the key issues faced was the lack of interest shown by the relevant authorities to facilitate the requests hence most datasets used for this research were open-sourced.

There are also various studies undertaken in the Ba Catchment to try flood modelling and hydrological mapping which often focus on the hard engineering solutions which could not be input into the three methodologies as it would require complex inputs which is beyond the skill of the researcher. The models have been prepared using the available datasets and it is laying the groundwork for future research using improved data inputs, especially in the HEC-RAS one-dimension flood simulation. There is a need for personnel training and capacity building to start using the freely available software to plan flood models. It will increase data collection of river flow, riparian vegetation, riverbed materials, and cross sections to start building a database of river characteristics in Fiji.

The lack of complete rainfall data is another challenge as inputs in flood modelling require complete datasets without averages so that results reflect the situation on the ground. There are manual stations across Ba Catchment that can incur human error when recording and submitting datasets to the Fiji Meteorological Service. The automatic stations are scarce and cover the middle to lower Ba Catchment. There need to be more automatic stations spread around the catchment to capture flow data and rainfall. This will assist the modellers to determine flood water lag times which can then be incorporated into the early warning system to advise people of the behaviour of the river and the approximate time for the river

break. Although the automatic stations are connected to transmit data to the server at the Fiji Meteorological Office, the stations failed to properly record the rainfall and river water level which resulted in missing data on the 2018 flood events in Ba. It is recommended that automatic stations are placed across the whole catchment for a better chance to generate accurate flood models and gain a deeper understanding of how the river characteristics work together during a flood event.

The use of satellite imagery is a way forward but is not particularly helpful to Ba Catchment as the flood extent is smaller compared to flood events experienced globally. The Ba Catchment is the 4th largest on Viti Levu and the impact it has is great on the people residing on the floodplain which is a common practice across the country. The use of SAR provides an opportunity to explore flooded waters in real time however the temporal and spatial resolution is a challenge since the catchment and river system is small and narrow to precisely map the flood extent using SAR only. The script in Googe Earth Engine was modified but the date of imagery after a flood is crucial in this method. The adjustments to the thresholding effect are required in the script which assists in the speckle filtering, a key filter in the methodology. The speckle reflectance impacts the flood output and further refinement is needed on the script to suit the conditions of Ba Catchment. There is also a need for training and capacity building on using remote sensing data for flood analysis and generating flood maps in the context of the Pacific Islands. The online remote sensing training available is tailored to suit large floodplains and replicability is a challenge to smaller catchments like Ba.

Chapter 5: Results

The results chapter presents the outcome of all methodologies aimed at answering the research question. Three methods were adopted to determine the most appropriate method to map flood risk zones based on the available datasets: i) Multi-Criteria Decision Analysis using Height at Nearest Drainage; ii) flood mapping using SAR imageries, and iii) one-dimensional flood mapping using HecRAS.

Each of these methods had its data requirements and was tested using local data collected through different authorities. The common data input in all methods was the digital elevation model, which was a combination of NASADEM, SRTM and LiDAR data. For the Height Above Nearest Drainage (HAND) results, the first part of the results will look at the flood extent result and the second part will look at the impact on land use and land cover of lower Ba Catchment. Results of SNAP and HEC-RAS are not analysed for land use land cover changes nor divided into zones for further interpretation.

The flood impact on people, infrastructure, and economy at the lower Ba Catchment is higher when compared to the middle and upper catchment as the administrative centre, major agriculture, and economic activity are concentrated here. The Ba Town and Rarawai sugar mill is situated at an elevation of 5.5 meters and is always impacted during a major flooding event. The HAND results were generated for the entire catchment area whereas the results from SNAP and HEC-RAS were generated for the lower Ba River. Therefore, the focus of the results is on the lower Ba River instead of the whole Ba Catchment. The results from each methodology of this research are discussed relating to flood extent output. The HAND result is generated from QGIS software using geospatial analysis. The SNAP result is generated using remote sensing analysis of SAR imageries. The HEC-RAS result is generated using a simple one-dimensional river flow analysis. Out of all, the HAND method provided

the most suitable risk map and was determined to be appropriate for the study site with the available datasets. The HAND flood risk map is presented in three zones. Zone one looks at the results between Ba Bridge to the river mouth, zone two looks at the results between Rarawai Ward to Ba Bridge, and zone three is focused individually on Navala Village and Toge Village.

5.1 Results Generated from Height at Nearest Drainage Method

Generating flood maps helps communicate risk to people and infrastructure. The result of land use land cover analysis (Figure 45) is utilized to further understand the flood impact in Ba Catchment. The HAND result shows the likelihood and extent of flooding in Ba Catchment (Figure 46a). The results for zones one and two are overlayed on LiDAR orthomosaic. However, zone three is overlayed on the ESRI base map as the area was outside the LiDAR coverage. The HAND model reclassification is based on the vertical distance to the Ba River channel network. A flood susceptibility class of 5 is the highest flood class in the model and is for all areas that are 0-2 meters above the river channel. The value ranges from 1 to 5 of which 5 is high risk and 1 is a very low risk of flooding (Table 9). The building outlines and road data were downloaded from Open Street Map which was edited to cover any missing roads and buildings within the selected sites. The missing buildings were identified after comparing the latest google earth imagery with open street map data and new buildings were digitized. The Open Street Map buildings and road data are clipped to Ba Catchment to assist in calculating the buildings and roads within the flood zone. There are 8873 building polygons and 1577 polylines representing the major and minor roads, bridges, and tracks in the Ba catchment.

Vertical distance to stream (m)	Flood susceptibility class
0-2	5
2-4	4
4-6	3
6-8	2
8-10	1
10+	0

Table 9 flood susceptibility class of vertical distance to channel network to determine flood extent surrounding lower Ba River.

Land use land cover analysis shows that the majority of the lower catchment is under agricultural activity with the upper catchment having heavily disturbed *talasiga* (fire scar). The results are utilised in checking the impact of floods on different land use and land cover.

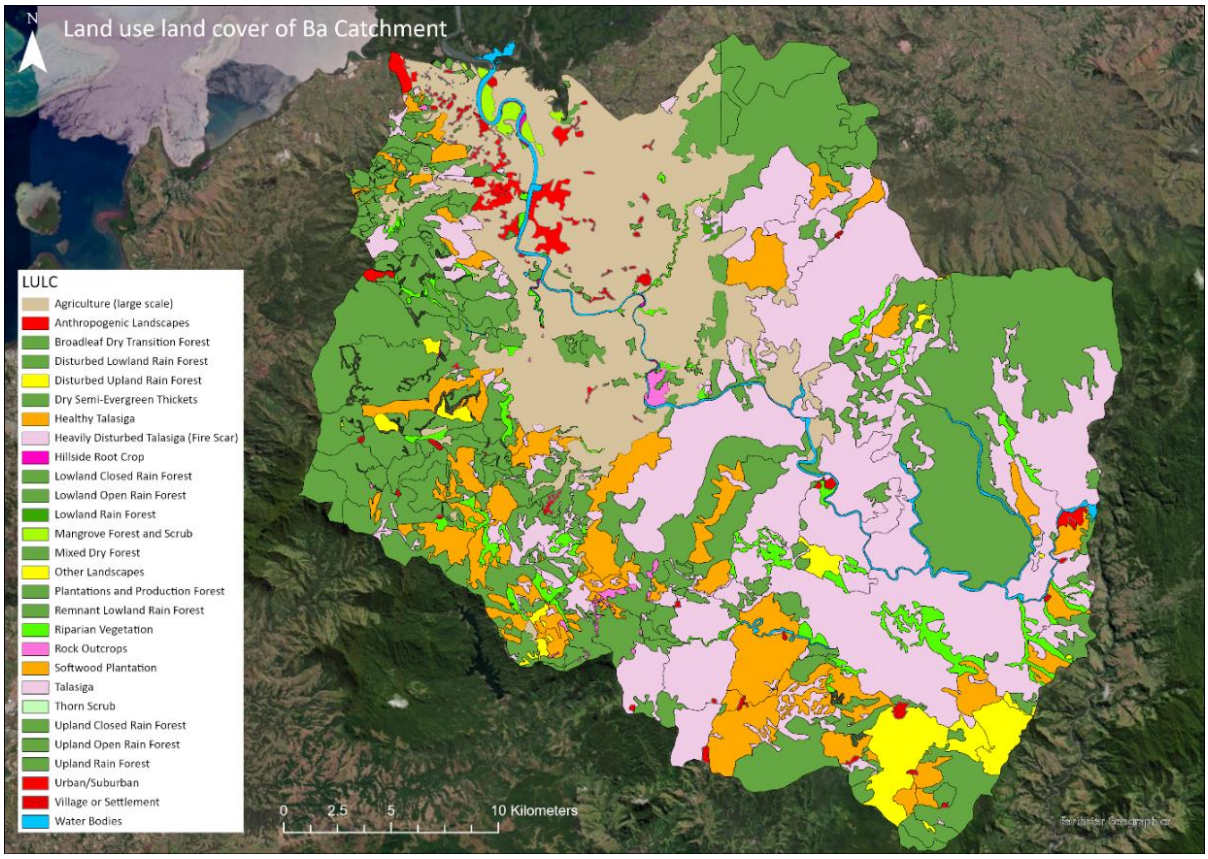

Figure 45 Land use Land cover classification of Ba Catchment through interpretation of satellite imagery and local knowledge. Map by Zoyha Nisha.

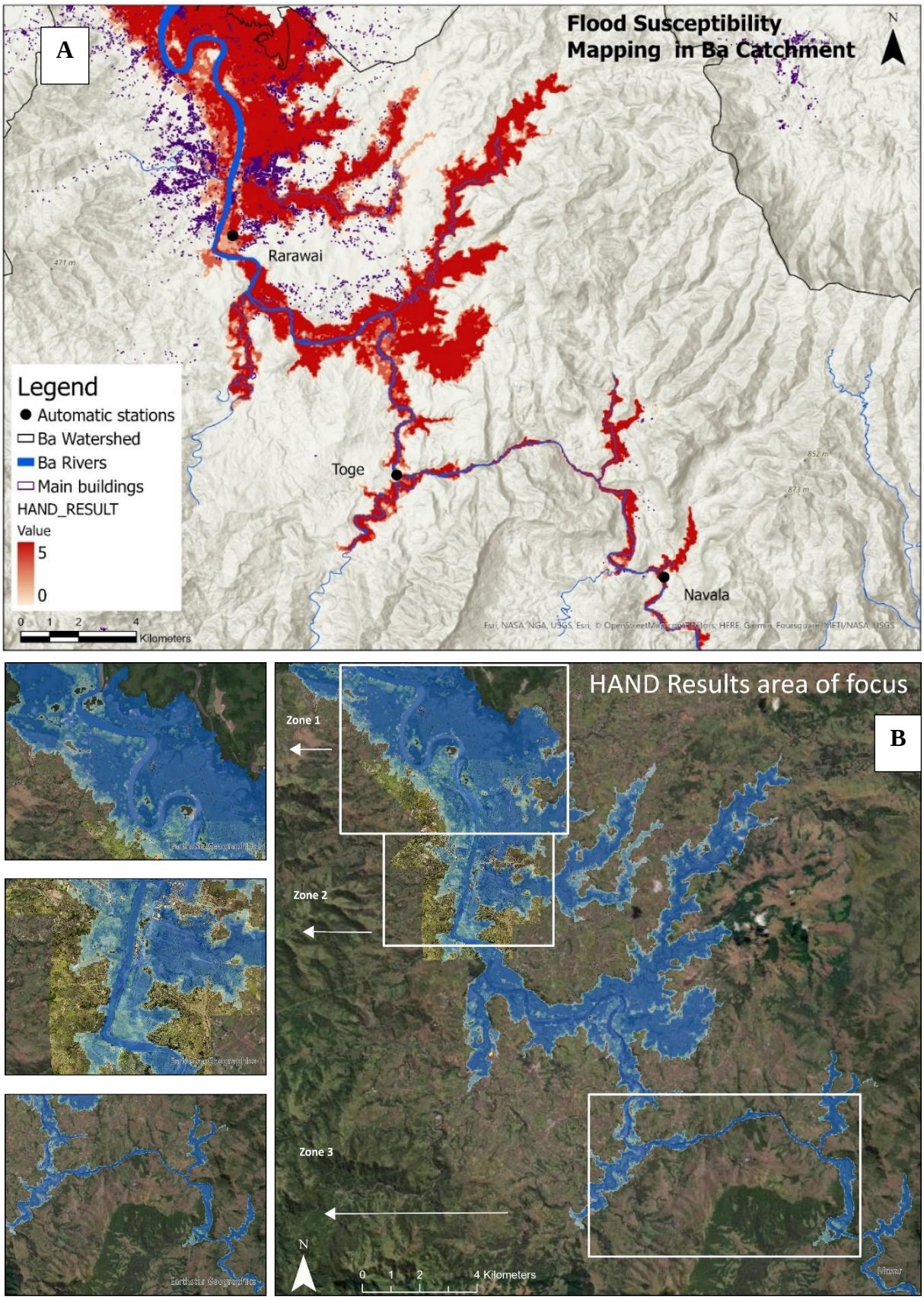

Figure 46 (a).Result of HAND model categorized in ranges between high, medium, and low and (b) further categorized in zones to discuss each area.

5.11 Zone one

Zone one covers downstream of Ba Bridge to the mangrove delta by the river mouth. The zone is home to ten villages totalling approximately 1633 buildings. The results show the entire zone as having medium to high flood risk (Figure 47). The elevation is approximately between 0.5 - 4.5m above mean sea level which makes it the most susceptible to widespread flooding in Ba Catchment as the topography is generally flat. The area is predominantly sugarcane and subsistence agriculture where some farmers have additional constructions on their lands such as small fertilizer storage sheds, small machinery sheds, piggeries/livestock sheds, and temporary accommodations for cane cutters engaged for the sugarcane harvesting season.

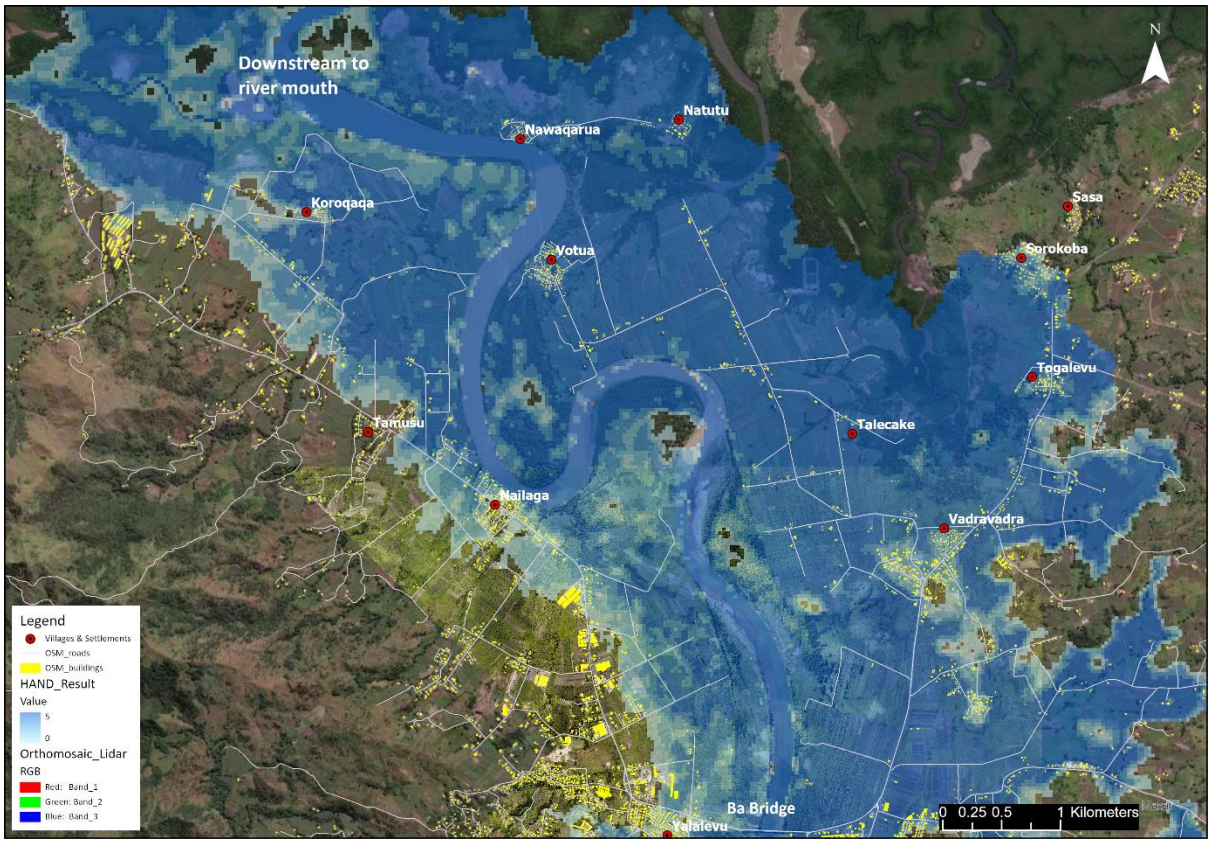

Figure 47 Flood extent in zone one shows 10 villages are directly impacted with flood heights of up to 4.5m

The HAND result is an indicative flood extent in zone one which shows many roads are also expected to be under flood waters which impact people's movement.

Land use land cover of zone one

The flood extent shows that the impact of flooding on the low-lying zone one is greatly felt by the sugarcane farmers in Ba Catchment. The land use land cover map of zone one shows that large-scale agriculture dominates and there is a remnant of lowland rainforest, mangrove forest and scrub, hillside root crop, and villages and settlements in the flood zone. The villagers that depend on large-scale agriculture and subsistence agriculture (root crops) are residing within the flood-prone extent and have built on resilience to flooding as people continue to reside in flood-prone areas. There are six evacuation centres for people within flood zone one, however, it is situated along higher elevations where flood risk is low in the zone. The evacuation centres are Koroqaqa Village Church, Votua Catholic School, Nailaga Village Church, Wailailai Sanatan Dharam Kanya Temple, Vadravadra Village Church, and Talecake Village Hall and Church (Figure 48).

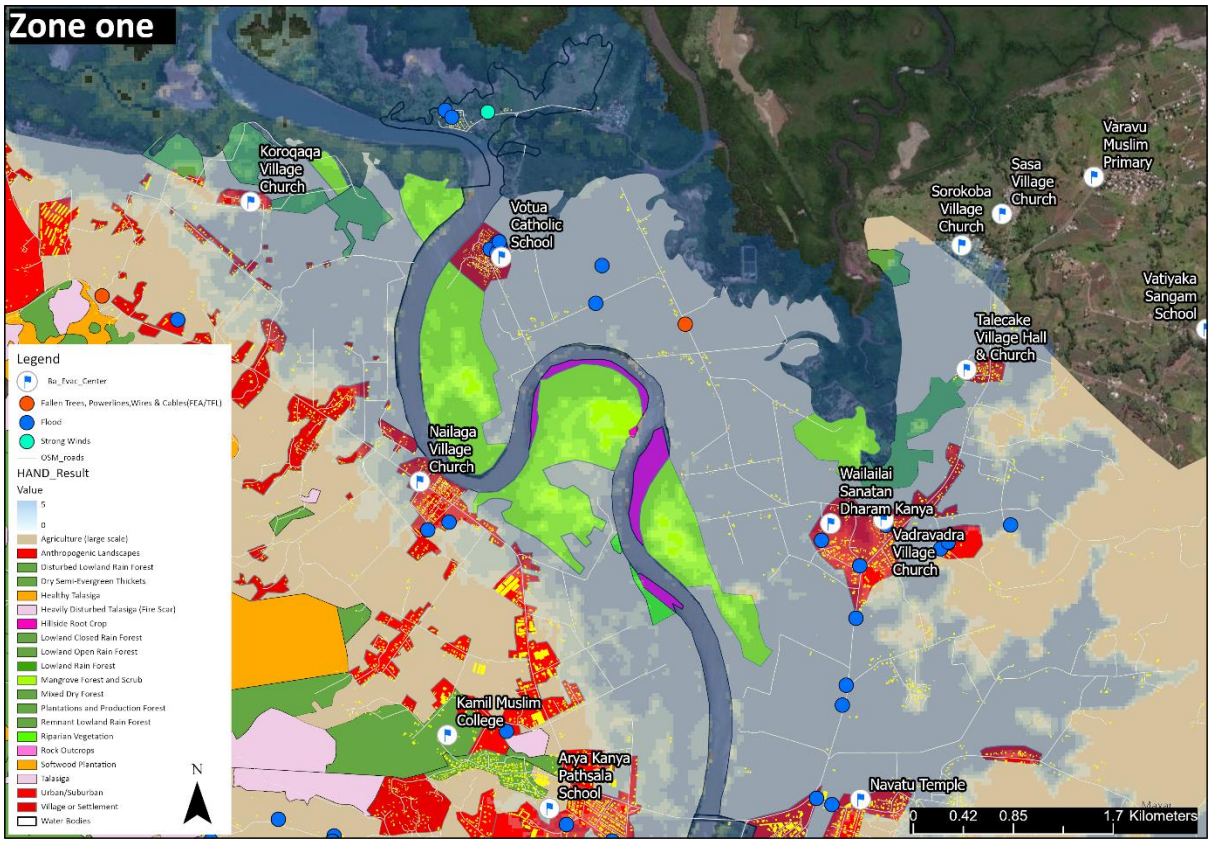

Figure 48 The land use land cover map of zone one is overlayed under the HAND result to ascertain flood extent. HAND result transparency (grey colour) shows mainly agricultural land is within flood extent.

5.12 Zone two

In zone two, each ward in the Ba Town boundary is analysed to measure the proportion of buildings within the flood extent. The five wards (Namosau, Varoka, Yalalevu, Varadoli, and Rarawai) together make up the entire Ba Town boundary. Most of the buildings are commercial and residential (Figure 49).

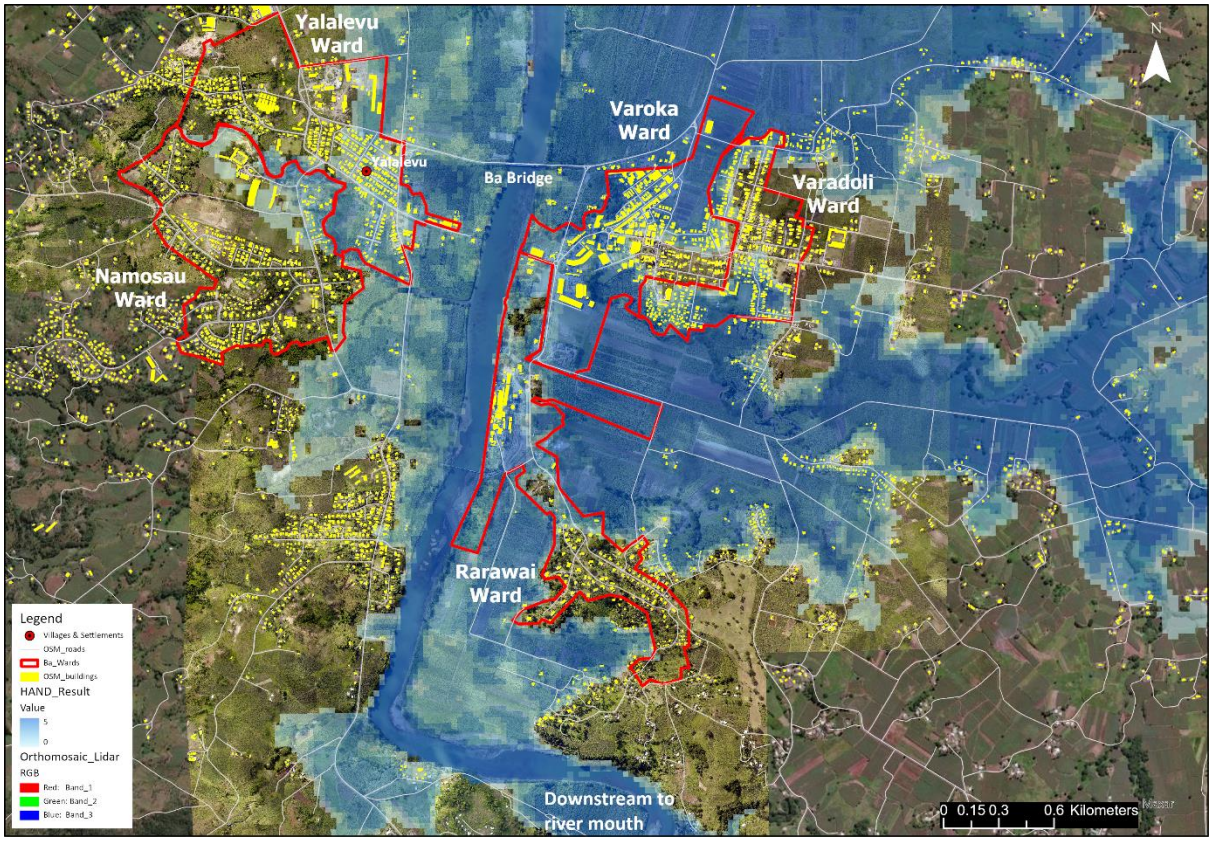

Figure 49 HAND result showing flood extent around Ba Town area and surrounding wards

Rarawai Ward

Rarawai ward is one of the most affected by floods as it is situated beside the Ba River (Figure 50). The results show areas near the Rarawai Mill to have a pixel value between 3 to 4. This would mean that the height of flood water around the Rarawai mill is about 2 meters to 6 meters. The history of flood levels affecting Rarawai Mill coincides with this result as discussed by McAneney, Honert, & Yeo (2017). The accuracy of this assessment is medium and there was also an estimation of flood water height inside the mill by using flood

level/mark records at the Ba railway bridge upstream and the level recorder at Ba Town downstream.

The ward contains mainly sugarcane plantations with a residential area along Rarawai Road. The sugarcane plantations are affected by flood heights of 2 meters to 6 meters as the elevation of the area is below 10 meters mean sea level and the terrain is generally flat making it ideal for sugarcane plantations which are also silted by the river deposits during floods. The Rarawai settlement, Fiji Sugar Corporation Staff quarters, and Field 25 settlement are also affected by flood waters between 2-6 meter heights as the area also has influx from Elevuka Creek. The road access to areas out of the ward is all blocked as the flood water impacts the Rarawai bridge and Rarawai road leading to the ward.

The total number of buildings digitized from the ESRI base map for the Rarawai ward is 206. This includes important buildings such as the Energy Fiji Limited power station, Rarawai School, Ba Court House, Rarawai Sugar Mill, and Fiji Sugar Corporation staff quarters. Out of 183 buildings, 36 are affected by flood waters in the ward. Most of these buildings are of the Rarawai Mill of Fiji Sugar Corporation (FSC). The ground truth information provided by the National Disaster Management Office shows that the ward has been affected by floods, the impact of strong winds during tropical cyclones, and damage to trees and electrical lines. The agricultural farmers are assessed by the Ministry of Agriculture and sugarcane plantations are assessed by the Fiji Sugar Corporation to estimate losses and assist farmers with seeds and seedlings and prepare mitigation plans to resume activity.

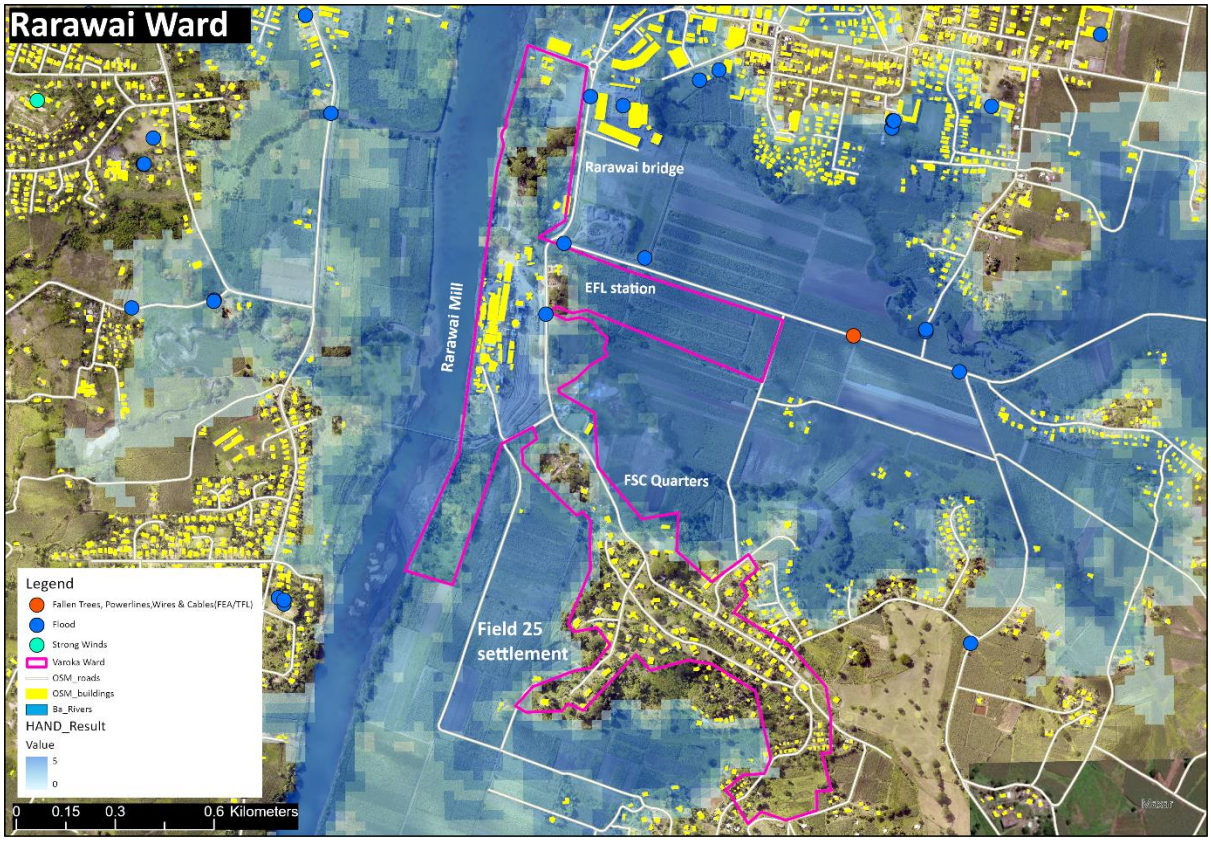

Figure 50 Flood extent in Rarawai Ward

Namosau Ward

The Namosau bridge is affected by flood waters, limiting access to the ward (Figure 51). The ground bulletin reported 0.65 meters of flood water on Namosau Bridge during the January 2018 floods (Force, 2018). Although many buildings in the ward are safe from flood waters, the result may be inconsistent with actual flooding reports as not all of Namosau Creek is part of the HAND analysis. The National Disaster Management Office data also have floods recorded within the ward and on the bridge of Namosau Creek. The ward boundary includes Xavier College and Govind Park which the results show as areas with low flood heights. The area was reported to have flooded during the January 2009 floods however a diversion in 2013 successfully eased the flooding of the area (Mathewsell, 2013). Out of 446 buildings in the ward boundary, 68 are within the flood zone as seen in the result. The flood waters are often from the creek running through the ward during small-scale localized floods however

the flood water reaches the ward from the Ba River during major events. Xavier College is one of the evacuation centres in the ward and was impacted by the 2018 flood caused by Tropical Cyclone Keni.

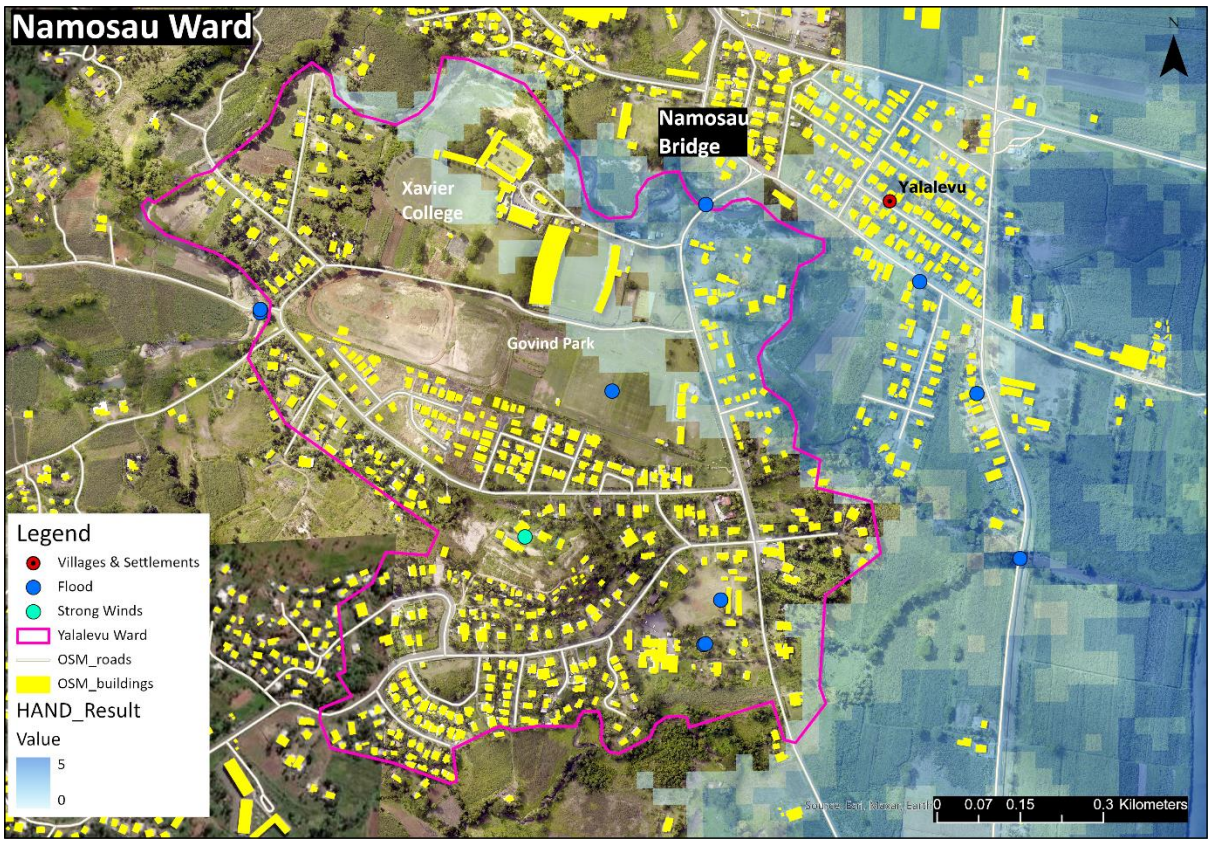

Figure 51 Flood extent in Namosau Ward

Varadoli Ward

Most of the area is at a higher elevation than the floodplain however there are also many buildings within the flood zone. The ward represents part of the Ba Town commercial and residential centre. There are 315 buildings in the Varadoli ward out of which 205 are within the flood zone (Figure 52). The contour of this ward ranges between 2.5m-7m in the flooded areas and 13-20m in the flood-safe zone. The flooded areas are along Navatu temple in the Varadoli ward north boundary which is impacted by 0-2m flood height. The results show that most of the area is not flooded however no two flood extents are the same. Flood waters may affect this ward due to high tides during flood events impacting the flood level. The schools,

AD Patel and DAV College are evacuation centres to support residents impacted by a disaster and are outside flood risk areas.

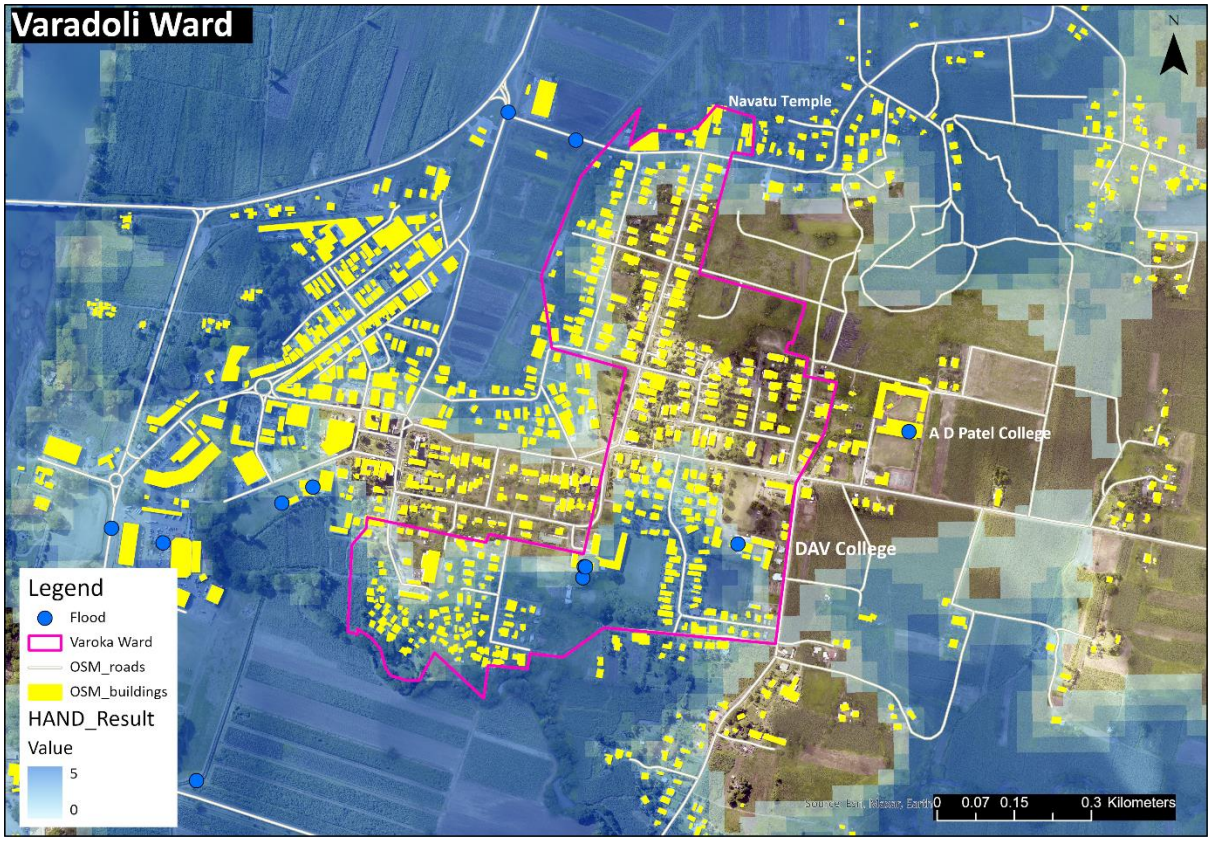

Figure 52 Flood extent in Varadoli Ward

Yalalevu Ward

There are 410 buildings out of which 201 are in the flood zone. This ward is generally a residential area and has some sugarcane plantations and a logging sawmill. As seen in the results, half of the ward falls in the flood zone with an estimated flood height of between 2 meters to 4 meters (Figure 53). The ward is by the Nestle Factory which experienced flooding on King's Road in 2018 (Force, 2018). The nearest evacuation centre for this ward is at Kamil Muslim College (by Nestle Factory) which was not affected during the 2018 flood and the site does not fall in the flood zone in the results however the site was flooded during tropical cyclone Winston in 2016. The area is likely to be affected by localized floods as Namosau

Creek runs along the Southern boundary of the ward with Namosau Bridge crossing also being impacted by flood waters. The main highway (King's Highway) is affected by flood waters below 2 meters which limits the movement of people and emergency services however the residents can move away to Kamil Muslim College for evacuation as the residential roads link towards it making alternative travel routes for people. the elevation of the ward is above 10 meters which protects residents during major flood events. The extent of the flood is along the low-lying elevations of the ward however, these areas are also nearer to the Ba River and Namosau Creek.

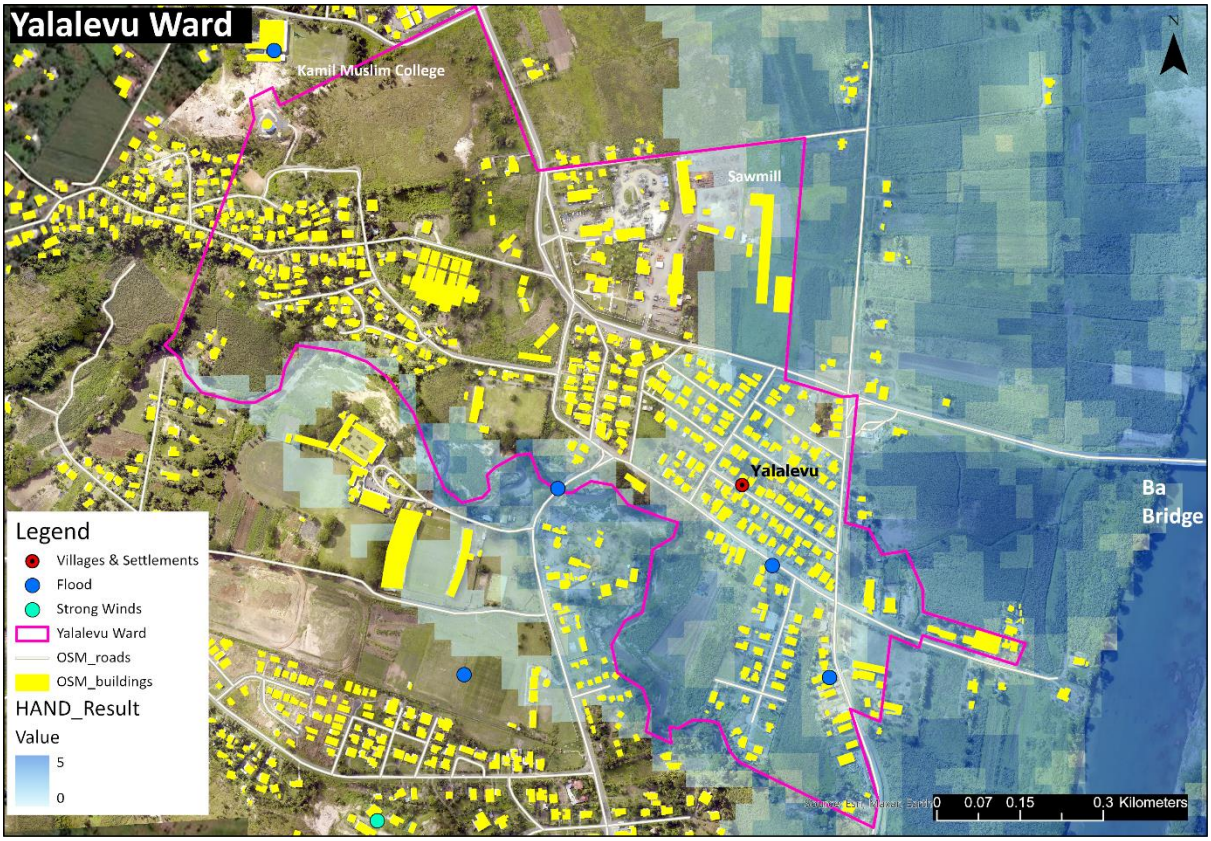

Figure 53 Flood extent in Yalalevu Ward

Varoka Ward

There are 267 buildings out of which 194 are within the flood zone making this ward the most affected in the Ba Town boundary (Figure 54). This ward represents the main Ba Town Centre. There are two fuel stations and all the commercial buildings within the ward. The other buildings are residential properties. The height of flood waters in Varoka ward is

between 0 to 4 meters. This flood height restricts access to low-lying areas. The results below show the majority of the ward as affected by flood waters hence increasing damage cost and risk to residents.

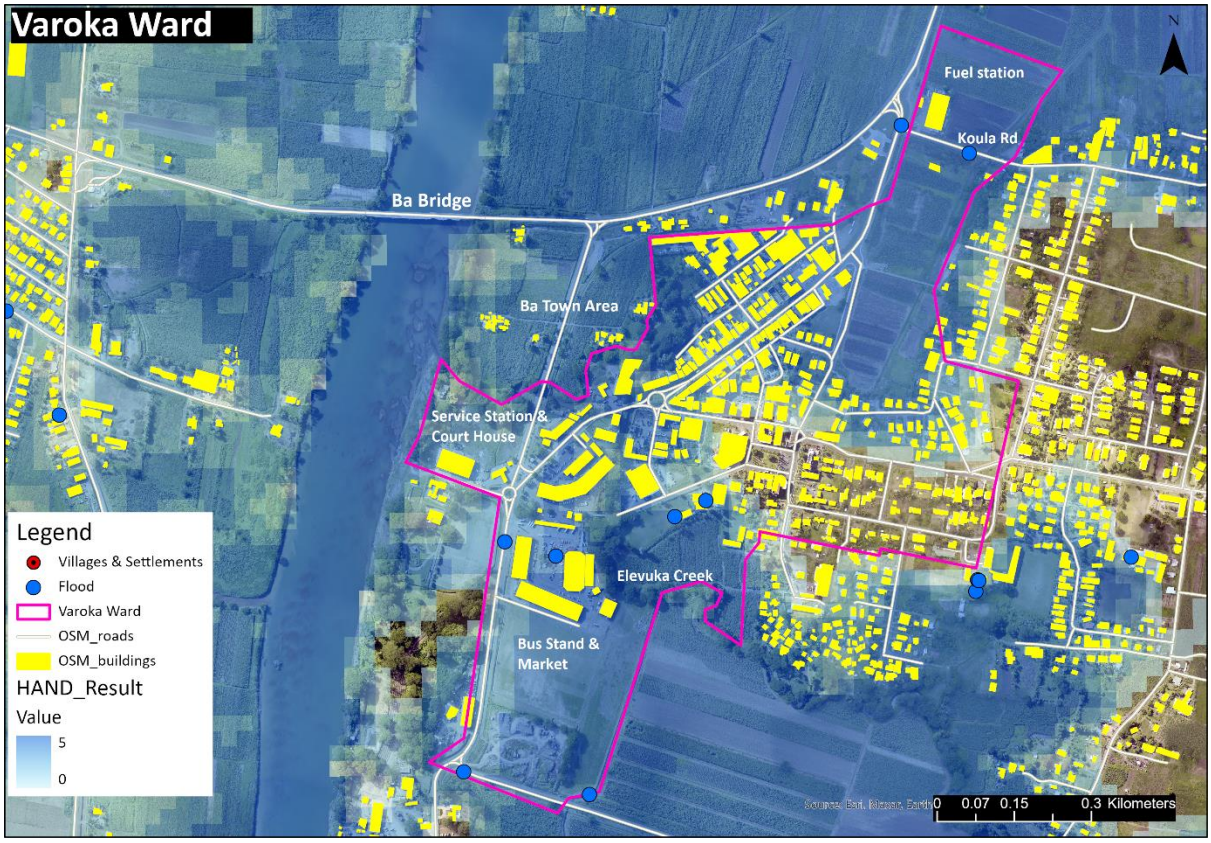

Figure 54 Flood extent in Varoka Ward

Land use Land cover of zone two

Analysis of land use and land cover show that zone two is highly populated and has a lot of buildings. There is some riparian vegetation along the river channel. A noticeable classification is the presence of disturbed lowland rainforest outside the Town boundary which can be attributed to the high surface water runoff into the streams and rivers. The disturbance and lack of good forest cover exacerbate sediment flow and contribute to soil loss and siltation of river channels. Areas that are not classified as urban, village, or settlements, and anthropogenic landscapes are agriculture. These are sugarcane plantations that contribute to Fiji's sugar export market. The map shows the extent of the HAND result and the land use

land cover classification of zone two (Figure 55). There are eight designated evacuation centres namely Arya Kanya Patshala School, Navatu Temple, Namosau Methodist School, Fiji National University Ba Campus, Vatulaulau Sanatan Dharam School, Nasolo Village Church, FSC Hall, and Rarawai FSC Primary School. Five of these evacuation centres are outside the flood extent while three are within the flood risk areas. Flood hazard has been ground truth all over the zone as per datasets provided by the Fiji National Disaster Management Office. The major transit roads and bridges are also impacted by flood water in the zone which can lead to high losses to infrastructure.

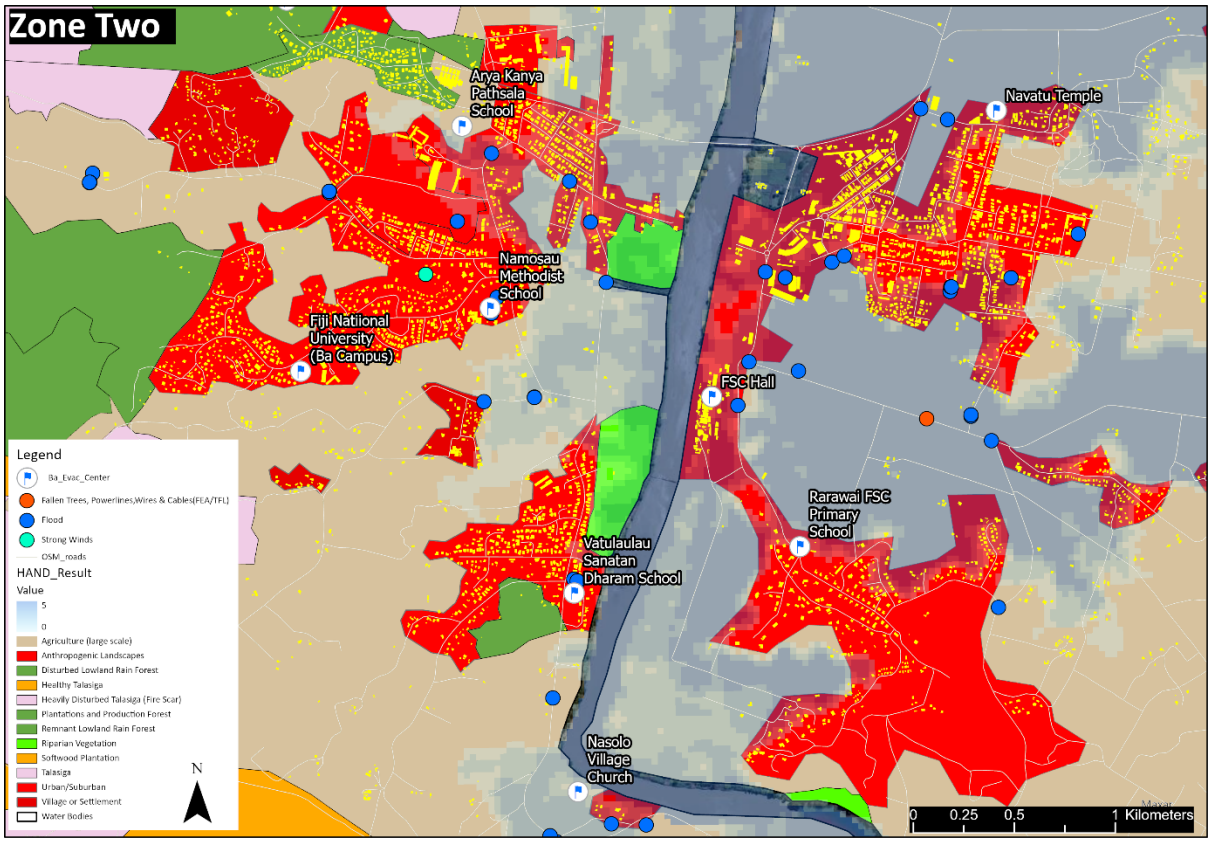

Figure 55 The land use land cover map of zone two is overlayed under the HAND result to ascertain flood extent. HAND result transparency (grey colour) shows mainly urban and agricultural land is within flood extent.

5.13 Zone 3

The extent of zone three is reduced to Navala and Toge villages. The flood extent varies across the zones as most areas are hilly upland and the flood zone is seen across the flood

plain by the two villages (Figure 56). The land use land cover analysis shows that there are scattered buildings, and the majority of the buildings are within the village boundary. There are few roads leading to the village however both are accessed via bridges that are within the flood zone as these bridges are below the flood plain and are constructed a meter above the riverbeds.

Figure 56 Zone three extent of HAND result

The remaining areas in zone three have heavily disturbed *talasiga* which refers to areas with dry grasslands and poor soil nutrients to support agriculture/forests (Figure 57). The area is intermixed with upland forests which are growing at an altitude between 600m-800m and land closer to the river is utilized for agricultural activities. There are some areas of healthy *talasiga* nearby the villages which hold forest cover. The exposed grassland is a factor contributing to the runoff into the rivers. The steep slopes of hilly areas surrounding the village boundaries represent the heavily disturbed *talasiga* which needs management and

can be restored with forest species that can thrive in these soil structures so that forests can help reduce runoff and slow down the flow of water into the river systems.

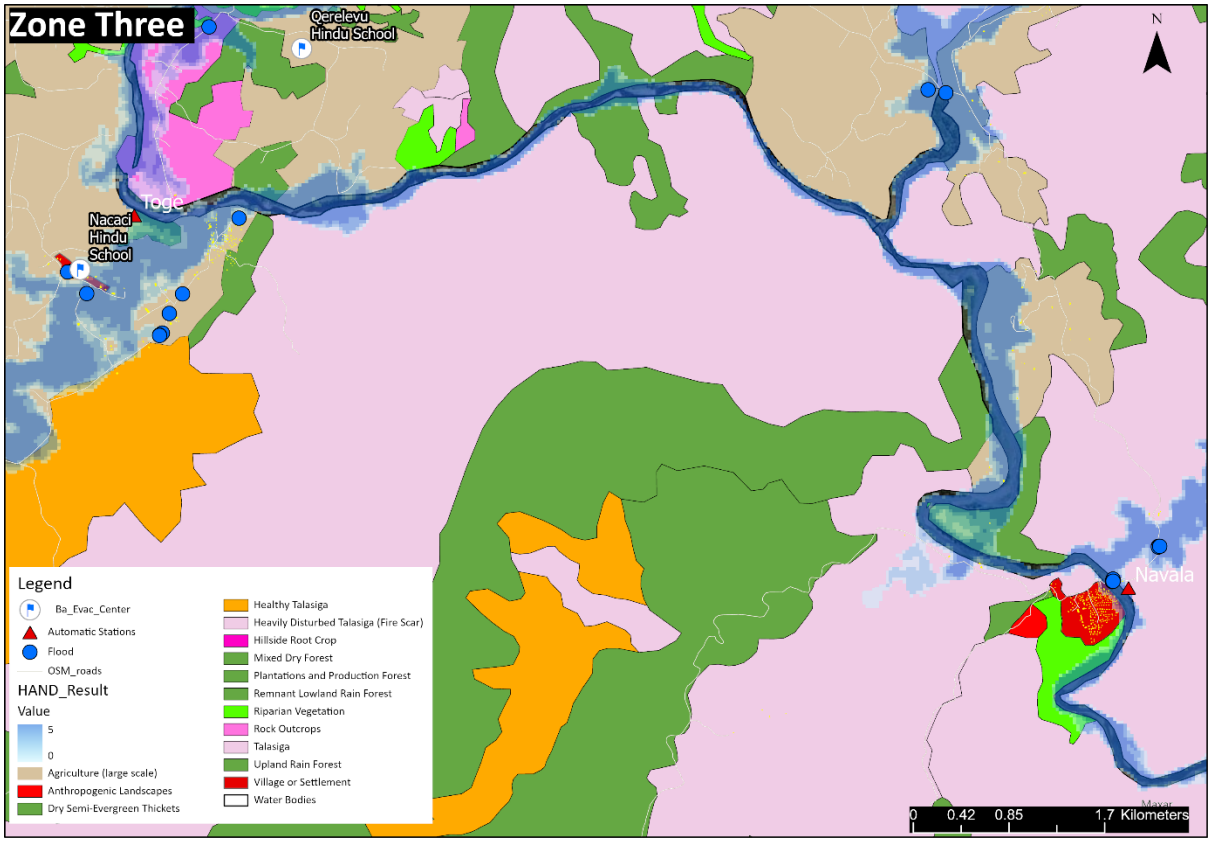

Figure 57 Land use land cover analysis of zone three shows the majority is Talasiga soil further classified as healthy and burnt. The flood extent is limited to low flood plains on the river bank where both of the villages is situated.

Navala Village

The village has 216 buildings out of which 32 fall within the flood zone. The flood heights estimated in the different areas of the village are between 6 meters to 8 meters in the results (Figure 58). The Navala crossing/ bridge was impacted in the 2012, 2016, 2018, 2019, 2020, and 2021 flood events as per ground truth data from the National Disaster Management Office.

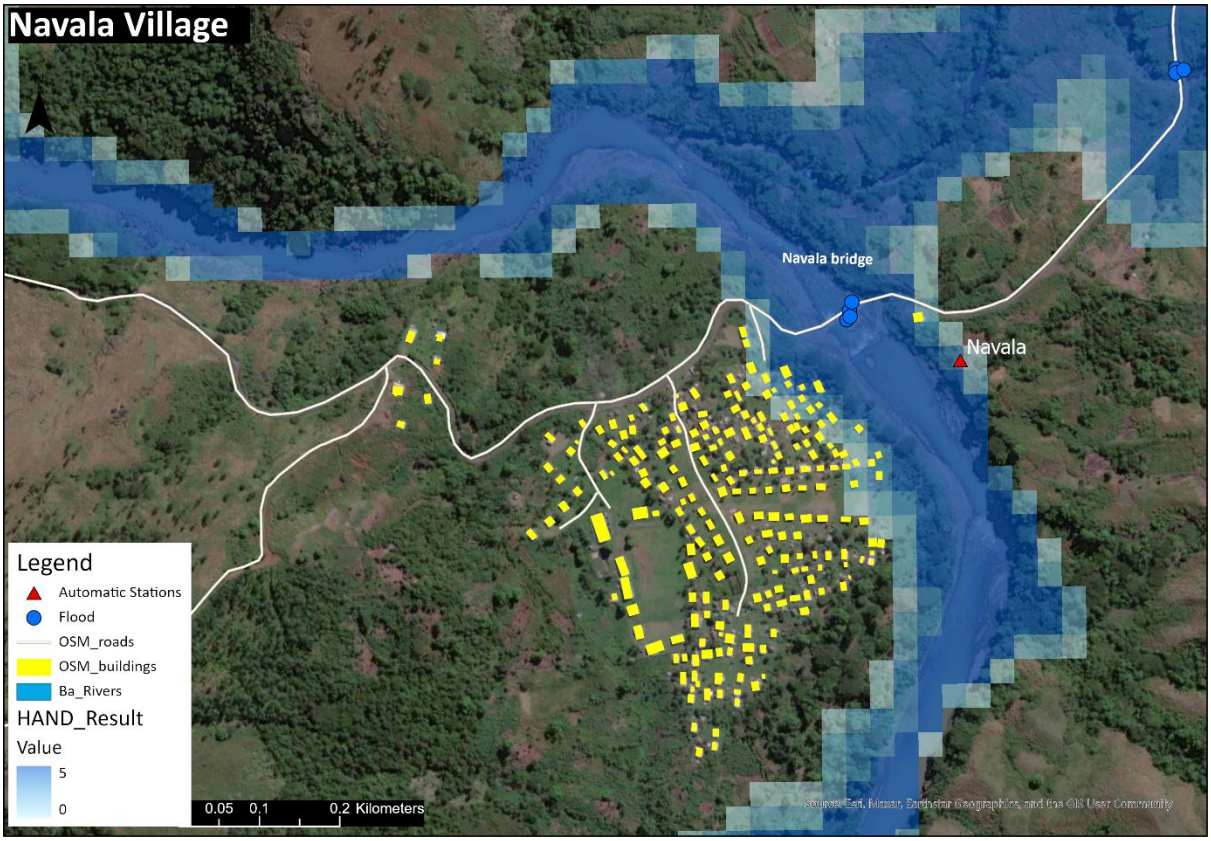

Figure 58 Flood extent in Navala Village

An automatic weather station is also situated along the riverbank which transmits to the satellite the rainfall and river water level data. This data is received in the system at the Fiji Meteorological Service office in Nadi to issue flood warnings. The height at which the automatic station is placed is also in the flood extent in the HAND result.

The land use land cover analysis of Navala Village shows that the majority of the surrounding areas of the village are classified as heavily disturbed *Talasiga* which is open grassland with very low forest cover (Figure 59). The area by the village has some riparian vegetation by the riverbank and the village is not involved in large-scale agriculture. The forest cover is not close to the village boundary, and this shows the large open *talasiga* grassland which impacts the runoff of sediments into the river during rainfall. The flood extent impacts largely the buildings in the village and the flood extent is limited to the flood plain which affects the subsistence agriculture and livelihood of the village. There is no

designated evacuation centre near the village and since most of the area is at a higher elevation than the flood plain, the village is largely safe during a flood event.

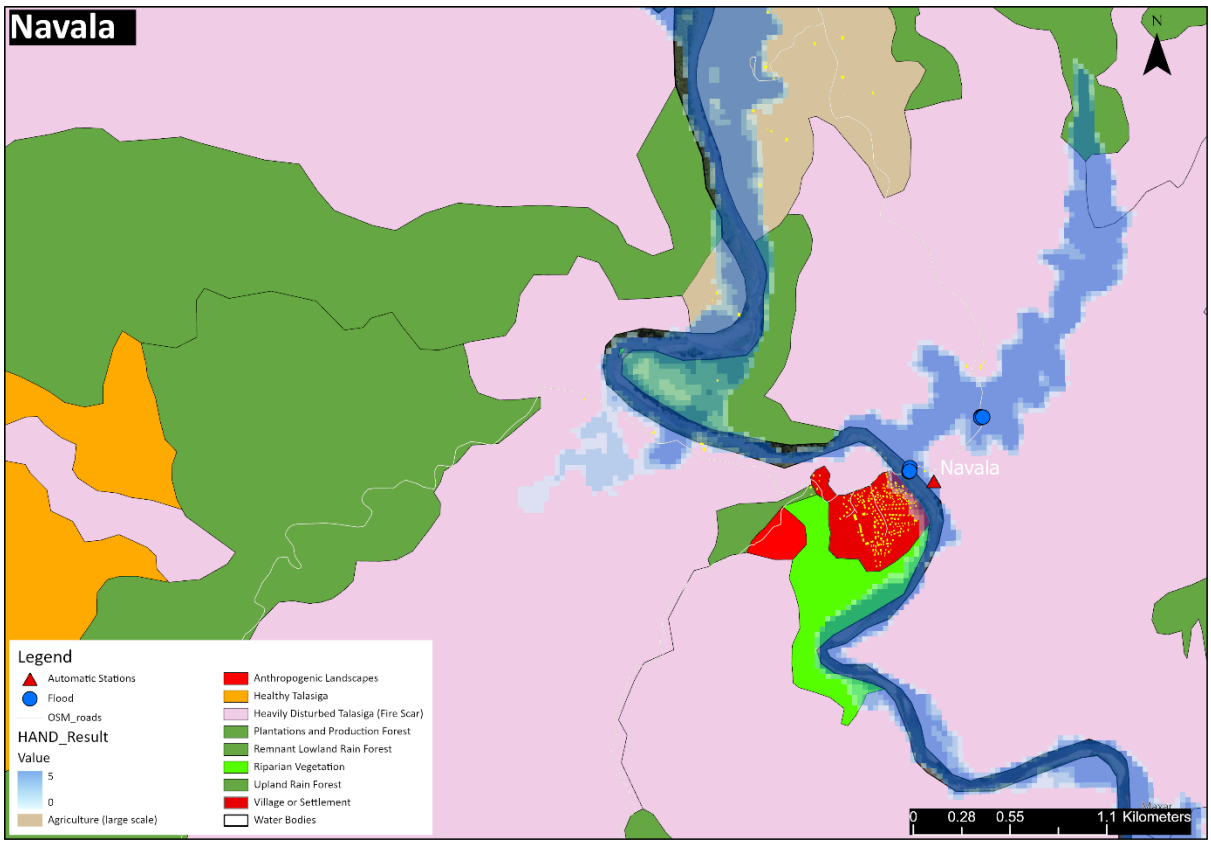

Figure 59 Land use land cover analysis of Navala Village

Toge village

The village has 104 buildings out of which 40 fall within the flood zone extent. The village is greatly impacted during large flooding events and the result estimates the flood heights to be between 4 meters to 8 meters in different parts of the village (Figure 60). Naloto District School is utilized as an evacuation centre that also falls within the flood zone in the results. There is only one designated evacuation centre in the area which is Nacaci Hindu School which is away from the village and roads leading to it are also impacted during flood events. Ground truth hazard data by the Fiji National Disaster Management Office show that the first and second Toge crossing/bridge were closed due to flood waters below two meters which is consistent with the results. The Ba River is merged with a confluence at Toge village which

affects the inflow of flood waters and increases the flow of water downstream. The results show a widespread flood extent which impacts the sugarcane plantations around the village. The bridge leading to the village is also flooded which restricts people's movement.

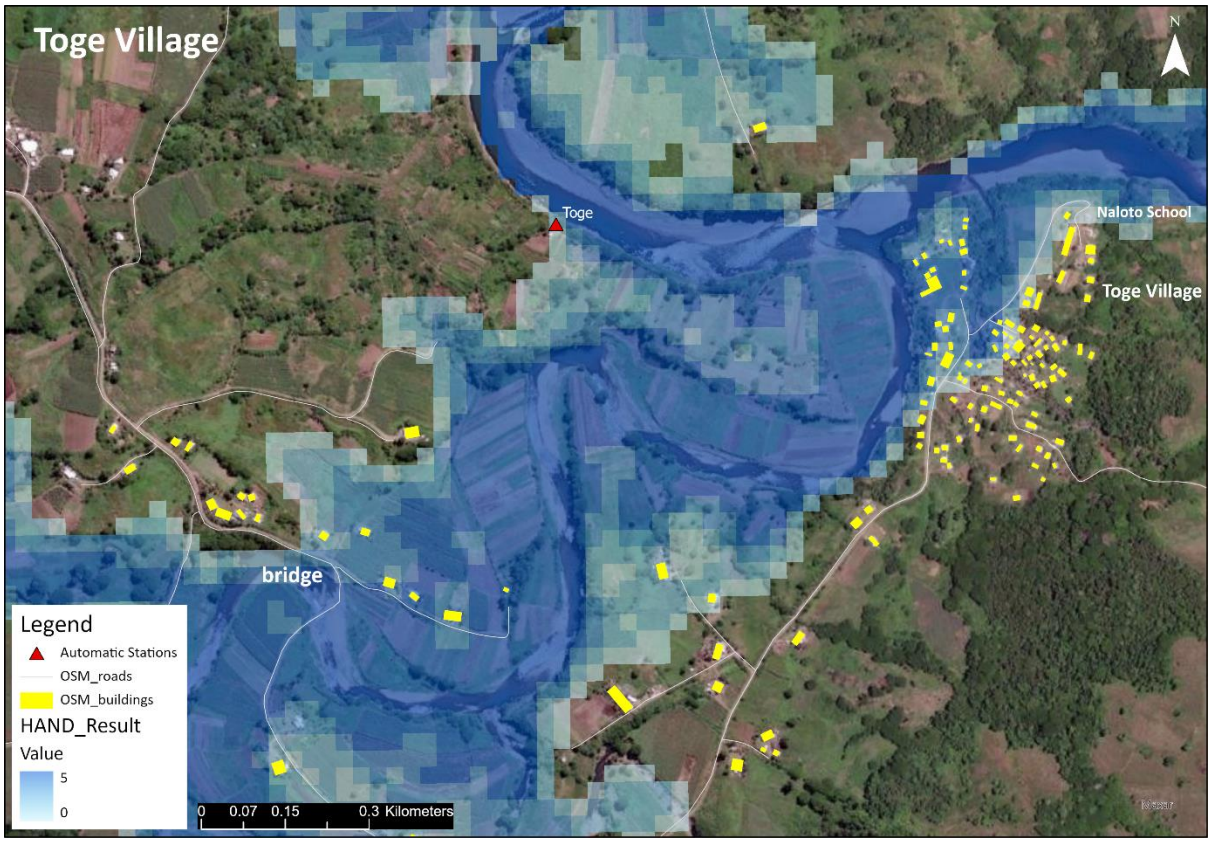

Figure 60 Flood extent in Toge Village

An automatic weather station is also placed on the banks of the river which transmits river water level data and rainfall data to Fiji Meteorological Services. However, it is noted from the rainfall data analysis that when a major flood event occurs and the station is underwater, the transmission of data is impacted. There is no record of the river water level at this crucial moment when it is highly important to gauge the critical water level in the river and ascertain the travel time of flow downstream to Ba Town and the river mouth.

The land use land cover of Toge village shows a large hillside root crop agricultural area (Figure 61). The majority of the land is utilized for large-scale agriculture and flood extent impacts the low flood plains. There is also *Talasiga* land near the village with very

little lowland forest cover and rocky outcrop which has exposed rock bedrock that cannot be utilized for any planting activity. There are flood hazards mapped near the village area that have been verified by the Fiji National Disaster Management Office.

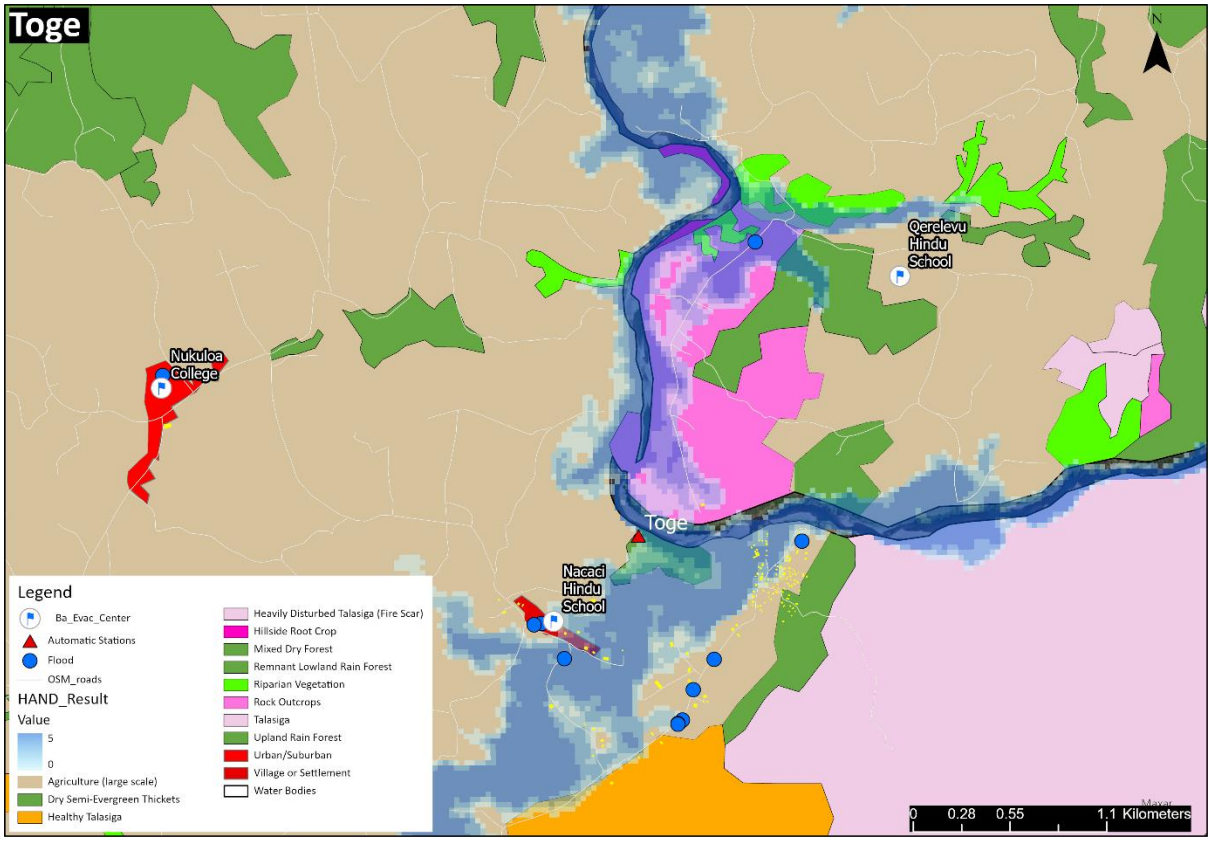

Figure 61 Land use land cover of Toge Village

5.2 SAR results validated using Google Earth Engine

The utilization of Synthetic Aperture Radar (SAR) imageries assists in identifying flood waters on land due to its capability to capture imageries. The SNAP result below shows that flood water was present in some areas in the lower Ba Catchment (Figure 62). The areas in red are depicted as flood waters being present on land during the time of SAR imagery capture. This analysis is of the 2018 flood event in April. The water-logged soil from sugarcane farms is reflected in the sensor and is shown more clearly at one site which is outside the Ba Town boundary and is in Zone 1 of the HAND results. The red colour depicting water presence is lighter in other areas and after masking out permanent water bodies, it shows areas where some water presence has been reflected. The result is displayed in Google Earth Pro to assist in validating areas of flood water.

Figure 62 results from SAR imagery which shows areas in red colour to have a presence of flood water

Since there is a high reflectance of cyan/ blue in the results, it was reclassified within the SNAP software to assist in identifying which areas were flood waters in the result as the red colour was mostly a lighter shade in many areas (Figure 63). The classification result assisted in better visualization and permanent water bodies were masked to remove from water/flood classification. The results show areas in the mountains, on the Western side of the imagery, to have flood water presence.

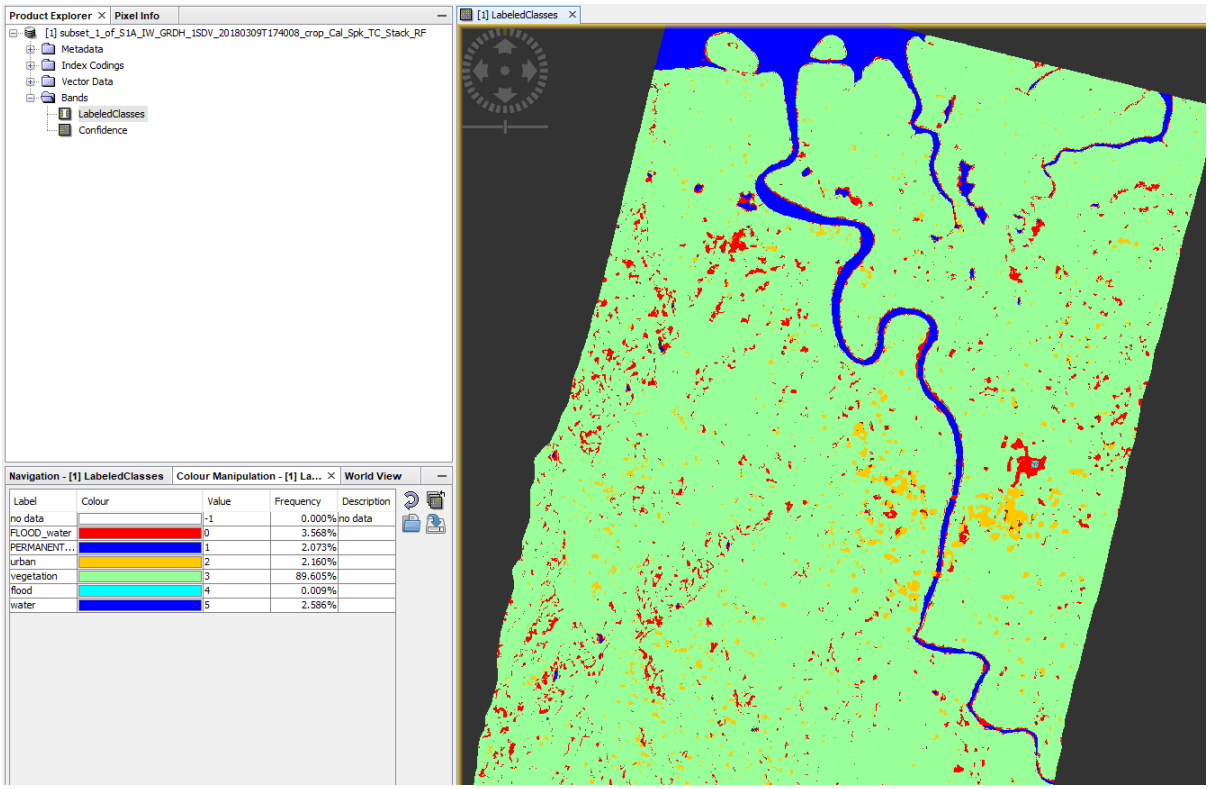

Figure 63 SAR results are manipulated into flood water, permanent water, urban, and vegetation classes to assist in analyzing the result

As a result of combined factors such as reflectance from bare ground and radar shadowing effects behind vertical objects such as vegetation, buildings, and topography, an increase in signal return is expected during flood conditions compared to non-flood conditions. This is because diffuse scattering may increase the corner reflection effect. During floods, the ability of microwaves to penetrate through the vegetation canopy is generally improved. This is because the presence of water in the vegetation canopy can

reduce the attenuation and scattering of the microwave signal, allowing it to penetrate deeper into the canopy and potentially detect the underlying floodwater.

However, the specific effects can depend on factors such as wavelength, polarization, and the type and density of vegetation present in the area. Therefore, L bands SAR sensors operating at about 23 centimetres have effectively detected forest floodings such as areas identified as red in the SAR output to be near riparian vegetation or large sugarcane farms. Typically, shorter wavelength SAR sensors (such as those operating at X and C bands) tend to have higher levels of canopy attenuation, volume scattering, and surface scattering from the top layer of forest canopies. SAR sensors with shorter wavelengths can have a negative impact on the detectability of flooding beneath vegetation due to increased double-bounce scattering.

Dual or quad-polarized SAR data provides more information on the ground's structural and geometric properties than single-polarized data. Polarimetric SAR imagery allows for a more precise differentiation between flooded and non-flooded forest areas. Following the analysis of imageries on SNAP, the Google Earth Engine (GEE) platform was utilized to automate the search and flood analysis by writing a simple JavaScript code. This allowed the flood hazard mapping of a few flood events rather than the 2018 April floods in Ba Catchment (Figure 64a-d). The code is provided in the appendix. Various factors can impact the result produced. The results produced in SNAP are by using the descending pass and VV VH polarization. With the code, both descending and ascending pass is analyzed to check if there are different results to show flood waters detected in SAR imageries.

GEE analysis of SAR imageries with ascending passes shows areas flooded as slightly different than descending passes. An important piece of information is that the after-flood imagery is dated 09/04/2018 for ascending pass whereas it is 02/04/2018 for descending pass.

This shows that the availability of imagery on the date of the flood event is crucial to deciding which is appropriate to use in the analysis. For the Ba flood events in April 2018, there were two tropical cyclones and flood events covering dates 02/04/2018 to 08/04/2018 and this has led to both passes showing flood waters. The results help to understand that there are certain differences expected from both polarizations, VV and VH. The VV polarization in both passes can show more flood waters detected than the VH polarization. The closest result from each pass and polarization to match the results from SNAP is the descending pass with VV polarization. The areas flooded in zone one HAND method is closely similar in descending pass.

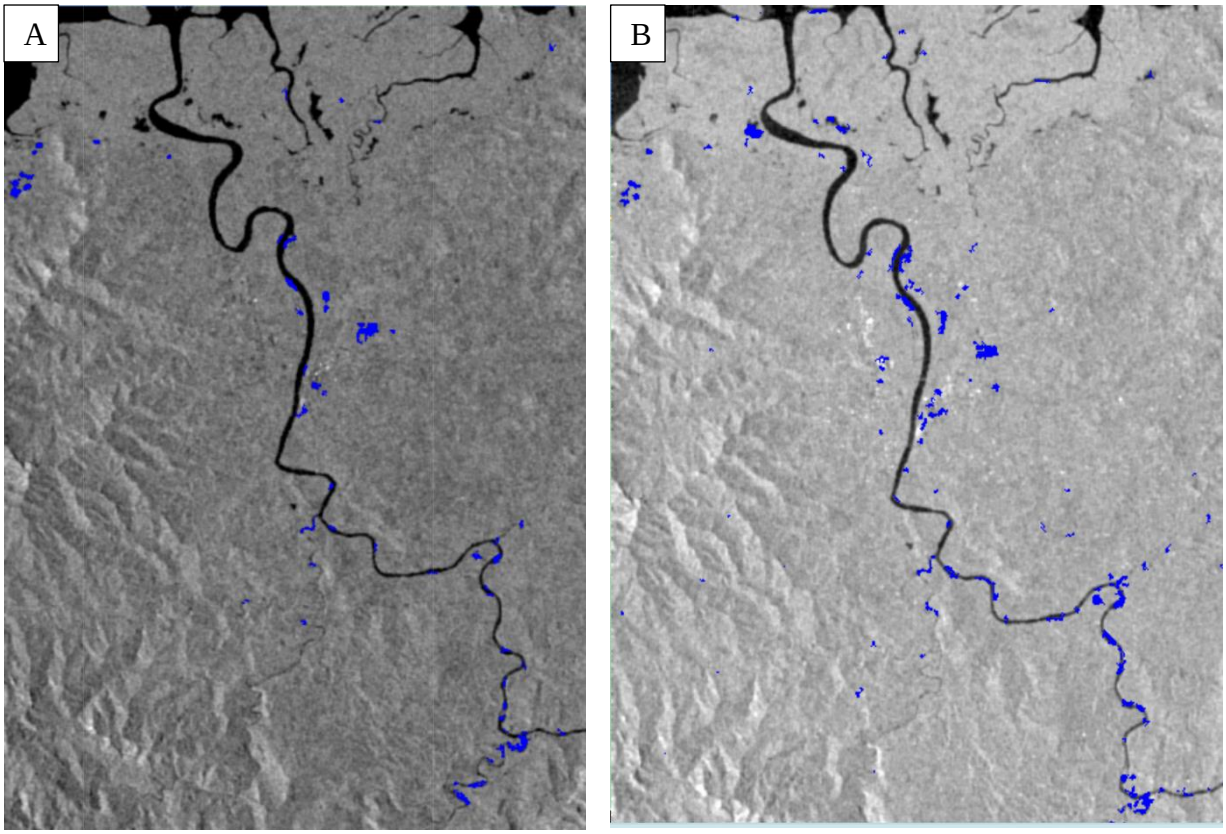

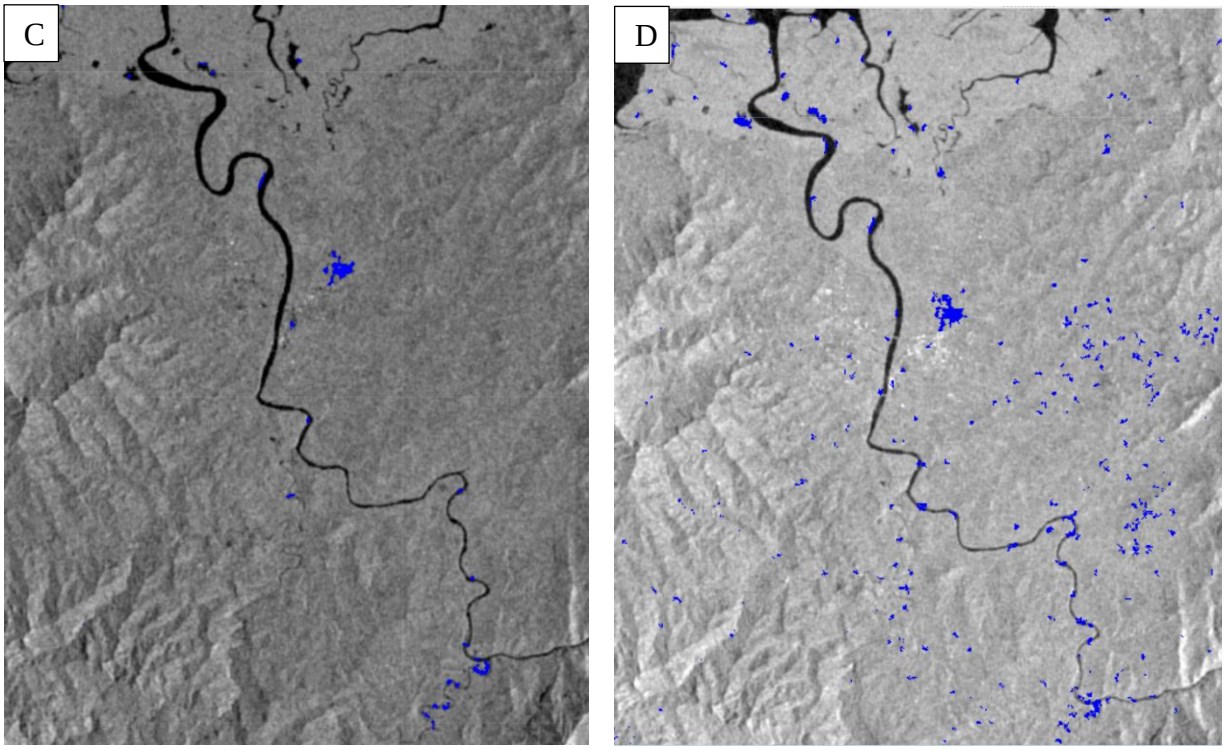

Figure 64 results of (a) VH Ascending, (b) VV Ascending, (c) VH Descending, and (d) VV Descending

5.3 HEC-RAS result

The one-dimensional simulation was designed and run in HEC-RAS to estimate flood extent using simple hydrological engineering methods. The simulation produced two different results which were due to the addition of the Ba Bridge in trial one and then the simulation was run without the bridge in trial two. The first 20km of river centrelines from the river mouth were digitized for this simulation as the LiDAR data was only of this coverage (Figure 65).

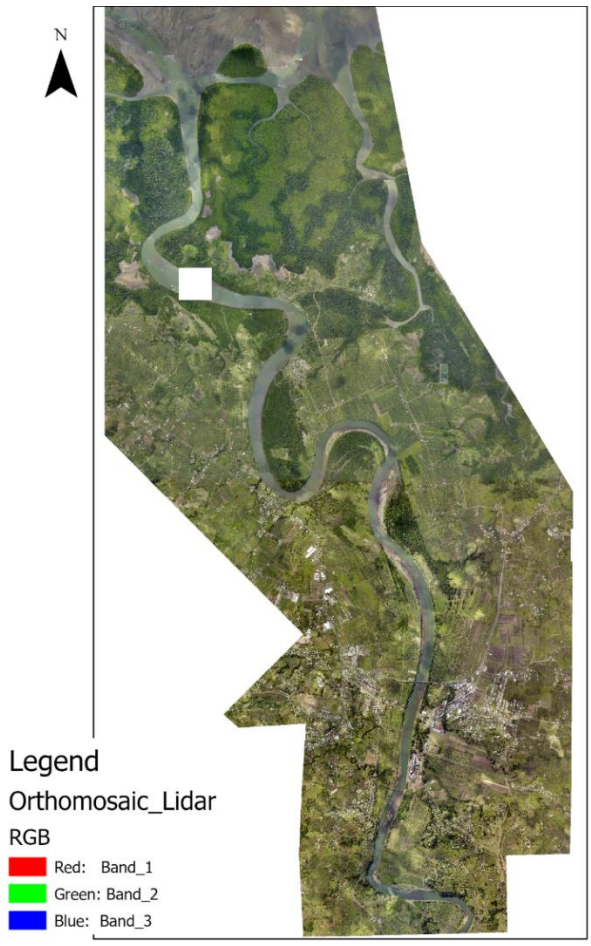

Figure 65 Orthomosaic of 434 LiDAR imageries to generate a DEM output

Below is the result for a selected slope calculation at each site and the Mannings coefficient is selected as 0.04 based on the natural character of the river and that flood waters affected the floodplain with vegetation cover. Manning's n will be input in the HEC-RAS model as an input to run the one- dimensional simulation. Manning's n is derived from the

roughness of surface features so that the flood model can be calibrated to depict real flood scenarios.

Toge slope = -0.0014

Navala slope= -0.0016

Mannings coefficient of roughness n = 0.040

The discharge was calculated using manning's n which is estimated below.

Table 10 Discharge estimate of the 2018 April flood at Toge and Navala Village.

Section	**Area (m^2)**	**Velocity (m/s)**	**Discharge (m^3/s)**
Toge section 1	1672	3.96	6614
Toge section 2	1883	3.32	6261
Toge section 3	2318	3.72	8643
Toge average		3.67	7173
Navala section 1	1655	4.20	6950
Navala section 2	1685	4.69	7907
Navala section 3	1527	4.28	6530
Navala section 2	1477	3.59	5301
Navala average		4.19	6672

The results generated with the bridge design showed that flood waters were throughout the floodplain and does not exceed the digitized bank lines (Figure 66). This result was restricted by the flow paths as no other tributaries were added to the design plan. The result also shows the estimated flood heights of the flow. The maximum flood height was 5.4m for the floodplains

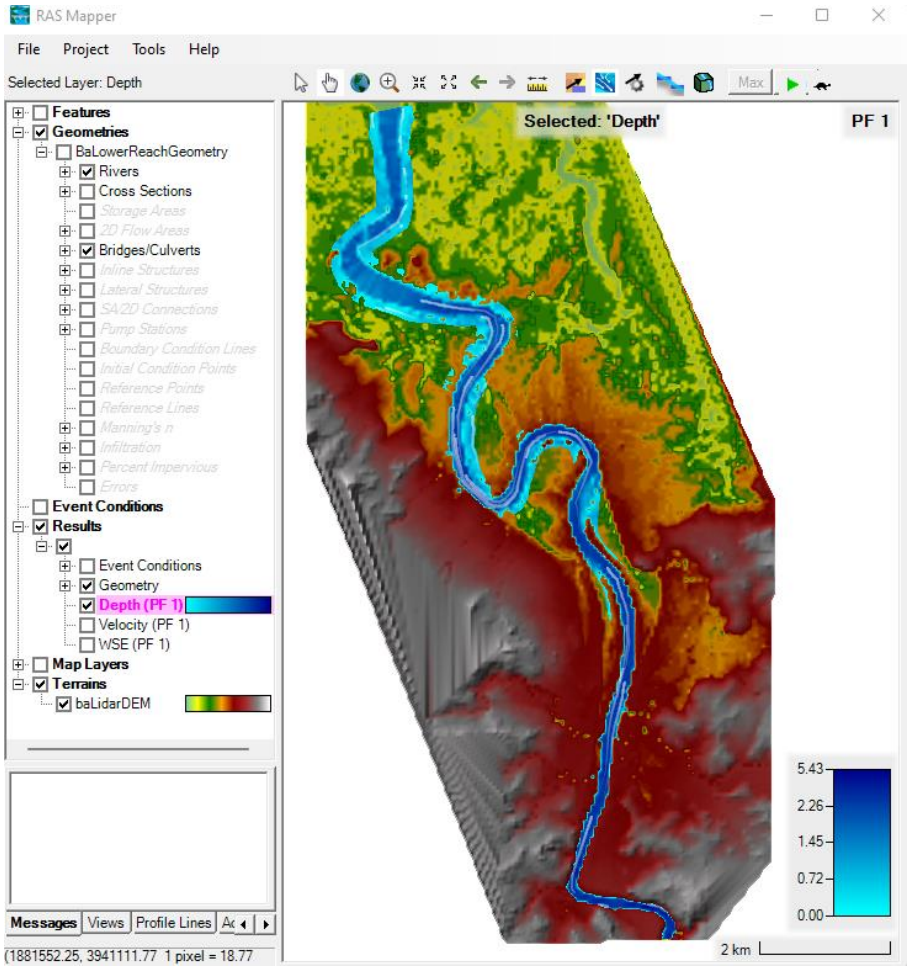

Figure 66 Plan 1 of one-dimensional flood simulation in HEC-RAS with Ba Bridge design added into the simulation

The second attempt to run a steady flow analysis without adding the bridge to the design plan produced a different result (Figure 67). The flood extent was different compared to attempt one as there were more widespread flood waters in zone one which was partly matching with HAND results. The removal of the bridge from the plan itself makes the model not fit for purpose as the real scenario on the ground is not reflected in the model. This attempt was undertaken to check if the first result was incorrect due to the improper design of the bridge. However, the flood extent generated in trial two shows the flood extent within the flood plains. Flood waters are along the riverbanks and are spreading mostly after the Ba Bridge towards the mangrove delta of zone one. The results also show a riverbank break after

the Ba Bridge. When comparing the HAND result with this, the area coverage is similar in the mangrove zone one by the river mouth.

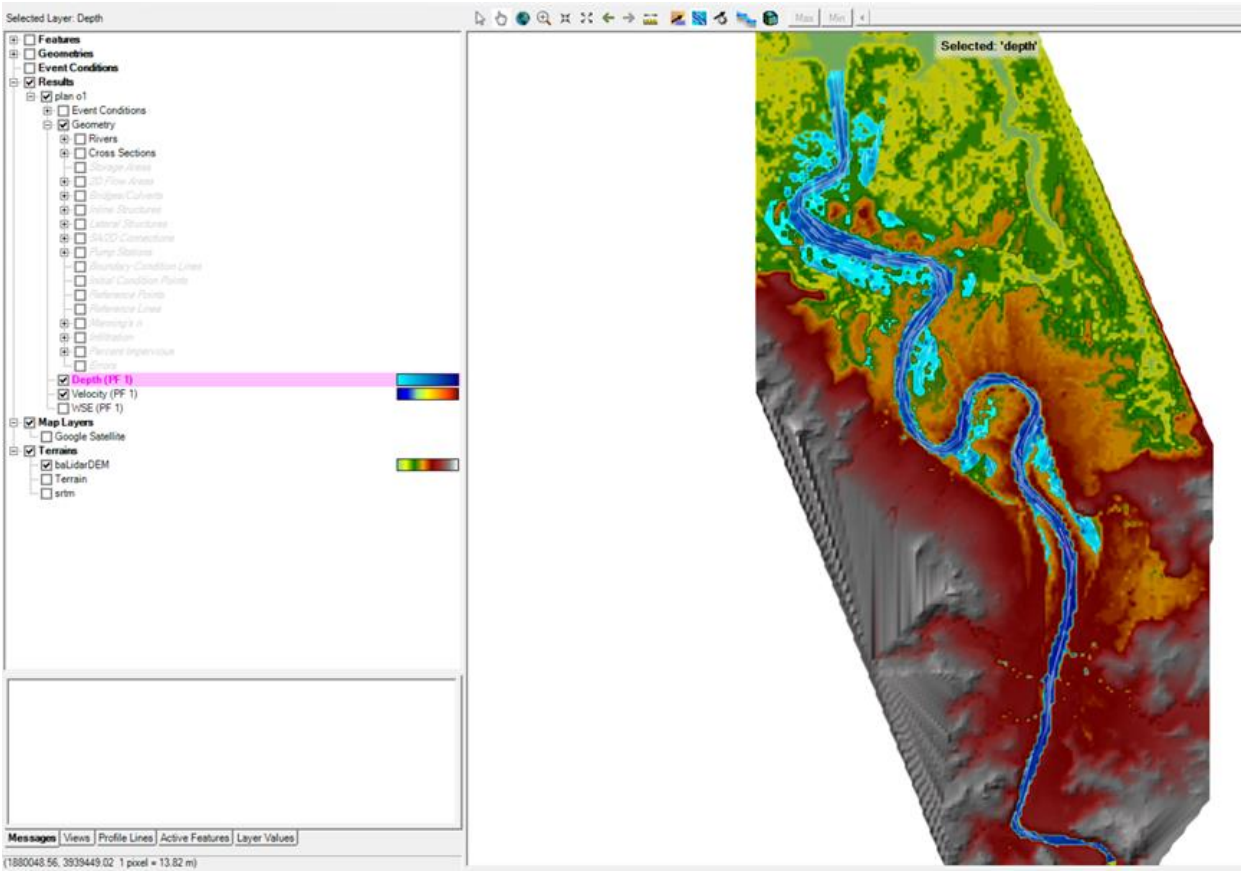

Figure 67 Plan 2 of one dimensional flood simulation in HEC-RAS without bridge design in the plan

The middle catchment was also attempted in trial three to see if the simulation was producing results that could be meaningful for zone three. The river and floodplain were digitized by the Navala and Toge villages as the cross-section data were available at these two locations. The result showed missing flows between meanders which is not the case during a flood event (Figure 68). The flow data and cross-sections were edited to recalibrate the plan however the results did not change which meant that the simulation required further calibration. The attempt to improve trial plan 3 was not carried out as the knowledge, skillset, and time were not sufficient to meet the planning needs of HEC-RAS flood models.

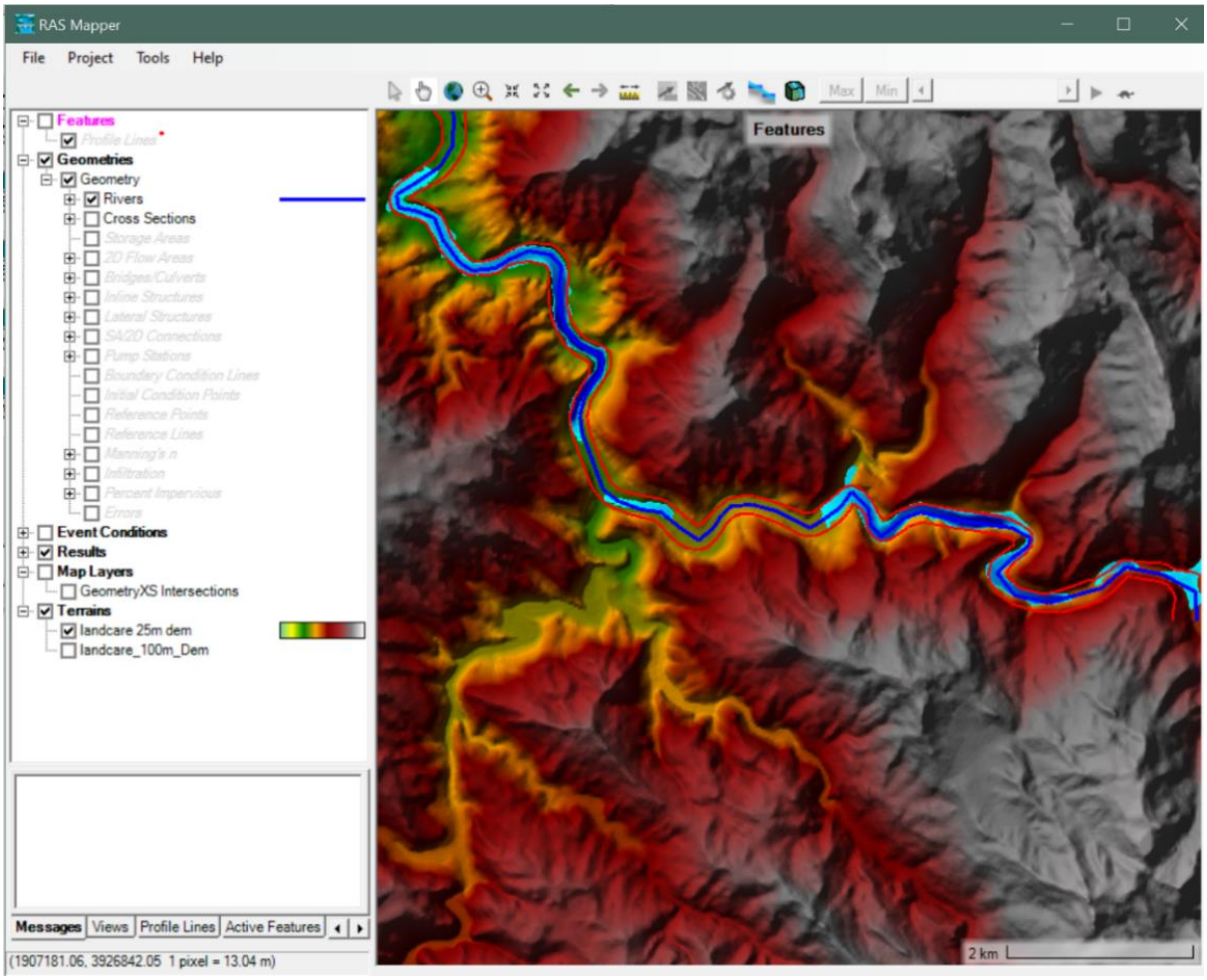

Figure 68 Trial three of the HEC-RAS model at Toge Village

Chapter 6: Discussion

Flooding is one of the most frequent natural disasters to impact Fiji. The purpose of this research is to identify the impact of flooding events in the Ba Urban area through the use of GIS tools and technology to map out the possible extent of flooding. The overall research question is to identify flood risk areas in Ba and the potential impact on the people and on different land uses of the catchment. This chapter discusses and summarizes the key findings of the results. Overall, the results show that the HAND method is most suitable to map flood risk areas in the Ba Urban area. This is because the data input was sufficient to produce a result that can be used to prepare flood risk maps for the Ba Urban area and along the middle catchment where Toge and Navala village is situated.

Height at Nearest Drainage (HAND) method

The HAND result is approximate because it neglects many details of the river hydraulics and flows over flood plains. More detailed approaches often demand time and resources unavailable in Fiji hence HAND method may be a helpful approach to get screening levels and real-time flood maps of Ba Catchment. Moreover, the conclusions are reinforced by Yeo et al.'s (2010) observations of flood heights at various points within Ba Town and the encompassing vicinity of the lower Ba Catchment. However, the lack of precise field validation data following each occurrence has led to the assessments being compared against a restricted dataset, primarily sourced from the Fiji National Disaster Management Office. However, it lays a groundwork for locations prone to flooding in Ba Catchment and validates the HAND results. The results are largely based on the river network generated from the NASADEM digital elevation model and then overlayed on the high-resolution LiDAR datasets provided by the Secretariat of the Pacific Community. The availability of LiDAR, even for a small cover, of Ba Catchment has helped fill the gaps identified by Paquette &

Lowry (2012) as improved elevation was generated from the LiDAR data to measure flood heights of HAND result.

The overall output of the HAND result provided the best method to map flood hazards in Ba Catchment which can assist in decision-making for flood preparedness. The three zones at Ba Catchment give a closer look at areas where most damages are expected. The most affected flood zone is Zone Two as there are various land uses within the flood extent. The impact on the economic activity of Ba Town is greatly affected by the flood followed by the loss of agricultural production leading to lower income, especially from sugarcane farmers. The elevation along zone two varies but since the Ba Town Center and all wards fall within the flood zone, it is essential to carry out development planning while bearing in mind the flood extent experienced in Ba Catchment. The cost of a flood event is also highest in zone two as there are many properties and infrastructure that suffer extensive damage such as washing away of bridges and roads, broken electricity powerlines and water pipes and damage to residential and commercial buildings (Lucas, 2020).

The impact on people within the flood zone amounts to the high vulnerability of communities (Irvine et al., 2020). The ten villages within zone one face damages to food, livestock and property during every flood as the elevation is below 5 meters above mean sea level. To experience localized flood and extreme flood events every year and continue to reside in flood-prone flood plains is due to traditional ties to the land and simply cannot relocate to another location as these lands have been their ancestral home and a sense of identity. As *itaukei* (native) landowners, the traditional protocols and linkage to land are a reason for the low willingness to relocate (McMichael, Katonivualiku, & Powell, 2019). Those who have purchased land through freehold or acquired land leases are faced with the burden to continue residing in flood-prone zones as purchasing another land comes with a high cost and mortgage which many are unable to afford in Fiji. The people continue to build

adaptation to floods and often resort to raising their houses on piles to minimize the impact of flood events.

The villages of Navala and Toge will also get damaged by flood waters as water flows downstream and an analysis of land use land cover has identified the low forest cover and presence of *talasiga* land to be a contributing factor of rapid runoff into the streams and main river tributaries (Stephens, Lowry, & Ram, 2018). The village is also in rural areas and is engaged mainly in agricultural activity apart from Navala Village being a tourism spot. The damage to infrastructure such as roads and bridges limits the movement of people after events and rebuilding of these infrastructures often takes time which disrupts data collection on infrastructure damages, socio-economic impact, and environmental degradation through loss of soil and riparian vegetation.

SNAP to analyse the SAR imagery method

For Fiji, the revisit period of satellite imageries is a limitation and localized floods last a few hours, and major flooding events do not last more than two days approximately. Therefore, the availability of SAR imageries on the exact date of a flooding event would provide the most benefit and coverage to monitor flood extents. The flood imageries of the next day or two are only suitable to show water-logged soil reflectance which can also help estimate the flood extent however it is unsuitable as flood events are followed by periods of heavy rainfall. This can lead to an overestimation of the flooding extent in an area.

The availability of freely available SAR imageries allows analysis of flooded zones in Ba Catchment which requires further calibration to the output and a way forward is to gather ground truth data to assist in deciding the parameters such as before and after image thresholding to differentiate between flooded pixels and surrounding cells. The outcome of SAR image analysis supports the theory that SAR imageries can be a way forward for flood

mapping in data-scarce regions. Historical imageries can be analysed to see the flood extent as SAR images are not affected by cloud cover which is widely present during the duration preceding a flood event (Stephens, Lowry, & Ram, 2018). The output generated by SAR analysis shows that speckle filtering needs further calibration as a lot of areas were showing to be flooded and a close examination of the results in google earth pro supported in identifying that majority of the results were false positive. The flood waters were being identified on the mountains on the eastern side of the Ba River which were present after masking was undertaken. This is an indication of waterlogged soil reflectance being classified as water present on soil and hence labelled as flooded areas.

When a radar signal from SAR interacts with a water surface, it usually results in a relatively smooth and specular reflection, leading to lower backscatter. However, when the radar signal encounters a rougher land surface, such as vegetation, buildings, or uneven terrain, it experiences more scattering and diffraction, causing higher backscatter levels. This change is characterized by a transition from low to high backscatter. This transition enables a clear delineation of water surfaces; the distinction between floodwaters and permanent water bodies by comparing the SAR image acquired during or soon after the flood with the corresponding archived image acquired before the flood event. For best results, both images must have the same geometrical characteristics, including paths in instance angle and the same frequency and polarization. In this analysis, descending pass and VV polarization were selected.

The Copernicus Emergency Mapping Service (EMS) is activated to assist in mapping and producing hazard maps, such as one generated for Ba, Fiji, after tropical cyclone Winston. According to Martinis (2010), the ability to detect the extent of flooding in SAR data is affected by various factors, including the surface roughness characteristics of both the water areas and the surrounding land, as well as system-specific parameters such as

wavelength, incidence angle, and polarization. The detectability is mainly dependent on the contrast between the water and the surrounding land. The mountainous region South, East, and West of Ba Catchment had resulted in a foreshortening effect which has impacted the results generated.

SAR can identify an exposed flood surface by reflecting the radar energy in a specific way, resulting in low backscatter and darker pixels in the SAR data. This happens because the flood surface acts as a specular reflector, scattering the radar energy away from the sensor (Martinis & Rieke, 2015). On the other hand, the areas surrounding the water surface usually show higher signal returns due to increased surface roughness. When higher SAR frequencies are used, there is a greater difference in contrast between the water and non-water areas (Martinis, 2010).

As a result, the use of X-band SAR is more appropriate for small-scale flood monitoring than longer wavelengths. An increase in water surface roughness due to wind increases the backscatter over water, decreasing the flood mapping capability. This is because the rough water surface scatters more of the radar energy back towards the sensor, resulting in higher backscatter values that can be misinterpreted as flooded areas. VV polarization provides the best discrimination between water and non-water terrain for the Ba Catchment although small ripples over the flood surface are observed. Also, when there is an increase in surface roughness, the ability to distinguish between water and land surfaces is more adversely affected by VV polarization than HH polarization.

There are various reasons why the flood extent in Ba Catchment might be overestimated. During flood mapping, certain objects can be confused with open water surfaces due to their similar backscatter. These objects include smooth natural surface features like sand surfaces and bare ground, as well as anthropogenic features like streets. In

addition, radar shadowing effects can occur behind vertical objects such as vegetation, buildings, and topography, which can also complicate flood mapping. In comparison to optical sensors, SAR provides a distinct advantage in detecting flooding beneath vegetation. This is due to several combined factors, including the ability of the radar pulse to penetrate the vegetation and the resulting backscatter from both the horizontal water surface and the lower part of the vegetation.

Various methods exist for detecting flooding in SAR data and are based on visual image interpretation, automatic thresholding, change detection procedures based on multi-temporal SAR data, contextual classifiers such as object-based approaches, region growing procedures, and contour models. Usually, several techniques are combined to improve flood mask extraction. Also, integrating auxiliary datasets such as digital elevation models, slope information, topographic indices, and land cover information can significantly support the flood mapping process.

Fully operational automatic flood mapping services exist based on SAR data such as Sentinel 1 and TerraSAR-X satellites. These services cover the whole process starting from automated data ingestion, pre-processing, classification, and dissemination. These services are beneficial in providing users with crisis information in near real-time. They are used, for example, to support the operational crisis response activities of the International Charter Space and major disasters. SAR is actively used for flood disaster management. An instance is the International Charter for Space and Major Disasters, which aims to establish a cohesive approach among global satellite data providers in delivering and acquiring space data to assist those affected by disasters. Most of the disasters for which the Charter is activated are caused by flooding, and for these, SAR sensors are the priority tasking. The Copernicus EMS also provides operational information on flooding events using a large constellation of SAR sensors from its partner agencies, and it supports all stages of the disaster lifecycle.

To minimize the risk of flooding, the existing measures undertaken by the Fijian Government include structural and non-structural measures across Fiji to protect from future flooding events. The Intergovernmental Panel on Climate Change (IPCC) reports increasing trends and extreme precipitation in areas already prone to such events. This implies that there may be more significant risks of flooding on a regional scale. The impact of these events and human lives and property is likely to rise, given population growth forecasts. The need, therefore, for information to support flood prevention and mitigation in the future can only increase.

The method of SNAP required downloading SAR imageries and conducting the analysis on each imagery one at a time. This method was coded on Google Earth Engine (GEE) to replicate the results of the 2018 April floods in the lower Ba Catchment. On GEE, it was easier to check for different parameters such as a change in polarization and incidence angles to see if the results had changed. The results differ when parameters are changed because of dates on which imagery was available and another possible reason can be the time of imagery taken. The closer to the flood event, the more flood waters will reflect the sensor and the estimation of flood extent can be accurately determined.

HEC-RAS one-dimensional simulation method

The outcome of this methodology largely depended on the data input. The digitization of geometries was conducted as accurately as possible. The input of flow velocity and slope data is calculated from the discharge and Manning's n equations. The input of these two equations determines the output of the simulation. The result generated from this method is also dependent on the input of the Ba Bridge plan. Since the engineering plan of the bridge was not available, the accuracy of the plan is low. The results also differ when the bridge plan is excluded from the simulation.

The flood extent outcome of the HEC-RAS simulation is not accurate because the model lacks the engineering needs of the simulation. Since Ba Catchment has various bridges, only the main Ba bridge is factored in. The focus is also reduced to lower Ba Catchment because of the lack of available datasets such as river flow data. The data was requested but not made available. The rainfall data is used to estimate the flow lag time from Navala and Toge downstream at Ba Town.

A reason for this HEC-RAS model not having proper simulation results can be that the riverbed elevations were not lowered to bed levels underneath the bridge decks. This would have ensured that the location of bridge abutments is correctly included in the model. The current piers and bridge decks were not designed using actual plans which impacted the flow simulation and over-estimated the flood depth in the flood plain.

The flood modelling using HEC-RAS is the first of its kind in Ba Catchment hence there are no studies to compare and measure the accuracy of the results. The only analysis of floods using HEC-RAS in Fiji is for Waidina Tributary in Rewa Catchment (Rathnayake & Arachchi, 2015). It also highlights the need for accurate data and planning for hydrological modelling. The one-dimension simulation will be successful with more accurate data input and full rainfall information. The precipitation datasets exhibited considerable data gaps, particularly during flood events, attributed to the submergence of monitoring stations situated within floodplain areas. The inclusion of authentic rainfall data holds the potential to enhance the accuracy of discharge and velocity computations within the simulation process (Rathnayake & Arachchi, 2015). There are also time and resource constraints with a lack of trained hydrologists in Fiji to utilise forecasting models (Tilly & Fakhruddin, 2020).

Summary

A generic hydrologic-hydraulic modelling workflow requires many complex numerical analyses and numerous input variables to represent complex reality. The reliability of these models highly depends on various primary data and high-resolution digital elevation models which are expensive to produce. Due to infrastructure development and natural causes, the topography changes over time. Flood models need to be updated frequently to represent current conditions, which may incur additional costs. When all available input data expertise is not present in the development of a hydrologic-hydraulic model, different geomorphic classifiers can delineate areas that are susceptible to flood using the HAND model. The HAND model utilizes the elevation differences along the water flow path to standardize the landscape and depict the local drainage capability. By doing so, it portrays the topography of potential water flow in the area. The relative drop in elevation, determined by HAND, is a useful indicator of the likelihood of flooding, and it correlates directly with the height of the river stage.

The three methodologies discussed have their advantages and disadvantages for flood mapping in Ba Catchment. Out of all, Multi-Criteria Decision Analysis using the HAND method provided the most suitable result. There is a scope for other methods to be used with accurate data inputs so that the resulting outcome can be improved. It also supports the idea that different flood mapping approaches can be utilized for Fiji where data is scarce and dependence on open source information is high which has low-resolution data to properly carry out analysis on small island countries (Tilly & Fakhruddin, 2020). The catchment sizes and flood extent also pose challenges therefore the need to have accurate ground-validated data will provide a way to improve flood models. The research question is answered as a flood hazard map is produced and a flood modelling attempt using SAR imageries and HEC-RAS simulation proved to be unsuccessful. The impact on different land uses along the river

is also discussed and this flood extent map can be further calibrated with more ground truth data to improve results.

Chapter 7: Conclusion and Recommendations

There were two goals of this thesis research. Firstly, to produce a flood hazard map of the Ba Catchment and secondly to identify the impact of a flood event on land use land cover along the river channel.

From the HAND method, the town centre is badly affected by every localized flood event however the shop owners and residents in the ward are resilient to flood events. During the flood warnings, the main activity is to move all store contents to the first floor to minimize flood damage. The first few areas to get affected are the Ba bus stand and market area as the Elevuka Creek runs through the town area. The relocation of the town centre is too large for a developing country like Fiji as major flood events affect once every few years. The analysis of flooding in Ba shows that food damage is every year and is most commonly affected by localized flash flooding.Therefore major flood events do cause the most damage however the local flood knowledge, early warning systems and community preparedness and response in the flood zones mean people in Ba Town are highly unlikely to relocate to a flood-free zone. The Ba Town Council and National Fire Authority assist in the town cleanup which is directly after the flood has receded and it assists the people affected by the flood in the town area. The commercial activity is halted until the entire area is clear and safe for businesses to resume safely which does lead to economic losses.

Methodologies of flood hazard mapping and modelling

The three methods tested for the analysis of the Ba River flood zone produced varied results. The flood extent is an estimate of a flood event and can change depending on how small or large scale a flood is. The main contributor to flood events is rainfall and Ba Catchment has experienced more flash flooding than a large events. A flooding event does not last longer than two days to cause extreme damage however it disrupts people’s lives and damages are

worse if the flood event is followed by tropical cyclones. The community and the Government are left to rebuild after each event which pushes a lot of debt on the Government and dependency on overseas aid. The methodologies explored in this research have shown that there is a lot of work that needs to be done in terms of data collection so that accurate flood models can be generated. The use of satellite imagery comes with the issue of temporal and spatial resolution. For Ba Catchment, the flood duration is small as the catchment is small compared to many other catchments worldwide. Therefore, having the imagery taken on the exact date of flooding would present the best results. This study presents the possibility to utilize open-source data to carry out flood mapping in Ba Catchment, Fiji. The method can be replicated in other catchments in Fiji to start flood hazard mapping activities.

The current land use of Ba Catchment is largely agricultural and forestry. The harvesting of sugarcane in agricultural land use zones exposes soil to erosion. Forest harvesting along the upper catchment also poses a risk of landslide and soil erosion. These activities generate revenue for the country and cannot be halted however management can be integrated into harvesting plans. The afforestation and reforestation of bare lands in the middle and upper catchment can provide a solution to runoff as it will help slow the rate at which water travels to the nearby streams. The land use at lower ba Catchment is largely agriculture intertwined with urban and industrial activity. The location of Ba Town by the river will always pose a risk of flooding. Results from this study shows the need for better land use planning to limit commercial activity and residential expansion within the wards of Ba Town boundary. The flood zone extent map is a step forward in identifying the flood risk zones so that town planners can incorporate flood extent in their planning schemes. Although development cannot be stopped, it would provide a long-term solution to move development into safer zones to reduce flood impact on people and property.

The solutions to minimize the impact of floods on the people of Ba largely involve incorporating expensive solutions such as hard engineering and river dredging. There is a minimal focus on introducing nature-based solution which includes planting riparian vegetation and mangroves to be the first line of defence from coastal inundation and flood risk on floodplains. The loss of soil and bank lines poses a risk of losing land during extreme flood events. The way forward to control soil loss is by planting trees along the riverbanks to hold the soil structure and slow the force of flood waters breaking on the floodplains. The communities in Fiji are closely linked to their traditional ties and are connected to their land. Awareness of soil and vegetation loss should be discussed alongside the loss of revenue and lives when creating awareness of flood risk. There are early warning systems in place to give ample time for residents to evacuate which has drastically reduced the number of lives lost during flood events however smart planning needs to be incorporated into reducing overall flood risk such as building houses on piles and away from flood plains. Hard engineering solutions such as building levees and dykes will also assist in flood management however the maintenance of these infrastructures is not within the capacity of small island developing states. The high cost of maintaining floodgates, and retention of dams and levees will require international funding, loans, or aid as Fiji will not be able to afford long-term maintenance plans. The river dredging has occurred in Ba River in the past, however, the solution lasts a short term because of silt buildup on the river beds due to improper agricultural practices. The effort to dredge needs to work hand in hand with catchment management through tree planting initiatives and improving agricultural practices such as intercropping so that soil is not left bare after harvesting a crop.

Limitations of the methodologies

The lack of national datasets in gridded or shapefile format is a limitation to accurately creating models that can help in planning adaptation and mitigation strategies for

communities residing on the floodplains. There is also a need for improvement in how agencies that collect datasets streamline the availability of this information as a lot of time is lost trying to facilitate the data release process. One of the key issues faced was the lack of interest shown by the relevant authorities to facilitate the requests hence most datasets used for this research were open-sourced.

There are also various studies undertaken in the Ba Catchment to try flood modelling and hydrological mapping which often focus on the hard engineering solutions which could not be input into the three methodologies as it would require complex inputs which is beyond the skill of the researcher. The models have been prepared using the available datasets and it is laying the groundwork for future research using improved data inputs, especially in the HEC-RAS one-dimension flood simulation. There is a need for personnel training and capacity building to start using the freely available software to plan flood models. It will increase data collection of river flow, riparian vegetation, riverbed materials, and cross sections to start building a database of river characteristics in Fiji.

The lack of complete rainfall data is another challenge as inputs in flood modelling require complete datasets without averages so that results are reflecting the situation on the ground. There are manual stations across Ba Catchment that can incur human error when recording and submitting datasets to Fiji Meteorological Service. The automatic stations are scarce and cover the middle to lower Ba Catchment. There need to be more automatic stations spread around the catchment to capture flow data and rainfall. This will assist the modellers to determine flood water lag times which can then be incorporated into the early warning system to advise people of the behaviour of the river and the approximate time for the river break. Although the automatic stations are connected to transmit data to the server at the Fiji Meteorological Office, the stations failed to properly record the rainfall and river water level which resulted in missing data on the 2018 flood events in Ba. It is recommended

that automatic stations are placed across the whole catchment for a better chance to generate accurate flood models and gain a deeper understanding of how the river characteristics work together during a flood event.

The use of satellite imagery is a way forward but is not particularly helpful to Ba Catchment as the flood extent is smaller compared to flood events experienced globally. The Ba Catchment is the 4th largest on Viti Levu and the impact it has is great on the people residing on the floodplain which is a common practice across the country. The use of SAR provides an opportunity to explore flooded waters in real time however the temporal and spatial resolution is a challenge since the catchment and river system is small and narrow to precisely map the flood extent using SAR only. The script in Googe Earth Engine was modified but the date of imagery after a flood is crucial in this method. The adjustments to the thresholding effect are required in the script which assists in the speckle filtering, a key filter in the methodology. The speckle reflectance impacts the flood output and further refinement is needed on the script to suit the conditions of Ba Catchment. There is also a need for training and capacity building on using remote sensing data for flood analysis and generating flood maps in the context of the Pacific Islands. The online remote sensing training available is tailored to suit large floodplains and replicability is a challenge to smaller catchments like Ba.

Appendix

Google earth engine script for flood hazard mapping using SAR imageries

```
// Load Sentinel-1 C-band SAR Ground Range collection (log scaling, VV co-polar)

var collection = ee.ImageCollection('COPERNICUS/S1_GRD')
.filterBounds(pt)
.filter(ee.Filter.listContains('transmitterReceiverPolarisation', 'VV'))
.select('VV')
.filter(ee.Filter.eq('orbitProperties_pass', 'DESCENDING'));
// Filter by date
var before = collection.filterDate('2018-03-01', '2018-03-20').mosaic();
var after = collection.filterDate('2018-04-01', '2018-04-09').mosaic();
// Threshold smoothed radar intensities to identify "flooded" areas.
var SMOOTHING_RADIUS = 50;
var DIFF_UPPER_THRESHOLD = -3;
var diff_smoothed = after.focal_median(SMOOTHING_RADIUS, 'circle', 'meters')
.subtract(before.focal_median(SMOOTHING_RADIUS, 'circle', 'meters'));
var diff_thresholded = diff_smoothed.lt(DIFF_UPPER_THRESHOLD);
var terrain = ee.Algorithms.Terrain(hydrosheds);
var slope = terrain.select('slope');
before = before.mask(slope.lt(5));
after = after.mask(slope.lt(5));
Map.centerObject(pt, 13);
Map.addLayer(before, {min:-30,max:0}, 'Before flood');Map.addLayer(after, {min:-
30,max:0}, 'After flood');
Map.addLayer(after.subtract(before), {min:-10,max:10}, 'After - before', 0);
Map.addLayer(diff_smoothed, {min:-10,max:10}, 'diff smoothed', 0);
Map.addLayer(diff_thresholded.updateMask(diff_thresholded), {palette:'0000ff'},'flooded
areas - blue',1)
```

Toge automatic station lacking rainfall data on flood event on 02/04/2018.

TOGE								
Sum of Daily Rainfall (mm)	**Column Labels**							
Row Labels	**2015**	**2016**	**2017**	**2018**	**2019**	**2020**	**2021**	**Grand Total**
Jan		**467.5**	**714**	**492.5**	**635**	**164.5**	**920.5**	**3394**
Feb		**667.5**	**820.5**	**628.5**	**228**	**167**	**496.5**	**3008**
Mar		**347.5**	**598.5**	**924.5**	**370**	**1022.5**	**456**	**3719**
Apr		**648.5**	**124**	**734.5**	**320.5**	**340**	**163**	**2330.5**
01-Apr		0	0	97.5	6	5	3.5	112
02-Apr		0	36.5	8	0	1.5	2.5	48.5
03-Apr		232	0	0	0	3	0	235
04-Apr		142.5	0	6	0	3.5	1	153
05-Apr		208	0	11.5	0	0	0	219.5
06-Apr		36.5	0.5	241	3	14	0	295
07-Apr		0	0	41.5	2	171	0	214.5
08-Apr		3.5	0	21	2	20	0	46.5
09-Apr		0	0	119	0	0	0	119
10-Apr		0	0	138	0	1.5	0	139.5
11-Apr		0	0	0	0	0	0	0
12-Apr		0	0	0	31	0	0	31
13-Apr		0	0	0	27	0	0	27
14-Apr		1	2	0	52	0	0	55
15-Apr		0.5	19.5	0	0	0	1	21
16-Apr		23	0	0	0	0	31	54
17-Apr		0	5	0	0	0	8.5	13.5
18-Apr		0	0	0	42.5	1	26	69.5
19-Apr		0	0	0	5	0	0	5
20-Apr		0	0	6	8	1	1	16
21-Apr		0.5	0	0	34	2.5	41	78
22-Apr		1	14	0	6.5	20.5	0	42
23-Apr		0	0.5	0	4.5	0	6.5	11.5
24-Apr		0	0	0	0	0	11	11
25-Apr		0	0	0	26.5	23	0	49.5
26-Apr		0	36	1	9.5	23.5	15.5	85.5
27-Apr		0	9	0	2	36	0	47
28-Apr		0	0	0	47	10	0	57
29-Apr		0	0	29.5	12	2.5	13	57
30-Apr		0	1	14.5	0	0.5	1.5	17.5

References Cited

Abedin, S., & Stephen, H. (2019). GIS Framework for Spatiotemporal Mapping of Urban Flooding. *Geosciences, 9(2)*, 77.

Ambroz, A. (2009). *Ba floods, economic costs, January 2009*.

Andrew, N. L., Bright, P., de la Rua, L., Teoh, S. J., & Vickers, M. (2019). Coastal proximity of populations in 22 Pacific Island Countries and Territories. *PLOS ONE, 14*(9), e0223249. https://doi.org/10.1371/journal.pone.0223249

Arcement, G., & Schneider, V. (1989). Guide for selecting Manning's Roughness Coefficients for Natural Channels and Flood Plains. https://pubs.usgs.gov/wsp/2339/report.pdf

Archer, L., Bates, P., Neal, J., & House, J. I. (2018). Modelling, Comparing TanDEM-X Data with Frequently-Used DEMs for Flood Inundation. *Water Resources Research*, *54*(4).

Bates, P. D., & De Roo, A. P. J. (2000). A simple raster-based model for flood inundation simulation. *Journal of Hydrology*, *236*(1-2), 54-77.

Bind, J., Chiaverini , A., Henderson , R., Measures , R., Paulik , R., Pearson , C., & Smart, G. (2014). *Nadi River Flood Risk Assessment*.

Buri, S., Fong, S., Honda, H., & Wagner, S. (2022). MSMEs in Focus: Insights on how MSMEs in Fiji are affected by extreme weather events and their readiness for disaster risk financing. Retrieved 07/11/2022, from https://www.uncdf.org/article/8002/msmes-in-focus-insights-on-how-msmes-in-fiji-are-affected-by-extreme-weather-events-and-their-readiness-for-disaster-risk-financing

Coenen, V., Overkamp, K., Pohl, I., & Bruijn, F. d. (2019). *DRR Mission Report Fiji: Scoping Mission for Flood Alleviation Measures for Ba & Rakiraki Towns (and associated water catchments)* (116224/19-016.139). https://english.rvo.nl/sites/default/files/2023/03/DRR-Team-Fiji-Scoping-Mission-Report-October-2019_0.pdf

Copernicus. (2022). *Sentinel-1 SAR User Guide - Definitions*. Copernicus. https://sentinels.copernicus.eu/web/sentinel/user-guides/sentinel-1-sar/definitions#:~:text=It%20is%20a%20measure%20of,unit%20area%20on%20the%20ground.

Disasters, C. f. R. o. t. E. o. (2022). *EM-DAT: The International Disaster Database* https://www.emdat.be/database

Donner, S. D., & Webber, S. (2014). Obstacles to climate change adaptation decisions: a case study of sea-level rise and coastal protection measures in Kiribati. *Sustainability Science*, 331–345.

Downton, M. W., & Pielke, R. A. (2005). How Accurate are Disaster Loss Data? The Case of U.S. Flood Damage. *Natural Hazards*, *35*(2), 211-228. https://doi.org/10.1007/s11069-004-4808-4

FBoS. (2018). *2017 Population and Housing Census*. Fiji Bureau of Statistics Retrieved from https://www.statsfiji.gov.fj/

Fiji, G. o. (2017). *Climate vulnerability assessment : making Fiji climate resilient*. http://documents1.worldbank.org/curated/en/163081509454340771/pdf/Climate-vulnerability-assessment-making-Fiji-climate-resilient.pdf

FMS. (2020). *Annual Climate Summary 2020*. https://www.met.gov.fj/aifs_prods/Climate_Products/2020annualSum2022.10.19%2012.02.59.pdf

Force, F. P. (2018, January 14). Western Division Flooding Report: Bulletin No. 3. *Fiji Sun Newspaper*. https://fijisun.com.fj/2018/01/14/western-division-flooding-report-bulletin-no-3/?fbclid=IwAR0jHsB_sK5twEC5Vyj3uZkeGB9dcBzcUzY8rB1LrPaoQPdvv3XomNh7G1w,%20Vatulaulau%20Road,%20Namosau%20Bridge%20and%20Rarawai%20Bridge%20were%20under%20flood%20waters

Forkuo, E. K. (2011). Flood Hazard Mapping using Aster Image data with GIS. *International Journal of Geomatics and Geosciences*, *1*(4), 932-950.

Gehrke, P., Sheaves, M., Terry, J. P., Boseto, D., Ellison, J., & Figa, B. S. (2011). Vulnerability of freshwater and estuarine fish habitats in the tropical Pacific to climate change. In *Vulnerability of Tropical Pacific Fisheries and Aquaculture to Climate Change* (pp. 369-461). Secretariat of the Pacific Community.

Hawker, L., Rougier, J., Neal, J., Bates, P., Archer, L., & Yamazaki, D. (2018). Implications of Simulating Global Digital Elevation Models for Flood Inundation Studies. *Water Resources Research*, *54*, 7910–7928. https://doi.org/https://doi.org/10.1029/2018WR023279

Holland, P. (2008). *Fiji Technical Report: An Economic Analysis of Flood Warning in Navua, Fiji.* (SOPAC Project Report No. 122, Issue.

Irvine, G., Pauli, N., Varea, R., & Boruff, B. (2020). A Participatory Approach to Understanding the Impact of Multiple Natural Hazards in Communities along the Ba River, Fiji. *Community, Environment and Disaster Risk Management*, 57-86.

JICA. (1998). *The Study on Watershed Management and Flood Control for the Four Major Viti Levu Rivers in The Republic of Fiji*.

JPL, N. (2013). *NASA Shuttle Radar Topography Mission Global 1 arc second* https://doi.org/https://doi.org/10.5067/MEaSUREs/SRTM/SRTMGL1.003

Kapoor, A., Alcayna, T., Boer, T. d., Gleason, K. B., Bivishika , & Heinrich, D. (2021). *Climate Change Impacts On Health and Livelihoods: Fiji Assessment*.

Kuleshov, Y., Mcgree, S., Jones, D., & Charles, A. N. (2014). Extreme Weather and Climate Events and Their Impacts on Island Countries in the Western Pacific: Cyclones, Floods and Droughts. *Atmospheric and Climate Sciences*, 803-818.

Kumar, V. (2010). Water Management in Fiji. *International Journal of Water Resources Development*, *26*(1), 81-96. https://doi.org/10.1080/07900620903392216

Kundzewicz, Z. W., Kanae, S., Seneviratne, S. I., Handmer, J., Nicholls, N., Peduzzi, P., Mechler, R., Bouwer, L. M., Arnell, N., Mach, K., Muir-Wood, R., Brakenridge, G. R., Kron, W., Benito, G., Honda, Y., Takahashi, K., & Sherstyukov, B. (2014). Flood risk and climate change: global and regional perspectives. *Hydrological Sciences Journal*, *59*(1), 1-28. https://doi.org/10.1080/02626667.2013.857411

Löschner, L., Herrnegger, M., Apperl, B., & Senoner, T. (2017). Flood risk, climate change and settlement development: a micro-scale assessment of Austrian municipalities. *Regional Environmental Change*, *17*, 311-322.

Lucas, B. (2020). Economic Impacts of Natural Hazards on Vulnerable Populations in FIJI. https://climate-insurance.org/wp-content/uploads/2021/01/Fiji-Economic-Impacts-Report-27Nov2020.pdf

Lumbroso, D., Titimaea, A., Penaia, A., & Bonte-Grapentin, M. (2008). *Samoa Capacity Building in Flood Risk Management* [Technical Report].

Lyu, H.-M., Wang, G.-F., Shen, J. S., Lu, L.-H., & Wang, G.-Q. (2016). Analysis and GIS Mapping of Flooding Hazards on 10 May 2016, Guangzhou, China. *Water*, *8*(10), 447.

Mark, O., & Djordjević, S. (2006). *While waiting for the next flood in your city*.

Martinis, S. (2010). *Automatic near real-time flood detection in high resolution X-band synthetic aperture radar satellite data using context-based classification on irregular graphs*.
Martinis, S., & Rieke, C. (2015). Backscatter Analysis Using Multi-Temporal and Multi-Frequency SAR Data in the Context of Flood Mapping at River Saale, Germany. *Remote Sensing*, *7*(6), 7732-7752.
Mathewsell, L. (2013, March 3). Ba Creek Diverted, Less Flood Impact. *Fiji Sun*. https://fijisun.com.fj/2013/03/03/ba-creek-diverted-less-flood-impact/
McAneney, J., Honert, R. v. d., & Yeo, S. (2017). Stationarity of major flood frequencies and heights on the Ba River, Fiji, over a 122-year record. *International Journal of Climatology*, *37*(2).
McMichael, C. (2019). Rising seas and relocation in Fiji. *Policy Forum*. Retrieved June 27, from https://www.policyforum.net/rising-seas-and-relocation-in-fiji/
McMichael, C., Katonivualiku, M., & Powell, T. (2019). Planned relocation and everyday agency in low-lying coastal villages in Fiji. *The Geographical Journal*, *185*(3), 325-337. https://doi.org/https://doi.org/10.1111/geoj.12312
Metherall, N., Beavis, S., Holland, E., & Vinaka, A. M. D. (2021). Characterisation of pH variations along the Ba River in Fiji utilising the GEF R2R framework during the 2019 sugarcane season. *Environmental Monitoring and Assessment*.
MetService. (2022). *Tropical Cyclone Monitoring*. Meteorological Service of New Zealand Ltd. https://about.metservice.com/our-company/national-weather-services/tropical-cyclones/
Mimura, N., & Pelesikoti, N. (1997). VULNERABILITY OF TONGA TO FUTURE SEA-LEVEL RISE. *Journal of Coastal Research*, 117-132. http://www.jstor.org/stable/25736091
Moishin, M., Deo, R. C., Prasad, R., Raj, N., & Abdulla, S. (2021). Development of Flood Monitoring Index for daily flood risk evaluation: case studies in Fiji. *Stochastic Environmental Research and Risk Assessment*, 1387-1402.
Muste, M., Thomas, D., & Bacotiu, C. (2019). Evaluation of the Slope-Area Method for Continuous Streamflow Monitoring. 38th IAHR World Congress, Panama City, Panama.
Naidu, P. N., Khan, M. G. M., & Jokhan, A. D. (2017). Assessment of sugarcane varieties for their stability and yield potential in Fiji. *The South Pacific Journal of Natural and Applied Sciences*, *35*(2), 20.
Naikaso, F. (2018). Initial damage for TC Josie and Keni stands at $91m. https://www.fbcnews.com.fj/news/initial-damage-for-tc-josie-and-keni-stands-at-91m/
Nobre, A., Cuartas, L., Hodnett, M., Rennó, C., Medeiros, G., Silveira, A., Waterloo, M. J., & Saleska, S. (2011). Height Above the Nearest Drainage - a hydrologically relevant new terrain model. *Journal of Hydrology*, *404*, 13-29. https://doi.org/10.1016/j.jhydrol.2011.03.051
OCHA. (2016, 16/05/2016). *Responding to Tropical Cyclone Winston*. https://www.unocha.org/story/responding-tropical-cyclone-winston
OCHA. (2018). Republic of Fiji: Tropical Cyclone Josie and Tropical Cyclone Keni Rapid Gender, Protection and Inclusion Analysis. https://reliefweb.int/report/fiji/republic-fiji-tropical-cyclone-josie-and-tropical-cyclone-keni-rapid-gender-protection
Okoye, C., & Ojeh, V. N. (2015). Mapping of Flood Prone Areas in Surulere, Lagos, Nigeria: A GIS Approach. *Journal of Geographic Information System*, *07*, 158-176. https://doi.org/10.4236/jgis.2015.72014

Paquette, J., & Lowry, J. (2012). Flood hazard modelling and risk assessment in the Nadi River Basin, Fiji, using GIS and MCDA. *The South Pacific Journal of Natural and Applied Sciences*, 33-43.

Pradhan, Y., & Ghose, M. (2012). Automatic Association of Strahler's Order and Attributes with the Drainage System. *International Journal of Advanced Computer Science and Applications(IJACSA), U.S ISSN : 2156-5570(Online) ,U.S, ISSN : 2158-107X(Print)*, *3*, 30-34.

Rathnayake, U., & Arachchi, S. (2015). Flood Modelling in Waidina Tributary, Fiji Islands. 3rd International Symposium on Advances in Civil and Environmental Engineering Practices for Sustainable Development,

Richards, A., Irving, C., McHattie, C., Wilcox, K., Matreja, T., Mitchell, E., Strachan, F., & Naikasowalu, T. (2021). *A Line In The Sand Investigating Black Sand Mining In Fiji*.

Rincón, D., Khan, U. T., & Armenakis, C. (2018). Flood Risk Mapping Using GIS and Multi-Criteria. *Geosciences*, 275.

Rincón, D., Khan, U. T., & Armenakis, C. (2018). Flood risk mapping using GIS and multi-criteria analysis: A greater Toronto area case study. *Geosciences*, *8*(8), 275.

RNZ. (2016, 25/02/2016). Fiji govt estimates Winston damage US$460 million. *Radio New Zealand International*. https://www.rnz.co.nz/international/pacific-news/297447/fiji-govt-estimates-winston-damage-us$460-million

RNZ. (2020). Fiji Govt says Cyclone Harold costs exceed $US40m. *Radio New Zealand*. https://www.rnz.co.nz/international/pacific-news/417430/fiji-govt-says-cyclone-harold-costs-exceed-us40m

RNZ. (2021). Cyclone Yasa damage to Fiji worth nearly $US250m. *Radio New Zealand*.

Sene, K. (2008). *Flood Warning, Forecasting and Emergency Response*. Springer.

Smith, C. F., Cordova, J. T., & Wiele, S. M. (2010). *The Continuous Slope-Area Method for Computing Event Hydrographs* [Scientific Investigations Report 2010-5241].

Speckhann, G. A., Chaffe, P. L. B., Goerl, R. F., Abreu, J. J. d., & Flores, J. A. A. (2018). Flood hazard mapping in Southern Brazil: a combination of flow frequency. *Hydrological Sciences Journal*, *63*(1), 87-100.

Stephens, M., Lowry, J., & Ram, A. (2018). Location-based environmental factors contributing to rainfall-triggered debris flows in the Ba river catchment, northwest Viti Levu island, Fiji. *Landslides*, 145–159.

Strahler, A. N. (1952). HYPSOMETRIC (AREA-ALTITUDE) ANALYSIS OF EROSIONAL TOPOGRAPHY. *GSA Bulletin*, *63*(11), 1117-1142. https://doi.org/10.1130/0016-7606(1952)63[1117:Haaoet]2.0.Co;2

Tilly, L., & Fakhruddin, B. (2020). *Fiji Disaster Risk Reduction and Resilience Activity Scope and Design* (Flood Warning System Recommendation Report Issue. https://www.tonkintaylor.co.nz/media/1628/18062020_flood-warning-system-report_-final-draft_clientfeedback-v1.pdf

Town Planning Act- Chapter 139- General Provisions. (1999). *Department of Town and Country Planning*. Retrieved November, from http://www3.paclii.org/fj/legis/sub_leg/tpagpftpsaa1999672.pdf

WMO. (2018). Fiji to Implement Flash Flood Guidance System. Retrieved 28/11/2018, from https://public.wmo.int/en/media/news/fiji-implement-flash-flood-guidance-system

Wright, N. G., Villanueva, I., Bates, P., Wilson, M., Pender, G., Neelz, S., & Mason, D. C. (2008). Case Study of the Use of Remotely Sensed Data for Modeling Flood Inundation on the River Severn, U.K. *Journal of Hydraulic Engineering*, *134*(5), 533 - 540.

Yeo, S. (2013). A Review of Flood Resilience in Fiji. International Conference on Flood Resilience: , Exeter, United Kingdom.

Yeo, S., Blong, R. J., & McAneney, J. (2007). Flooding in Fiji: findings from a 100-year historical series. *Hydrological Sciences Journal*, 1004-1015.
Yeo, S., Esler, S., Taaffe, F., Jordy, D., & Bonte-Grapentin, M. (2017). *Urban Flood Risk Management In The Pacific*.
Yeo, S., Mcgree, S., & Devi, S. (2010). *Flooding in the Fiji Islands between 1840 and 2009*.
Yeo, S. W. (2000). *Ba Community Flood Preparedness Project: Final Report*. https://purl.org/spc/digilib/doc/a6v3c
Yeo, S. W., & Blong, R. J. (2010). Fiji's worst natural disaster: the 1931 hurricane and flood. *Disasters*, *34*(3), 657-683.
Zheng, X., Maidment, D. R., Tarboton, D. G., Liu, Y. Y., & Passalacqua, P. (2018). GeoFlood: Large-Scale Flood Inundation Mapping. *Water Resources Research*, *54*(12), 10-13.